CHARGE STRATIFICATION

FOR

AN INTERNAL COMBUSTION ENGINE

A thesis

submitted in fulfilment

of the requirements for the degree

of

Master of Engineering (Mechanical)

in the

University of Canterbury

by

CHRISTIAN CHANDRAKUMAR ZAVIER

Department of Mechanical Engineering

University of Canterbury

1991

To My Mother

CONTENTS

ABSTRACT

The effect of charge stratification on the lean mixture combustion in a Ricardo E6 single cylinder, variable compression, spark ignition engine has been investigated. The charge stratification process involved injecting small amounts of pure methane gas into the engine cylinder through a modified spark plug just prior to ignition, at a relatively low pressure. Methane injection timing and methane injection duration (or injection rate) were controlled electronically and varied over a range of values. The charge stratification experiment was performed with two different types of inlet mixture. They were :-

(1). gasoline fuel injected into the inlet manifold

(2). methane gas carburetted through the inlet manifold

To examine the effects of charge stratification, a few optimisation studies were undertaken prior to the main combustion experiments.

A combustion chamber simulation was performed to visualise the effects of the velocity field on the injected methane gas. For this a constant volume bomb was built with the same bore as that of the Ricardo engine cylinder. A typical set of velocity fields around the spark plug gap location were established using hot wire anemometry, and relevant positions of the injected methane gas at different times from the injection point in the simulated velocity field were captured through Schlieren photography.

The present work has led to the following conclusions:-

(1). lean limit of the inducted fuel mixture is extended through the charge stratification process

(2). effectiveness of charge stratification is well pronounced at lean air - fuel ratios

(3). HC emission is higher with stratified charge combustion compared with base line operation

(4). CO emission with stratified charge combustion is almost the same as or little lower than with base line operation, at leaner air - fuel ratios

(5). the initially small and compact shape of the injected methane gas appearing in the Schlieren photographs could have a positive influence on the flame initiation phase.

ACKNOWLEDGEMENTS

I thank most sincerely my supervisor Dr. R.K.Green for the advice and encouragement given throughout this work and finally for the help in the thesis write - up itself. I also thank Prof. D.C. Stevenson for the help in setting up the light source for the Schlieren photography.

I wish to extend my special thanks to Mr. R.E. Tinker and Mr. E.W. Cox for their willing support in constructing the experimental set - up and for the continuous help during the entire experimental work. Their valuable hints in solving technical problems are also much appreciated.

I wish to thank Mr. G.R. Harris for his willing help during the hot wire anemometry work. I also like to thank Mr. B. Sparks for his co - operation especially during most part of the Schlieren photography work. Thanks also to Messrs. O. Bolt, H.J. Anink, G.L. Leathwick and H.A. Mobbs for their help at various occasions.

I like to extend my appreciations to my fellow post - graduate students, particularly Neil Glasson for having constructive discussion on this work and for the help in solving many computer oriented problems.

At last not least I wish to express my gratitude to Mrs. Ann Shearer for kindly giving her time to the proof reading of this thesis.

LIST OF ABBREVIATIONS

ATDC	after top dead centre
A/D	analogue to digital
BP	brake power
BTDC	before top dead centre
CO	carbon monoxide
CO_2	carbon dioxide
D.C	direct current
EGR	exhaust gas recirculation
Ford PROCO	Ford Programmed Combustion
Honda CVCC	Honda Controlled Vortex Controlled Combustion
HC	unburnt hydrocarbons
M.A.N	Maschinenfabrik Augsburg Nurnberg
MBT	minimum advance for best torque
NO_x	oxides of nitrogen
TCCS	Texaco Controlled Combustion System
TDC	top dead centre
WOT	wide open throttle
bsfc	brake specific fuel consumption
o.d	outer diameter
ppm	parts per million

r.m.s.	root mean square
r.p.m	revolutions per minute
% vol.	per cent volume

LIST OF TABLES

LIST OF PLATES

LIST OF FIGURES

CHAPTER 1

INTRODUCTION

1.1 INTRODUCTION

The reciprocating internal combustion engine is by far the most common form of engine or prime mover. One of the main types of internal combustion engine is the spark ignition engine, in which the fuel is ignited by a spark. The advantages inherent in the spark ignition engine include its versatility, power - to - weight ratio and the cost of manufacture, which enables it to compete favourably with other types of engine. Hence the spark ignition engine has continued to grow with modern refinements aimed at improving performance within the constraints of the four - stroke cycle. Problem areas currently receiving attention by spark ignition engine manufacturers include fuel economy improvement and exhaust emissions control.

1.2 FUEL ECONOMY

The fuel economy of an engine is characterized by the efficiency with which the fuel is burnt in the engine. Although this is only one of the criteria by which the performance of an engine is assessed, its importance was realised after the second world war when it was found that 60 per cent of the total tonnage to a combat theatre was made up of petroleum products (36). Then came the Middle East oil crisis in 1973, which, because of subsequent

increased oil prices raised the public awareness about fuel economy to a significant level. This situation had a major impact on many developing countries, who have to import oil from overseas and even on developed countries like New Zealand where oil accounts for about 15 per cent of total import expenditure (113), the major part of the oil consumption being attributed to road transport. Apart from this, if one looks at the world oil status it can be seen that the ratio of oil reserves to the production has been decreasing steadily since 1950 (9). This scenario had led many countries to form energy planning committees and required the automobile manufacturers to improve their engine design with fuel economy in mind.

In addition to the standard engine operating parameters like air - fuel ratio, speed, load and spark timing, the fuel economy of a spark ignited engine is also influenced by other factors including physical properties of gasoline, mixture preparation and type of lubricant.

1.3 EXHAUST EMISSIONS

During the last three decades considerable attention has been focussed on the causes and effects of air pollution. Automobiles represent one of the most serious sources of air pollution. More than 80 per cent of the emissions originating from transportation are generated by gasoline powered vehicles. The major pollutants in automobile emissions are unburnt hydrocarbons, carbon monoxide and oxides of nitrogen. Although hydrocarbon emissions can occur from the crankcase, carburettor and fuel tank, the major part of emissions and the most difficult to overcome are those

contained in the exhaust gases.

In addition to these pollutants, the formation of CO_2 is an inescapable consequence of the combustion of hydrocarbon fuels in air. Although in the past it has not been considered as a dangerous pollutant, its role in the Greenhouse effect (Section 1.3.2) may well require reduction of this gas in the future.

1.3.1 Sources of exhaust emissions

(a). Unburnt hydrocarbons (HC)

Wall quenching, incomplete combustion, misfire, absorption and release of fuel by the oil layers inside the engine cylinder are found to be the main causes for the existence of hydrocarbons in the exhaust emissions. Patterson et al.(88) has suggested that the effect of engine variables on HC emission should be considered in four steps as follows :-

(1). formation of quench regions in the combustion chamber

(2). post - quench oxidation in combustion chamber

(3). fraction of HC leaving combustion chamber and

(4). oxidation in the exhaust system

These four steps can be put into a equation form as follows :-

HC emission in the exhaust =step(1) - step(2) - step(3) - step(4)

HC emission levels depend on engine variables such as combustion chamber shape, compression ratio, air - fuel ratio, charge dilution, spark timing, speed, induction system design, wall roughness and load (16,29,52,53,81,88).

Daniel (28) has shown from his experiments using propane as the fuel, that the unburnt hydrocarbons exhausted into the atmosphere, contained original fuel hydrocarbons ($C_3 H_8$) and non - original fuel hydrocarbons (lower order hydrocarbons). He concluded that the non - original fuel type hydrocarbons might have been produced by cracking of propane during expansion and exhaust process.

Besides this, Adamczyk et al.(1) found that the type of oil present in the cylinder has an influence on the amount of HC emissions in the exhaust.

(b). Carbon monoxide (CO)

Incomplete combustion due to insufficient air in rich - running engines is found to be the main cause of the formation of this particular pollutant. With lean air - fuel ratios it has been noticed (45) that the flame quenching at the combustion chamber wall makes a significant contribution to the total CO in the exhaust, as well as to the partial oxidation of HC during the exhaust process.

The following reaction is generally considered to be the dominant reaction, affecting CO in combustion systems, containing large quantities of water vapour

$$CO + OH \longrightarrow CO_2 + H \qquad (1.1)$$

Newhall (80) and Pischinger et al.(92) have shown that CO concentration values are the same as the equilibrium values at the start of the expansion process. However, as the expansion process continues, an increasing deviation from equilibrium occurs.

If reaction (1.1) is at all times in equilibrium, then the relative levels of CO and CO_2 will be controlled solely by the existing levels of OH radicals and H atoms.

$$[CO]/[CO_2] = f\{[H]/[OH]\} \qquad (1.2)$$

Further Newhall (80) has shown that during the expansion process [H]/[OH] is increasing to very high values. Therefore $[CO]/[CO_2]$ must be correspondingly greater than for total equilibrium and as a consequence there is an excess of CO.

(c). **Oxides of nitrogen (NO_x)**

High peak combustion temperatures inside the cylinder and the mixture residence time at high temperatures are thought to be the causes of the generation of this pollutant according to the Zeldovich chain reaction (79)

$$O_2 \longrightarrow 2O \qquad (1.3)$$

$$O + N_2 \longrightarrow NO + N \qquad (1.4)$$

$$N + O_2 \longrightarrow NO + O \qquad (1.5)$$

According to Heywood (45) although NO forms in the flame front and post - flame gases, there is both experimental and theoretical evidence to suggest that NO formation at the flame front is generally small compared to that in the post - flame gases at typical gas pressures and temperatures of a spark ignition engine. NO concentrations freeze early in the expansion stroke for lean mixtures and later in the expansion for rich mixtures.

The important engine design and operating parameters which affect NO formation are compression ratio, combustion chamber shape, engine

speed, air - fuel ratio, inlet mixture temperature and pressure, spark timing, charge dilution and fuel type (10,16,57,81,88).

Besides these, Robison (99) from his experiments has shown the influence of humidity of intake air on the exhaust NO_x, where increased humidity is found to decrease the exhaust NO_x concentration.

1.3.2 Effects of exhaust emission

(a). Greenhouse effect

It is well known that the suns radiation, by virtue of its high temperature, is concentrated in the ultra-violet, visible and near infra-red wavelength ranges. In contrast the re - radiation from the surface of the earth is concentrated at the longer wavelengths, in the region of infra-red radiation. As the combustion of the hydrocarbon fuel continues, there will be a gradual increase of carbon dioxide (CO_2) in the atmosphere. Carbon dioxide and water vapour in the atmosphere are absorbers of radiation but primarily in the infra-red, not in the visible range. Consequently they pass solar radiation without much interference but they absorb and re - radiate much of the terrestrial radiation emitted from the earth which in turn may make the environment much warmer.

(b). Photochemical smog

This is another form of air pollution in which oxides of nitrogen and highly reactive groups of unburnt hydrocarbons such as olefins play a major role, in the presence of ultra-violet light to form a photochemical smog.

The following reactions are thought to take place (89)

$$NO_2 + \text{sunlight} \longrightarrow NO + O \qquad (1.6)$$

With the aid of a third body (M) in the reaction environment,

$$O + O_2 + M \longrightarrow O_3 + M \qquad (1.7)$$

$$O_3 + NO \longrightarrow NO_2 + O_2 \qquad (1.8)$$

Apart from this, highly reactive olefins react with oxygen atoms to give organic radicals R and R^1

$$O + \text{olefin} \longrightarrow R + R^1O \qquad (1.9)$$

$$R + O2 \longrightarrow RO_2 \qquad (1.10)$$

(peroxy radical)

These peroxy radicals can yield an oxygen atom to NO to form NO_2, whereby ozone(O_3) will be built-up.

The other radical R^1O might be an aldehyde. The aldehydes are eye irritants. The peroxy radical RO_2 (from reaction (1.10)) can also donate an oxygen atom to sulphur dioxide to form sulphur trioxide (SO_3). This compound can then react with water to form sulphuric acid as

$$SO_3 + H_2O \longrightarrow H_2SO_4 \qquad (1.11)$$

The acid forms a mist of fine aerosols which cause a marked decrease in visibility.

In addition to these reactions, another reaction may occur as follows

$$RCOO + NO_2 \longrightarrow RCOO\,NO_2 \qquad (1.12)$$

(PAN)

PAN (Peroxy acetyl nitrate) is a very potent eye irritant as well as a compound which causes damage to plants.

All of these products are thought to combine to form the photochemical smog sometimes present in the air. Although this peculiar form of air pollution was observed in Los Angeles, California, back in 1940, it has only received detailed attention since the late sixties as the number of vehicles operated with gasoline has greatly increased. This has resulted in Californian authorities setting up very stringent emission level standards (18,27) (Table 1.1) over the years compared to rest of the world.

Photochemical smog is characterised by a decrease in visibility, irritation of throat and eyes, a distinctive odour and damage to crops and building materials.

1.3.3 Emission control methods

Emission control devices have been developed by the automobile manufacturers to treat pollutant laden exhaust gases before they are emitted into the atmosphere. These devices include :-

(a). Thermal reactor

This is positioned at the exhaust manifold and provides for complete burning of HC and CO. An incorporated air pump sends fresh air into the exhaust gas so that there will be plenty of O_2 to react with HC and CO. It is this further combustion that keeps the temperature high in the thermal reactor. In addition, the thermal reactor has an internal volume of about four times that of a standard exhaust manifold, so that gas resides in the thermal reactor for a longer time and HC and CO therefore have longer to react with

the excess O_2 supplied.

(b). **Dual catalytic converter**

This is made up of two catalyst systems and mounted in the normal exhaust line. In the first stage NO_x is reduced by using a reduction catalyst into N_2 and O_2 and subsequently, in the second stage HC and CO are oxidized with the aid of air supplied by an incorporated air pump.

(c). **Three - way catalytic converter**

Recent development of the dual catalytic converter has led to the three - way catalytic converter. As the name implies all three pollutants HC,CO and NO_x are treated simultaneously.

However the operation of any catalyst system is liable to be affected by the lead in the gasoline. Moreover the effective operating range is confined to a narrow band very close to the stoichiometric air - fuel ratio. The method of achieving such precise control of air - fuel ratio is through the use of a **Lambda** sensor (Plate 1.1) in the exhaust coupled to a feedback loop to control the fuel flow (Fig.1.1).

Although combustion generated pollutants are dependent on various engine operating variables, they all primarily depend on the air - fuel ratio supplied to the engine, as in the case of fuel economy (Fig.1.2). From this one may come to the conclusion that a good compromise could be established between fuel economy and exhaust emissions only if an engine could be designed to operate on the lean side of the air - fuel ratio.

1.4 LEAN BURN ENGINES

Lean burn engines are one of the obvious answers to the legislation limiting the amount of exhaust pollutants and to the demands of an energy - conscious society. However with lean mixtures, the power output is reduced, but since we do not use the maximum power very often on the road it seems desirable to explore the possibilities of using lean mixtures as a means of better fuel economy at part load. The reason for the higher part load fuel economy is that the lower flame temperature reduces the mean specific heat of the gases and heat losses to the chamber walls. Moreover throttling and pumping losses are reduced.

The application of lean burn engine technology to emission control does pose two problems. They are :-

(1). lower exhaust temperatures which are not conducive to further oxidation of the exhaust gas in the exhaust manifold and

(2). oxygen rich atmosphere in the exhaust which makes the catalytic reduction of NO_x impracticable, so the exhaust gas re - circulation (EGR) has to be employed.

The first problem has been overcome by using port liners (2) and in terms of durability this system with a thermal reactor, is much superior to the catalyst system. One further consideration of lean burn concept on emission control is that NO_x emissions are highly sensitive to changes in air - fuel ratios.

Engine operation with lean mixtures can lead to other undesirable

combustion characteristics, unless proper control is exercised. These include misfire, slow burning and an increased level of cycle by cycle variation, resulting in poor fuel economy, increased emissions and poor driveability of the vehicle.

1.4.1 Misfire

Misfire is a condition that usually occurs in lean burn engines when the air - fuel ratio of the supplied mixture to an engine cylinder is increased, and a limit is reached whereby the mixture fails to burn every cycle due to failure of flame initiation or failure to sustain flame propagation. Misfire in an engine is described as failure of the mixture to ignite (97) or as Hansel (41) suggested it is likely that the kernel could leave the spark gap but fail to develop into a flame front.

It is difficult to identify this lean limit in practical systems like engine combustion chambers. Quader (97) in his experiments defined the lean limit as the mixture stoichiometry at which about 0.5 - 0.8 per cent of the cycles have motoring condition (i.e. no ignition) while Tanuma et al.(107) defined it as the largest air - fuel weight ratio for operation without misfire. Hattori et al.(44) have defined as the mixture strength providing 10 per cent misfired cycles. Sometimes the lean limit is defined on the basis of hydrocarbon emissions, like Burt et al.(17) who have defined it as the mixture strength that produced the same specific hydrocarbon emissions as did maximum power mixture strength.

Besides these, Bolt et al.(13) further classified the lean limit concept

into spark ignition lean limit (related to combustion initiation) and true flammability lean limit (related to flame propagation).

It has been found that the lean limit of air - fuel ratio is influenced to different extents by several engine variables. These include mixture preparation (41,49,97), type of fuel (42,97), charge dilution (41,97,102), compression ratio (12,39,69,97), intake mixture temperature (12,97,107), intake mixture pressure (12), number of spark plugs and spark plug location (83,97,107), spark timing (39,102,107), spark energy (24,44,102,107,114), spark plug electrode geometry (5,24,44,102,107), combustion chamber shape (39,97,107) and mixture motion (13,17,41,44,65,69,107).

Kalghatgi (54) in his experiment used a fuel additive of potassium alkyl salicylate as a spark aider and observed a marked improvement in the lean misfire limit.

1.4.2 Slow burning

With lean operating spark ignition engines, because of decreased energy liberation per unit volume of mixture, partial burn cycles may exist. This is a condition where ignition occurs but flame propagation is not complete, by the time that the exhaust valve opens. It is anticipated that this condition might occur due to one of the following reasons :-

(1). flame may have been extinguished during the expansion

(2). burning being too slow to allow complete flame propagation

Peters (91) in his experiment found that, out of 34 per cent partial

burn cycles, 32.5 per cent was with cycles with slow but continuous burning.

Many studies have shown that the slow burning cycles in the lean operating spark ignition engines are related to various engine variables. They include mixture quality (41,66,87), charge dilution (21,41,57,70,87), mixture motion (13,41,68,70,87), combustion chamber geometry (3,68,70), initial pressure (13), and spark plug gap location (70).

Mayo (70) has shown that increase in compression ratio, reduced only the ignition delay (i.e. the time required to burn first 10 per cent of the charge) not the burn time (i.e. the time interval required to burn the 10 - 90 per cent of the charge). But Peters (91) in his studies concluded that the initial stage of combustion has an influence on the subsequent burning rate of the charge. Moreover, Clarke (21) has showed that injecting gasoline directly into the cylinder made the burning process so slow, that depending upon droplet size and distribution, gasoline was still in the process of oxidation when the exhaust valve opened.

1.4.3 Cycle by cycle variation

The possibility of running spark ignition engines with lean mixtures for improved fuel economy and reduced exhaust emissions, especially at part - load conditions, has always been confronted with a stumbling block, known as vehicle surge. This is simply a phenomenon associated with unsteady power output of the engine. This power fluctuation is caused by the fact that combustion is not the same from one cycle to the next in a given cylinder and that there are often differences between cylinders.

The cylinder to cylinder combustion variation has been shown to exist and is often attributed to the variation of air - fuel ratio between cylinders. Patterson (87) found that a standard deviation air - fuel ratio of 1.45 for an average air - fuel ratio of 16.6 with a conventional carburettor at 1200 r.p.m, while Hansel (41) in his work noticed that air - fuel ratio ranged from 14.3 to 20.2 with an average of 16.0, for 30 m.p.h road load condition. This variation in air - fuel ratios may be caused by poor manifold design or carburation problems.

The cycle by cycle combustion variation is based on the variation of the flame propagating rate inside the combustion chamber. Consequently, Patterson (87) has readily observed these combustion differences as variations in cylinder pressure development. The cyclic variation was shown to increase as the air - fuel ratio moved away from stoichiometric in the lean direction (40) where maximum variation in peak cylinder pressure was increased by 60 per cent for a change in air - fuel ratio from 15:1 to 20:1. Later Hansel (41) showed that cycle by cycle variation would increase when the air - fuel ratio moves away from the stoichiometric, either in lean or rich directions. It is generally concluded from the engine experiments and modelling (7,13,26,67,70,87), that increasing the combustion rate would reduce the cycle by cycle combustion variation. This was explained by Patterson (87) as although both fast burn and normal systems have the same cyclic spread of pressure rate (i.e. maximum value - minimum value), systems with the faster combustion will have low cyclic variation relative to the mean value, thereby minimising the power fluctuations. Also Clarke (21) and Komiyama et al.(57)

noticed that cycle by cycle variations are least when there is a short ignition delay period.

The cycle by cycle combustion variation is found to be influenced by many engine variables, such as mixture quality (41,87), mixture ratio (21,25,41,42,87), spark timing (42,70,87,107), exhaust residual gas (21,41,57), type of fuel (13,21), compression ratio (7,21), number of ignition points and spark plug location (21,70,83) and mixture motion (13,21,22,41,67,87).

Regarding combustion chamber shape, although Mayo (70) has found in his experiments that introduction of squish area reduced the cycle by cycle variation. However Tanuma et al.(107) and Lucas et al.(64) have noticed that there is no significant difference due to squish action, instead Tanuma et al.(107) and Clarke (21) revealed the necessity for compact volume around the spark plug for smooth operation of the engine.

In addition, Clarke (21) has showed from his experiment that direct injection of gasoline into the cylinder, where all the fuel burns at the surface of the droplets, resulted in combustion varying from one cycle to the next.

1.4.4 Fuel economy of lean burn engines

Harrow et al.(42), in their experiment with a Ricardo E6 single cylinder engine, showed that at WOT, when the air - fuel ratio was increased from 14:1 to 17:1 there was approximately 8.5 per cent decrease in indicated specific fuel consumption, but with a 9 per cent reduction in indicated power. Similarly Nakajima et al.(78) with their newly developed dual plug Z fast burn Nissan engine, showed approximately 8.7 per cent fall in brake specific fuel

consumption for a change in air - fuel ratio from 14:1 to 20:1. It is also noted (17), in all the three types of car engine tested, good fuel consumption was generally obtained over the air - fuel ratio range of 17:1 - 22:1.

Moreover, Patterson (87) estimated that an improvement of 10 per cent to 20 per cent in specific fuel consumption can be achieved, if cycle by cycle variation of combustion, a common phenomenon in lean burn engines, is avoided.

1.4.5 Exhaust emissions of lean burn engines

It has already been noted in Fig.1.2, that exhaust emissions decrease as the mixture ratio moves towards the lean side. There is however a limit as to have lean, an engine may be operated. Again Harrow et al.(42), in their experiment, found that at 1000 r.p.m, when the air - fuel ratio was changed from near stoichiometric ratio of 14.5:1 to 19:1, specific HC, CO and NO_x emissions were decreased by approximately 0.5, 0.25 and 5.5 g/kW h respectively. But after an air - fuel ratio of 19.5, the HC emission especially tends to increase, maybe because of the problem of misfire, as did the CO emission level.

In contrast, it was shown that with Nissan Z fast burn engine (78), at 1400 r.p.m and MBT, it was not possible to attain the Japanese 1978 NO_x standard of 0.25 g/km with the lean burn concept, but it was obtained with the combination of stoichiometric mixture and EGR.

NO_x emission is found to be affected by the cycle to cycle variation in peak pressure (108). For a change of peak pressure from 40.5 bar to 45.6 bar,

approximately 1000 ppm increase of NO_x occurs, at a lean mixture air - fuel ratio of 17.8:1.

1.5 INTRODUCTION TO THE PRESENT WORK

As shown in the preceding sections, the real advantages of the lean burn pre - mixed charge engine cannot be realised, because of its inherent drawbacks like, misfire, slow burning and cycle by cycle combustion variation. These conditions result in poor fuel economy and higher exhaust emissions.

Although stratified charge combustion was recognised as a way to achieve the advantages of the lean burn concept many years ago, it has recently attracted researchers, after the imposition of stringent emission standards. Consequently, many design concepts have emerged on the principle of stratified charge combustion (43) (refer Chapter 2 for details). As a pre - requisite for the charge stratification, a readily ignitable fuel mixture, in the vicinity of the spark plug, must be provided generally either by auxiliary carburettor - intake valve combination (30) or fuel pump - nozzle combination (8,73). The latter combination has been used in almost all open chamber stratified charge engine designs. This arrangement involves fairly high pressure fuel injection into swirling air, so that a relatively rich mixture will form near the spark plug by the time ignition is required. In such circumstances, there is always a possibility that fuel could disperse away from the spark plug thus forming a very lean mixture which is difficult to burn. This condition would render it impossible for an engine to achieve a gain in lean mixture limit operation over the pre - mixed homogeneous charge

engine. Moreover this could result in excessive HC emission, especially at light loads, as observed by Wood (111).

However, it has been found possible to keep the relatively rich mixture cloud around the spark gap just before ignition, by using a reasonably low pressure fuel injection system. Pitt et al.(95) have used a solenoid injector to inject a gaseous fuel towards a spark gap at a low pressure, a short time before the ignition, thereby burning very lean mixtures.

Considering all these facts, a unique arrangement is envisaged for introducing the fuel (in this case methane gas) in the vicinity of the spark gap near the time of ignition, at a reasonably low pressure. To achieve this, a commercially available spark plug was modified to allow methane gas to be injected in the vicinity of the spark electrodes. As a consequence a turbulent mixture puff is formed in the region of the spark electrodes. Hence a lean pre - mixed mixture could be richened in the vicinity of the electrodes thereby producing a stratified charge. Upon ignition of the puff by the spark, the flame produced should burn the very lean mixture in the combustion chamber.

This idea has been put into operation with a Ricardo E6 single cylinder, variable compression, research engine, to study its performance, while

(1). gasoline fuel is injected into the inlet manifold and

(2). methane gas is carburetted through the inlet manifold

In addition to these tests, hot - wire anemometry and schlieren techniques have been used with a combustion chamber simulation testing, to

study the effects of charge motion on the relatively rich fuel cloud in the vicinity of the spark electrodes.

PLATE 1.1 Lambda sensor (heated type)

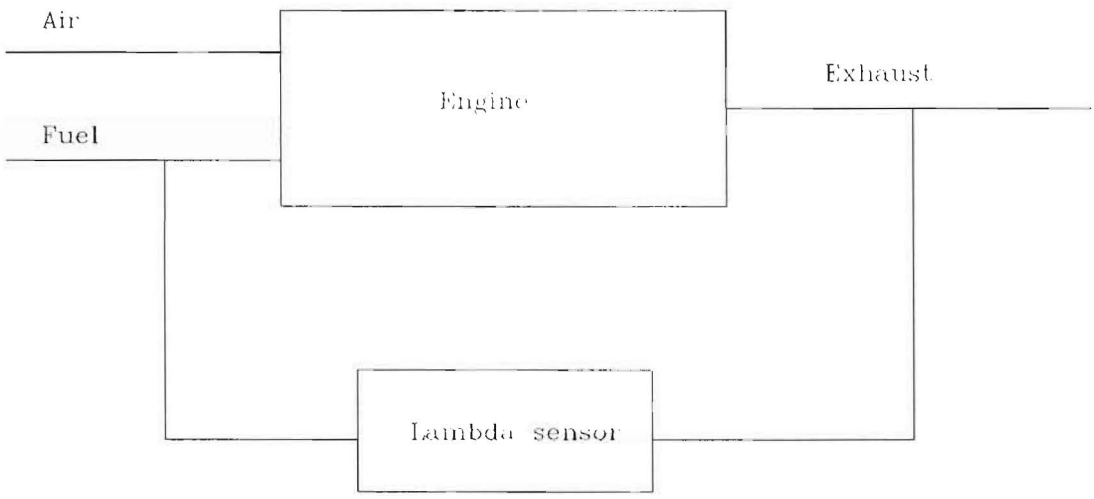

Fig.1.1 Closed loop control system of Lambda sensor

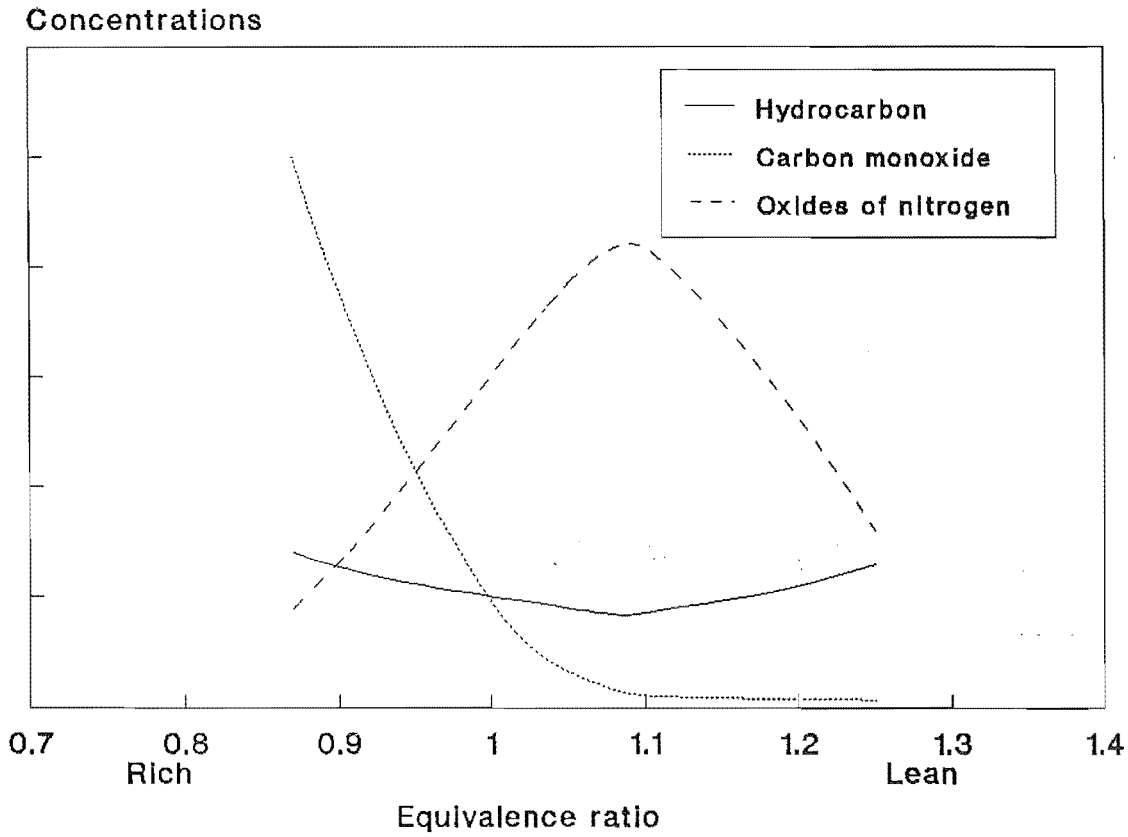

Fig.1.2 Pollutant concentrations vs equivalence ratio for a spark ignition engine

equivalence ratio = (actual air - fuel ratio)/(stoichiometric air - fuel ratio)

Year	HC (g/m)*	CO (g/m)*	NO_x (g/m)*
1972/73	3.2	39.0	3.0
1974	3.2	39.0	2.0
1975/76	0.9	9.0	2.0
1977/79	0.41	9.0	1.5
1980	0.39	9.0	1.5
1981/82	0.39	7.0	0.7
1983	0.39	7.0	0.4
1985	0.41	7.0	0.4
1987	0.41	7.0	0.4
1989	0.41	7.0	0.4

TABLE 1.1 State of California emission regulations

(g/m)* - gram/mile

CHAPTER 2

LITERATURE REVIEW

2.1 INTRODUCTION

The disadvantages associated with lean burn engines (Section 1.4.), have been partly attributed to the homogeneity of the air - fuel mixture at the time of combustion. Quader et al.(90) have concluded, that for lean operation some kind of heterogeneous condition, and possibly bulk stratification, is necessary.

The search for the better fuel consumption and low exhaust emissions, especially at part - load condition, has led to the development of the stratified charge engine. The advantages claimed for the stratified charge engine include improved efficiency, low exhaust emissions and greater fuel tolerance.

2.2 BASIC PRINCIPLE OF CHARGE STRATIFICATION

The principle behind charge stratification is to have a readily ignitable air - fuel mixture in the vicinity of the spark plug, and a weak mixture in the remainder of the combustion chamber at the time of ignition. Upon ignition of the relatively rich mixture by the spark, the flame produced should burn throughout the weaker mixture which may be non - combustible if used in conventional homogeneous charge operation. Although the mixture

is part rich and part weak, since the volume of weak charge is greater than that of the rich part the overall effect is to have lean combustion.

2.3 STRATIFIED CHARGE ENGINES

Although there is no universal definition, a stratified charge spark ignition engine may be defined as an engine with intermittent combustion initiated by a spark plug, where the element of mixture ignited by the spark plug is not typical of the mixture in the remainder of the working gas, over some portion of the engine operating regime.

Depending on the combustion chamber configuration (i.e. divided or open) and the method of fuel addition into the combustion chamber (i.e. fuel injected or carburetted), stratified charge engines are classified into different groups (Table 2.1) (43).

A few decades ago, the stratified charge engine appeared to be an attractive alternative to the unsuccessful lean burn pre - mixed charge engines. This made some automobile manufacturers consider the development of these engines. Although most of these developments have ended up at the prototype level, some engines have gone into production. e.g. **Honda CVCC** engine.

2.4 DEVELOPMENT OF STRATIFIED CHARGE ENGINES

2.4.1 Ford Combustion Process (FCP)

This is basically an open chamber, spark ignited, low pressure direct injection, charge stratification process (8,43,105). The mixture stratification is

achieved by a combination of air swirl and injection timing. A cup - in - piston is used to enhance the air swirl in this system. The injection and ignition timings are optimised to give a satisfactory performance over the load and speed ranges. Fuel injection is usually carried out during the compression stroke, although at low speed and light load the injection duration overlaps the spark timing. As the load and speed increases, the injection timing is slowly advanced relative to the spark timing.

When this process was incorporated into a multi - cylinder engine, an average fuel economy improvement of 30.8 per cent was recorded in comparison with a standard carburetted engine.

Although the Ford combustion process engine produced a significant improvement in fuel economy and maximum power equal to that of a carburetted version, the emission characteristics were far short of long range objectives. This has resulted in the development of the Ford **Pro**grammed **Co**mbustion (Ford PROCO) Process which is similar to the Ford combustion process, but employing two spark plugs to facilitate the use of a highly diluted charge.

In this process, NO_x are reduced by the higher EGR rates. The resulting increased HC and CO are oxidized by a catalyst and possibly a low thermal inertia exhaust manifold. Although there is a loss in fuel economy due to the introduction of emission control measures, the Ford PROCO engine fuel economy is still comparable with a standard carburetted engine.

2.4.2 Texaco Controlled Combustion System (TCCS)

This is an another prominent stratified charge system. Although the combustion chamber arrangement resembles that of the Ford PROCO, it follows the Texaco combustion process (TCP) (4,43,73). This involves a co - ordination of air swirl, high pressure direct cylinder fuel injection and positive ignition. The incoming unthrottled air is forced to swirl by means of a suitably designed intake passage and cup - in - piston arrangement, so that the swirl ratio (swirl ratio is defined as the ratio of swirl speed to engine speed) approaches 10 during the combustion event. Fuel injection is usually carried out near the end of the compression stroke, when the combustion is about to begin. This combustible mixture is burnt as rapidly as it is formed.

Load is controlled purely by the amount of fuel injected into the combustion chamber. Since the fuel is ignited by a spark plug as soon as it comes into the combustion chamber, the octane or cetane number quality requirements are eliminated. This advantage shows the multi - fuel capability of the system. Because of its heterogeneous combustion nature, the specific power is limited by the smoke level.

Since this system has low exhaust temperatures due to excess air operation, the exhaust thermal reactor could not be used as a means of controlling exhaust emissions. Therefore catalytic treatment is chosen to reduce the amount of HC and CO emissions. Since the exhaust gas of a stratified charge system tends to remain stratified at light loads, a swirl reactor is installed prior to the catalyst bed to promote mixing and continued combustion. Idle inlet air throttling is employed, to further reduce HC and

CO. NO_x are reduced by the combination of retardation of fuel injection and ignition and water cooled EGR.

The TCCS design is operated in the turbocharged mode as well as in a naturally aspirated condition. The turbocharge mode of operation is to offset the losses in performance suffered with the emission controlled naturally aspirated engine. Although HC and CO emissions with the turbocharged mode are low, the catalytic bed is still used, but not the aforementioned swirl reactor. Again NO_x are reduced with the EGR.

2.4.3 M.A.N. FM system

The necessity to improve the multi - fuel capability of the M.A.N. "M" diesel engine has led to the development of the M.A.N. " FM " system (19,43,71). Unlike its diesel version, the mixture in this system is ignited by a spark plug, while fuel is deliberately injected on to the surface of the piston bowl near the top dead centre thus forming a fuel film at the surface. Because of the higher temperature of the piston, the fuel evaporates and is carried into the spark plug region by the swirling air. The greater part of the heat required for further evaporation is supplied by flame radiation. The rate of mixture formation, therefore, is a function of the existence and intensity of the combustion itself.

When gasoline is used as the fuel, because of its low auto - ignition nature compared to diesel, the fuel has to reach the spark plug in order to become ignited. This condition requires a greater injection advance for the gasoline fuel relative to diesel fuel. In order to avoid adjusting the injection

advance for different fuels, an appropriate position for the spark plug in relation to the injector nozzle has been found. Although different locations of the spark plug have their own advantages, in this system the plug is located on the opposite side of the piston bowl from the injector. In addition to this, the spark plug electrodes are modified to minimise the electrode disturbance on mixture formation. The modified spark plug has a ground electrode of equal length, arranged parallel to the centre electrode.

The multi - fuel capability of this system has been further demonstrated by running the engine with methanol and ethanol (19). Moreover the exhaust emissions are reduced by using an exhaust catalyst system.

Meurer (72) has summarised the advantages of the M.A.N. " FM " system saying that it can operate with low peak pressure, may be supercharged and will cold start even with unblended methanol. Its disadvantages at its present stage of development include :- reduction in volumetric efficiency due to swirl, requirement for a special spark plug.

2.4.4 Honda Controlled Vortex Controlled Combustion (Honda CVCC)

Unlike the previous systems, this is a divided combustion chamber, (i.e. a new auxiliary combustion chamber is formed where the spark plug is located in the conventional engine) three valve configuration (30). Auxiliary and main chambers are connected by a torch passage. There is a special carburettor to supply rich mixture to the auxiliary chamber only, along with a

small auxiliary intake valve and a separate inlet passage.

During the induction stroke, the inlet valves of both chambers open while a lean mixture and a rich mixture are supplied to the main and auxiliary chambers respectively. Besides this, a part of the mixture which has entered the auxiliary chamber flows into the main chamber through the torch passage and mixes with the lean mixture. Then during the compression stroke, a portion of the main chamber mixture which is formed during the induction stroke enters the auxiliary chamber. Because of these mixing processes, a three - zone charge stratification (i.e. relatively rich mixture at the spark plug, lean mixture in the main chamber and an intermediate rich mixture at the torch passage) is achieved at the time of ignition. This intermediate mixture is ignited by the flame initiated in the auxiliary chamber and forms the torch, thereby burning the lean mixture in the main chamber.

The outcome of this controlled combustion is reduced peak temperature in the main chamber, which is advantageous for reducing NO_x emission. But at the same time, the average gas temperature remains comparatively high during the expansion and exhaust strokes, which should oxidize HC and CO with the aid of a thermal reactor.

In a further development along this line to improve the fuel economy of this system, Yagi et al.(112) have changed the geometry of the torch passage. Instead of the original single straight portion, it has straight and tapered portions and three passages branch off from the orifice of the tapered portion to the periphery of the main combustion chamber wall. This modified system has yielded low fuel consumption values by allowing the use of higher

compression ratios.

2.4.5 Volkswagen Pre - Chamber Injection stratified charge system (VW - PCI system)

This is another divided combustion chamber stratified charge system but the fuel is injected into the pre - chamber rather than carburetted as in the case of Honda CVCC (15). During the preliminary single cylinder engine research work, different combustion chambers were considered. They included :-

(1). open chamber with a recess in the cylinder head, in which fuel is injected immediately before the ignition. This displaces the misfire limit but only a little.

(2). combustion chamber with a pre - chamber which is about 5 per cent of the total compression volume. The fuel is injected into the pre - chamber, this further displaces the misfire limit.

(3). combustion chamber with a pre - chamber but the fuel is carburetted into the pre - chamber through an auxiliary intake valve. This incoming mixture is more or less of stoichiometric ratio and produces a further shift in the lean limit. But this has produced high HC emissions and the use of the third valve has deemed to be expensive.

After considering all these options, a spherical pre - chamber which is approximately 25 - 30 per cent of compression volume with a relatively large transfer passage to the main combustion chamber was chosen. In this the fuel is injected into the pre - chamber while the lean mixture is introduced into the main chamber either by port injection or carburetion. The injector nozzle and the spark plug are arranged in sequence in the flow direction so that the spark plug receives a mixture produced by blending the incoming air with fuel already dispersed in air.

Load regulation is achieved primarily by adjusting the mixture strength introduced into the main chamber. The orientation of the transfer passage, which produces the swirl, promotes the mixture preparation in the pre - chamber.

Further tests have revealed that the volume of fuel delivered to the pre - chamber has to be varied if minimum emission values are to be achieved, and with increased load, the amount of fuel injected into the pre - chamber must be reduced to avoid soot formation. It has been shown that about 20 - 35 per cent and 13 per cent of total volume of fuel has to be injected into the pre - chamber in order to achieve the minimum emissions and minimum fuel consumption respectively.

Vehicle dynamometer tests have indicated the necessity of a thermal reactor to improve the HC and CO emissions while the NO_x emissions are still lower than the conventional engine, even without EGR.

2.4.6 Mitsubishi Combustion Process (MCP)

This is basically an open chamber, fuel injected, charge stratification system (75,76). The spark plug has been located between the centre and the edge of the combustion chamber to meet its design requirement of high power and low emission. A fuel injector with a variable retraction delivery valve has been developed to provide the optimum injection timing for all operating conditions. The multi - fuel capability of this system has been demonstrated by running with kerosine. These engines were mass produced in Japan, to install in agricultural machines.

Apart from the reciprocating engines with the stratified charge combustion system, Curtiss - Wright Corporation has developed the stratified charge rotating combustion engine (51). This is another open chamber configuration and is capable of operating with a wide range of fuels. This work is now being undertaken by the John Deere Company of Illinois.

2.5 FLAME PROPAGATION IN A STRATIFIED CHARGE MIXTURE

When a flame is propagating through a fuel mixture, a change in the mixture concentration will lead to corresponding changes in the following factors, namely

(1). flame velocity

(2). amount of heat generated at the flam front

(3). heat transferred to the unburnt mixture

(4). flame temperature

(5). temperature of the burnt gases

The change in flame velocity with the mixture concentration has been demonstrated by Karim et al.(55), with a homogeneous mixture of methane in air, over a range of mixture concentrations.

The convective flow of active species from the hot burnt gases to the unburnt mixture depends on the flame temperature. Therefore, with a non - homogeneous mixture, if the flame velocity and the flame temperature are in the reducing mode, then the temperature difference between the hot burnt gases and the flame front would increase. This could result in a high rate of convective mass transfer of active species into the unburnt mixture and consequently an increase in the rate of flame propagation.

Karim et al.(56) have studied the flame propagation in a stratified mixture of methane and air inside a long transparent cylindrical tube. It has been noted, that when the flame was propagating along a concentration gradient, from near stoichiometric to fuel lean mixture, the observed flame velocities were higher than the corresponding quasi - homogeneous values. If this observation is viewed together with the fact that was established for a non - homogeneous mixture in the previous paragraph, then it might be concluded that the flame propagation in the stratified charge mixture will not be supported much by the convective mass transfer of active species. Therefore, the rate of flame propagation will not be very different from the quasi - homogeneous case. This was further demonstrated by Liebman et al.(62), who have shown that the upward flame speeds in layered and homogeneous methane - air mixtures were comparable.

Flame propagation through the stratified charge in an engine cylinder has been investigated by using mathematical models. Westbrook (109) has shown, from his open chamber model study, combining numerical methods with detailed reaction mechanism, that the flame speed was considerably higher than the homogeneous case, at an early stage of the combustion, i.e. until about 0.2 ms. This was followed by a rapid drop in flame speed as the flame entered into a mixture of exceedingly lean condition. As a result, with the stratified charge model, it took 3 ms to consume all the fuel, where it took only 0.7 ms with the stoichiometric homogeneous model.

Further, Girard et al.(37) have shown with the single cylinder modelling study, that the combustion duration of stratified hydrogen - air and propane - air mixtures was reduced, compared to that of homogeneous mixtures, at a range of lean overall air - fuel ratios.

Although the flame propagation study in the divided chamber configuration is complicated, it has been analysed through combustion modelling. Syed et al.(106) have shown that the jet velocity at the throat exit in an engine begins to rise as the flame develops in the pre - chamber and reaches a peak approximately when the flame appears in the main chamber with a subsequent decrease. This explains the faster initial mass burning rate in the main chamber and the initial large energy release rate.

Sakai et al.(100) have shown from an experiment with a single cylinder engine with a pre - chamber, that although the combustion duration of the torch ignited engine was longer than that of the conventional engine, it has a large energy release rate at the early part of the combustion. Later

Sakai et al.(101) have taken flame photographs on a quartz piston engine to show the faster flame propagation rates at the early part of the combustion. This trend has also been observed by Pischinger et al.(93).

2.6 EFFECT OF AIR MOTION ON A STRATIFIED CHARGE ENGINE PERFORMANCE

It has been seen in Section 2.4., that charge stratification in the stratified charge engines, especially with the open chamber configuration, is dependent upon the air motion inside the combustion chamber (8,19,73). The air motion inside the combustion chamber could generally be in three different forms, namely

(1). swirl

(2). turbulence

(3). squish

2.6.1 Swirl

This is a bulk rotational motion of the gas, approximately about the cylinder axis. This is an inlet induced, three dimensional, unsteady motion. Swirl could be generated and varied by the shape of the inlet port and with shrouds on the inlet valve.

2.6.2 Turbulence

This is an irregular condition of flow in which the various quantities show a random variation with time and space co - ordinates. It can be

generated by the inlet process and/or squish. Turbulence contributes to small scale mixing of fuel and air.

2.6.3 Squish

This is an inward radial motion of the gas originating from the small clearance region between the piston top and the cylinder head, as the piston approaches the top dead centre (TDC).

It can be seen from the above that the air swirl is generally responsible for the bulk movement of the air - fuel mixture while turbulence governs the degree of mixing of fuel and air inside the combustion chamber. Since the transient location of the mixture cloud relative to the spark plug is determined by the air swirl, it might well be said that the air swirl has a dominant influence on the charge stratification process in the stratified charge engine and on its performance.

This phenomenon has further been demonstrated by Fansler et al.(35) who have shown that the low frequency random fluctuations of the swirl centre would result in cycle to cycle variation in the air - fuel ratio at the spark plug which in turn affects the ignition and early flame growth. It has also been noted that at higher swirl levels, although squish itself does not have any significant influence on the air - fuel distribution at the spark plug, depending on the injector location, injection timing etc., the air - fuel distribution is influenced by the complex flow field, produced by the combined effect of swirl and squish.

Witze (110) has studied the influence of air motion in a single cylinder, direct injection stratified charge engine with a shrouded intake valve. It has been noted that the shroud orientation, giving high swirl and low turbulence, results in faster burning rates, which has led to little cyclic variation during combustion. This was because, a combination of high swirl and low turbulence produced the condition of greatest stratification.

Similarly, Pischinger et al.(94) have performed an experiment on a single cylinder, divided chamber, pre - chamber injected engine with different types of intake valve. It has been found that a test with the shrouded intake valve, produced good fuel economy and low emissions when compared with a low consumption production engine at that time. Moreover, out of those three types of intake valve tested, the shrouded valve has generated the maximum swirl and shortest burn time.

2.7 POLLUTANT FORMATION IN STRATIFIED CHARGE ENGINES

As we have seen, with the lean burn pre - mixed charge engines, the generation of pollutants such as HC, CO and NO_x is an inescapable consequence of combustion of hydrocarbon fuel in air. Such pollutant formation can be expected, even with the stratified charge engines, but at different levels.

2.7.1 Unburnt hydrocarbons (HC)

From Section 1.3.1., it can be seen that the major source of unburnt hydrocarbon emission is the wall quenching effect.

Westbrook (109) has shown from his numerical model of single cylinder, open chamber, charge stratification process, that although the fuel has been kept away from the chamber wall before it is consumed, volume flame quenching appears to result in an excessive amounts of HC. This has been explained by the fact that the flame speed drops rapidly as the flame begins to propagate through exceedingly lean mixture. This effect has been further examined by Johnston (50) and Lancaster (60) who have shown that a fuel lean region exists, after fuel injection, which is too lean to support combustion of the fuel mixture, causing the volume quenching.

Moreover Fansler et al.(35) have predicted from flow field observations, that at high loads, liquid fuel is accumulated at the bottom of the piston bowl where the squish generated turbulence is not enough to evaporate the fuel in time for burning and has resulted in excessive HC emission.

It has been found that at light loads the HC emission with direct injection spark ignition engine is higher than that of a pre - mixed spark ignition engine. Glovanetti et al.(38) attribute this effect to the deteriorating fuel injection behaviour at light loads. This conclusion seems to agree with the results obtained by Balles et al.(6), from a study with a direct injection stratified charge engine. They have found that the cyclic variation of the injection system performance and the combustion behaviour (in terms of heat release) increases, as the load decreases.

Further, Wood (111) and Oblander et al.(82) have also observed this trend and concluded that in addition to the formation of fuel lean regions, the

resulting low exhaust temperatures makes the after burning process of the combustion products more difficult at light loads. This could result in excessive amounts of HC. Moreover, Heywood (45) has suggested that the cup - in - piston configuration usually seen in open chamber stratified charge engines might have rendered high surface to volume ratio and has led to the increased HC emission.

With the divided chamber configuration, as Purins (96) noted, the higher surface to volume ratio could be the cause of the greater HC emissions. In addition to this, Newhall et al.(81) have suggested that the fuel spray deposition on the pre - chamber wall could also result in excessive HC emissions.

Additionally, Syed et al.(106) have predicted through their combustion modelling study of divided chamber configuration, that the turbulence mixing at the connecting throat area may cause unburnt fuel pockets to be trapped behind the flame front.

2.7.2 Carbon monoxide (CO)

Although the overall air - fuel ratio of the mixture burning inside the stratified charge engine is lean, an increase in the CO emission level at certain loads, compared to conventional engines, is not uncommon.

Wood (111) has concluded from his experiment with a direct injection stratified charge engine that the larger regions of over rich fuel - air mixtures were responsible for the increase in CO emission, at high loads. This trend has also been noted in the work carried out by Oblander et al.(82), where a

large increase in CO emission occurred, compared to the conventional engine, as the load increased. Again the lower exhaust temperatures with lean mixtures at light loads makes the after burning of CO much more difficult and has led to the high CO emissions.

In the case of the divided combustion chamber, Krieger et al.(58) have predicted, through the physical model for jet ignition combustion, that the rich burnt mixture present in the pre - chamber after the flame propagation appeared to be the most significant source of CO. This prediction has been supported by the results obtained by Ogasawara et al.(84) where it was found that the CO formation in the primary chamber dominated the overall CO concentration.

2.7.3 Oxides of nitrogen (NO_x)

Blumberg (11) has shown from his single chamber model study, for lean overall air - fuel ratios, with rich to lean mixture stratification, that insufficient difference in stratified mixture air - fuel ratios (i.e. difference between relatively rich mixture air - fuel ratio and weak mixture air - fuel ratio) has resulted in high NO_x emission. This is due to the fact that the first element to burn coincides with the air - fuel ratio, corresponding to maximum NO_x in homogeneous conditions, which was thought to be the cause of high NO_x emission. This conclusion has been further supported by the measurements made by Lavoie et al.(61), on a single cylinder Ford PROCO engine.

It has also been shown (82), that the relatively high temperature

during combustion within the rich mixture cloud is responsible for the high amounts of NO_x, in direct injection stratified charge engines.

In the case of the divided chamber arrangement, De Soete (31) has concluded that the explosive nature of the combustion inside the main chamber is responsible for the high NO_x production. A similar effect to this trend has been noted by Ogasawara et al. (84), where it has been found that for richer pre - chamber air - fuel ratios, the contribution from the main chamber to the overall NO_x emission is dominant, because the residual combustible gas comes from the pre - chamber, burning inside the main chamber.

Besides this, it has been found (46,84), that for very lean overall air - fuel ratios, most of the NO_x is produced inside the pre - chamber.

2.8 FUEL ECONOMY RESULTS WITH STRATIFIED CHARGE ENGINES

It has been reported (103), that the 6.6 litre, V8 Ford PROCO engine has produced 20 per cent improvement in fuel economy, compared to a carburetted engine of the same size. Similarly, it has been noted (74), that a reduction of 30 per cent in specific fuel consumption was achieved with the TCCS powered engine, relative to a conventonal engine of the same output.

Furthermore, Ciccarone et al.(20) have shown, that a direct injection stratified charge engine powered car has produced fuel economy improvements of 15 per cent during cruising and 7 - 20 per cent during urban driving conditions, when compared to a gasoline engine with the same

acceleration performance characteristics.

With the divided chamber arrangement, Date et al.(30) have shown that approximately 10 per cent improvement in fuel economy was achieved, with the CVCC engine powered vehicle. But it has also been shown (59), from the studies on a single cylinder engine with a scavenged pre - chamber, that although the fuel consumption is comparable with a conventional engine at light and medium loads, it is a little higher than than that of the conventional engine at high loads.

2.9 EXHAUST EMISSION RESULTS OF STRATIFIED CHARGE ENGINES

It has been recorded (4) that a turbocharged TCCS engine powered vehicle, even without emission control measures, has low emission values, compared to a standard carburetted version. Moreover, the Ford PROCO engine powered vehicle has showed a marked reduction in exhaust emissions relative to its carburetted counterpart.

In the case of divided chamber configuration, it has been reported (30) that a CVCC powered vehicle has generated very low emissions of varying degrees, depending on the type of vehicles tested. But Kuck et al.(59) have shown that except for CO emission at high loads, generally exhaust emissions are lower than that of the conventional engine.

1	2	3	4	5	6	7
SINGLE CHAMBERS			DUAL CHAMBERS		SINGLE CHAMBER	
FUEL INJECTION			CARBURETTORS			
Early Injection Into moving air	Late Injection Into moving air	Combustion Controlled by wall evaporation	Fuel Injection Into prechamber also fuel addition to main chamber	Mixture supplied by carburettor(s) separate prechamber inlet valve		Two strokes exhaust diluent engines Miscellaneous
EXAMPLES						
Ford Proco FCP Mitsubishi Hesselman Witsky	Texaco TCCS Curtiss - Wright Deutz	Man F - M Porsche	Newhall VW Huber Porsche Broderson	Honda CVCC Nilov Heintz GM Ford Nissan Walker	I . F . P	Ricardo Jessel Kushul Nice YOCP

TABLE 2.1 Classification of Stratified Charge Engines (43)

CHAPTER 3

EXPERIMENTAL APPARATUS

The apparatus used for this experimental investigation may be divided into two sections. They are:-

(1). apparatus for the engine combustion experiments

(2). apparatus for the combustion chamber simulation

3.1 APPARATUS FOR THE ENGINE COMBUSTION EXPERIMENTS

(refer appendix 1 for detailed specifications)

All engine combustion experiments have been carried out with the Ricardo E6 / MK6 variable compression ratio research engine (Plate 3.1). Engine power absorption was through an electric swinging field direct current type dynamometer and was driven by the engine through a flexible coupling. Brake power output of the engine was measured with a spring balance - torque arm arrangement which was connected to the dynamometer.

3.1.1 Air meter

The air flow into the engine was measured with an **Alcock** viscous flow meter. The pressure drop across the meter was measured with a variable slope manometer. This pressure drop was used in conjunction with the meter calibration constant to calculate the air flow into the cylinder.

3.1.2 Engine controller

The dynamometer was controlled by a **KTK** regenerative system which enabled the engine to be run in three different modes, namely,

(1). motoring : the dynamometer was used purely as an electric motor to motor the engine.

(2). load : the dynamometer was used purely as a dynamometer and absorbed the power generated by the engine, for power measurement.

(3). fixed speed : the dynamometer was used both as a dynamometer and as a motor. It would automatically change from one to the other to hold the speed constant, even if the engine ceased to fire.

3.1.3 Exhaust gas analyser

Horiba exhaust gas analyser (Plate 3.2) was used to measure the concentration of exhaust gas species, such as HC,CO, CO_2 and O_2. Exhaust gas for the analysis was tapped from the exhaust pipe, approximately 2 m from the exhaust valve.

3.1.4 Fuel supply system

Since the engine combustion experiments were carried out in four different arrangements, the fuel supply system for the each arrangement will be described below.

(a). Base line operation with gasoline fuel

A Bosch fuel pump was employed to supply gasoline to the solenoid injector from a 9 litre overhead tank at a pressure of 2 bar. The injector was fitted on the inlet elbow. The injector was actuated by a signal from an infra - red trigger unit at the rear of the engine cam shaft. Moreover the variable duration of the injector opening was controlled electronically which in turn controlled the fuel admitted into the engine cylinder. The injector unit was powered by a 12 V battery through an amplifier unit.

The fuel flow was measured with a flow meter, by recording the time taken for 50 ml of fuel to be consumed by the engine. The fuel line was water cooled to stop the formation of vapour bubbles which could upset the fuel flow measurement.

(b). Charge stratification of a gasoline engine with methane gas

This is the centre piece of the present research work described in this thesis. In addition to the fuel supply system described in (a), methane gas was introduced in the vicinity of the spark gap around the ignition timing.

To accomplish this, a commercially available NGK spark plug was modified (Plate 3.3), in such a way that a Bosch solenoid injector (hereinafter methane injector) would inject a small amount of methane gas through this spark plug just before the ignition. The methane injector was mounted on to the modified spark plug through a non - return ball valve (Plate 3.4). This non - return valve was employed to prevent any exhaust gases coming into contact with the methane injector. The needle end of the methane injector was water cooled, by having a brass sleeve which encompasses the methane injector and the non - return valve. Both ends of this sleeve were sealed with room temperature vulcaniser compound to avoid cooling water leakage. The methane injector with an operating voltage of 3 V, was powered by the 12 V ignition coil supply through a series resistance of 8.2 ohms.

The injection timing and the injection duration of the methane injector was controlled electronically and could be varied. This involved a second infra - red trigger unit which was mounted on the same cam end as the gasoline injector, but approximately at a diametrically opposite position. The variation in the injection timing was achieved by sliding the infra - red trigger unit just above the circumference of the slotted wheel, mounted on the rear end of the cam shaft (Plate 3.5). The position of the infra - red trigger unit with respect to TDC (i.e. injection timing) was read off from a scaled, fixed solid disc, mounted co - axially with the slotted wheel. But the injection duration was varied by means of a rotary switch (Plate 3.6) which linked the infra - red trigger unit and the methane injector. This variable injection

duration determined the amount of methane flow that was admitted through the spark plug.

The methane gas supply system (Fig.3.1) was made up of a methane gas cylinder of 170 bar pressure, a high pressure regulator and a surge chamber - 1 to minimise any fluctuations on the regulator side. An on - off valve was fixed next to this surge chamber to cut - off the gas supply in an emergency. The methane flow rate through the spark plug was measured with the rotameter - 1 which was accompanied by the surge chamber - 2, to eliminate any fluctuations in the flow meter reading due to intermittent gas injection.

Apart from this, a line gas filter with a sintered filter element was fixed in the gas supply line to trap any foreign matter from entering the methane injector and possibly affecting the injector performance. The gas line pressure was further monitored by a pressure gauge which was also used as an indicator to ensure that no exhaust gas flowed back through the methane injector. The gas piping was completed with 1/4 inch. stainless steel pipes and 1/4 inch. **Swagelok** fittings except between the line pressure gauge and the methane injector, where a 1/4 inch. flexible metallic hose was used for convenience. All pipe joints were sealed with **Loctite** compound to avoid any gas leaking.

(c). Base line operation with the methane gas

For this part of the experiment, the gasoline supply was disconnected and a gas carburettor fitted just under the air meter in place of a straight inlet

pipe. The gas carburettor was preceded by a regulator and a fuel controller, to reduce the pressure just below atmospheric pressure and to meter the gas flow respectively. There was no methane gas injection through the spark plug.

Again the gas was supplied from the same gas cylinder as mentioned in (b), but a new gas line of 1/4 inch. stainless steel pipe branched off after the surge chamber - 1 for gas carburetion. Further, the methane flow rate through the gas carburettor was measured with the rotameter - 2 which was accompanied by the surge chamber - 3 for the same reason stated above.

(d). **Charge stratification of a methane gas fuelled engine**

The fuel supply system for this arrangement was the combination of systems described in (b) and (c), except for the gasoline fuel supply. The methane gas supply system for the whole experiment is shown in Fig.3.1.

3.1.5 Ignition system

This was a variable ignition timing arrangement where the timing could be varied between TDC and 60°BTDC. This was made up of an amplifier unit, an ignition coil and an infra - red trigger unit. The amplifier was powered by a 12 V battery. A commercially available NGK spark plug was used with a gap setting of 0.64 mm.

3.1.6 Tachometer

Both digital and analogue facilities were available and were driven by a pick up from a 50 tooth wheel mounted on the end of the dynamometer.

This tachometer has a measuring range of 0 - 60 rev/s.

3.1.7 Thermocouples

Temperature measurements were accomplished with thermo - couples connected at different points in the engine set - up. The temperatures measured included, ambient, air inlet, cooling water in, cooling water out, fuel and exhaust gas.

3.2 APPARATUS FOR THE COMBUSTION CHAMBER SIMULATION

(refer appendix 2 for detailed specifications)

It was necessary to study the effects of charge motion inside the combustion chamber on the injected methane puff. This determined the process of flame initiation especially with overall lean mixture operation. For visualising these effects, a Schlieren photography method was employed to take records of the methane puff at different periods of time between start of injection and taking of photographs. This necessitated the simulation of the typical charge velocities around the spark plug location. Consequently, hot wire anemometry was used to establish these velocities around the spark plug.

3.2.1 Constant volume bomb arrangement

Because of the practical problems that could arise from using the Ricardo engine combustion chamber for Schlieren photographic work the idea of having a constant volume bomb was conceived. The bomb was made out

of mild steel and has outside dimensions of 130 mm x 130 mm x 140 mm (Plate 3.7). Moreover it has a bore of 76.2 mm, the same size as the Ricardo engine cylinder. A small variable speed D.C motor was mounted at the bottom of the bomb so that its shaft was vertical. This motor was used to rotate a small fan attached on the motor shaft to simulate the velocity field around the spark gap. The base plate of this bomb has provisions for purging the gas remaining inside the bomb and for the electrical connections to the D.C motor. The top cover of the bomb was made in such a way that it accommodates the spark plug and provides a clear view of the spark gap when looked at through the glass windows, inserted on the opposite sides of the bomb. These windows were used as an optical access for the Schlieren photography. The spark plug hole was also used to accommodate the hot wire probe for establishing the required charge velocities around the spark gap, to be used in the later Schlieren photography work.

3.2.2 Schlieren apparatus

The Schlieren technique is used in many areas of science and engineering and enables observation of substances that are colourless, transparent and non - luminous. Such substances are normally impossible to observe by direct visual or normal photographic methods. The technique is based on the gradient of refractive index caused by the varying density across the field under consideration.

Several different types of light source may be used in Schlieren photography; an argon jet light source was used for this research work which

made it possible to take instantaneous photographs of the methane puff. Argon gas for the light source was supplied from a standard gas cylinder. The gas pressure was reduced to 5 cm of water at the light source entry (as recommended in (47)), by using a regulator - restriction valve arrangement.

This apparatus basically comprises two aluminium coated concave mirrors of 150 mm diameter, a knife - edge and a light source. The light from the source is reflected by the first mirror, and passes through the test section. It is then reflected by the second mirror and passes through the knife - edge to form an image on the screen. The location and direction of these mirrors can be adjusted with the appropriate screws incorporated in the mirrors, so that a required range of the test section can be obtained. Similarly the aperture of the knife - edge can also be changed to sharpen the image on the screen, using appropriate screws on the knife - edge.

Furthermore, a delay circuit was employed to produce a time delay between the point of injection and the point of triggering the light source, in order to visualise the position of the methane puff at various time intervals.

Methane gas was supplied to the injector - spark plug assembly mounted on the constant volume bomb from a standard gas cylinder of 170 bar, so that a methane puff was generated around the spark gap. The Schlieren photography arrangement is shown in Plate 3.8.

3.2.3 Hot wire anemometer

A **DISA** hot wire anemometer was chosen to measure the mean velocity and turbulence around the spark gap as it has excellent sensitivity at low velocity, good spatial resolution and is relatively easy to use (Plate 3.9). The hot wire anemometer was operated in the constant temperature mode (33). In this mode a sensor heating current is supplied that varies with the fluid velocity to maintain constant sensor resistance and thus constant sensor temperature.

Since the output voltage of the constant temperature anemometer is a non - linear function of the flow velocity, a **DISA** lineariser was incorporated into the anemometer system. The D.C component of the hot wire signal corresponds to the mean flow velocity and was measured by a D.C voltmeter. Similarly the A.C component of the output signal corresponds to the fluctuating component and this was measured by a r.m.s. voltmeter. An adapter was made to hold the hot - wire probe (Plate 3.10) at the spark plug position in the constant volume bomb set - up. The block diagram showing the hot - wire anemometer velocity measurement system is shown in Fig.3.2.

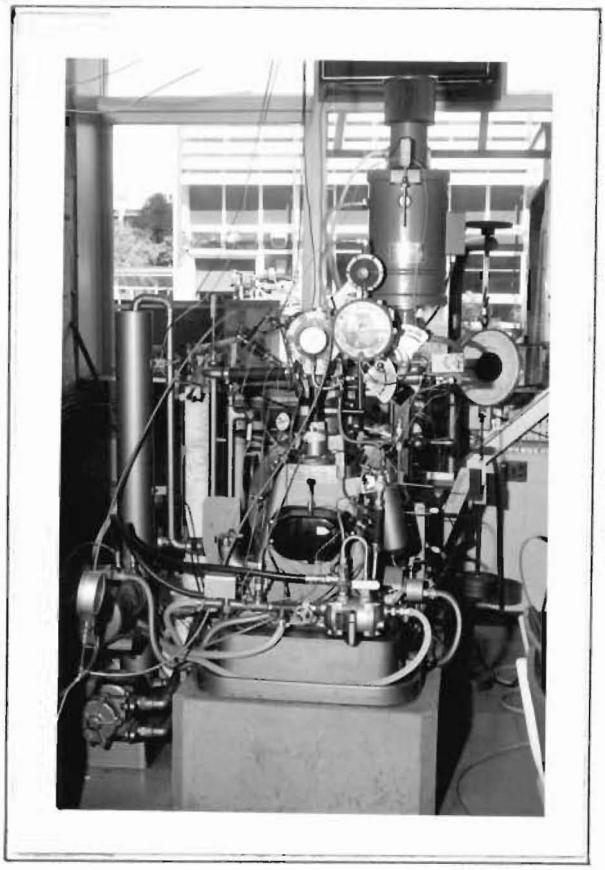

PLATE 3.1 Ricardo E6 variable compression single cylinder engine

PLATE 3.2 Horiba exhaust gas analyser with the sampling tube

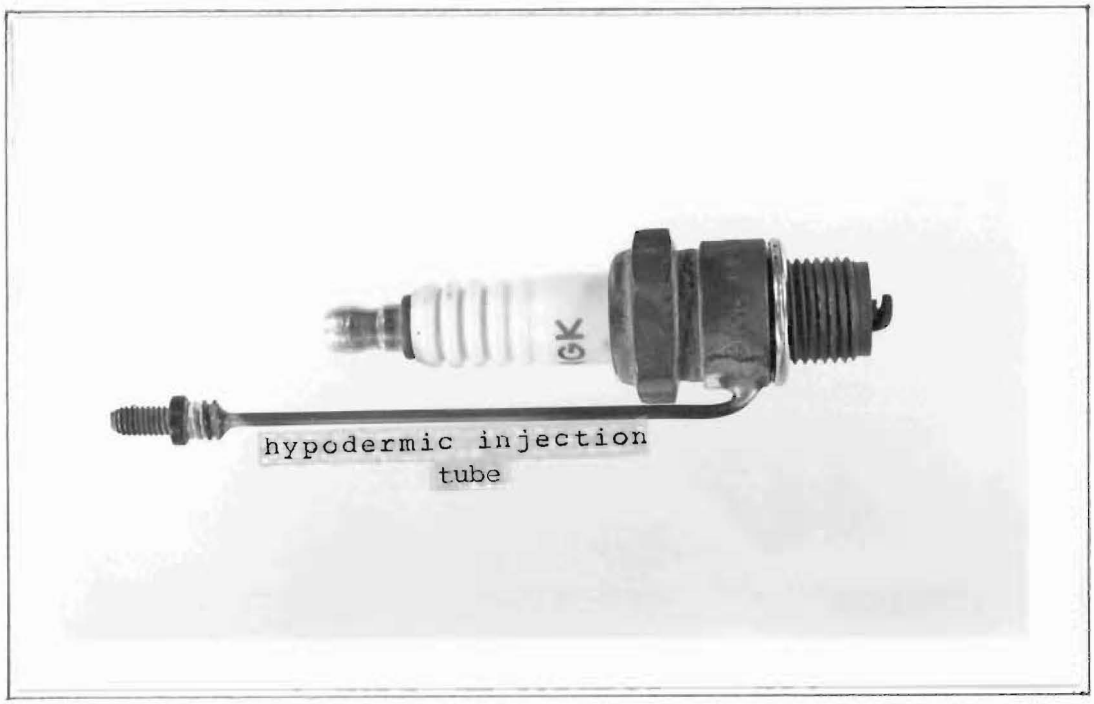

PLATE 3.3 Modified spark plug for stratified charge operation

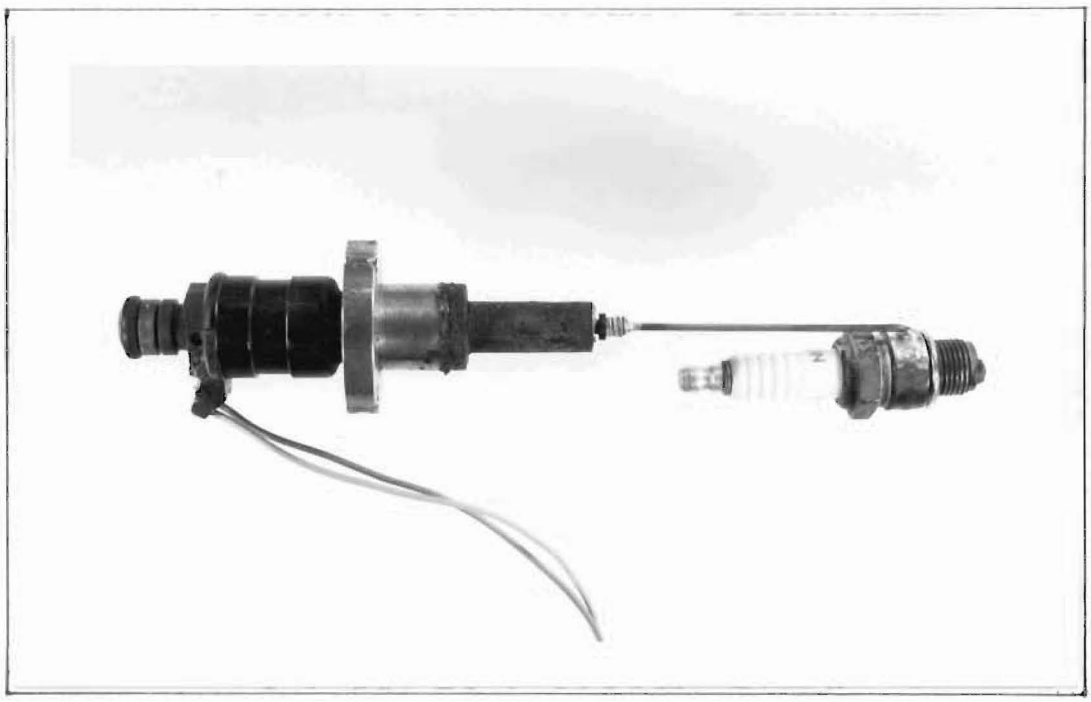

PLATE 3.4 Methane injector - non - return valve - spark plug assembly

PLATE 3.5 Methane injection timing variation arrangement

PLATE 3.6 Methane injection duration control arrangement

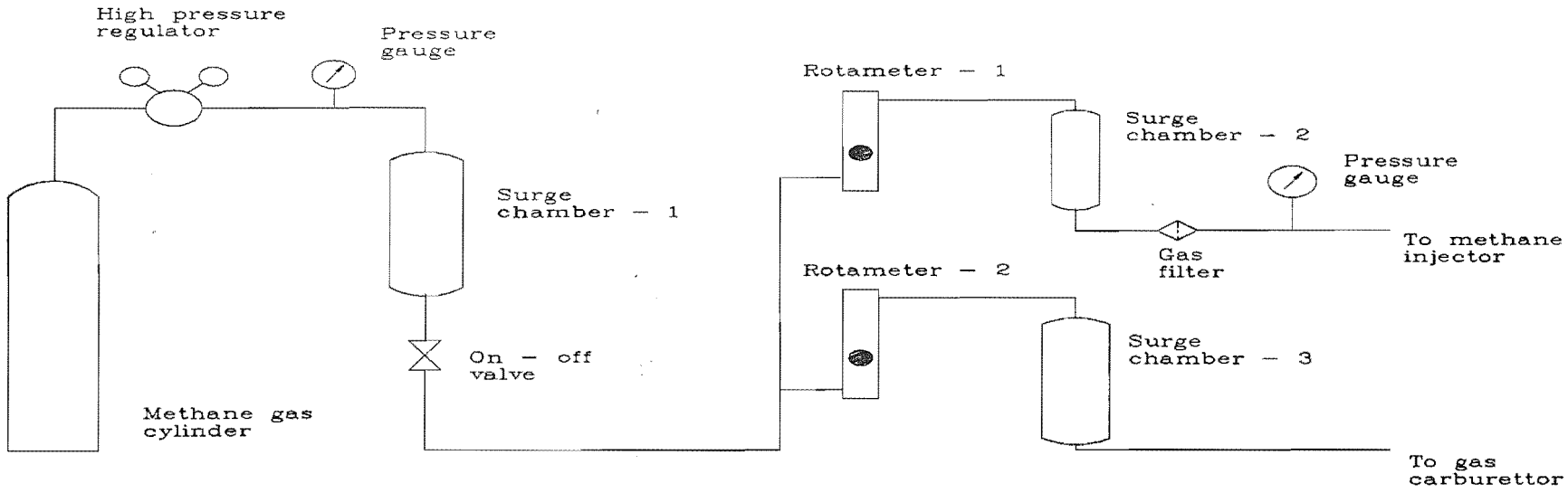

Fig. 3.1 Schematic diagram of the gas supply system

PLATE 3.7 Constant volume bomb set - up

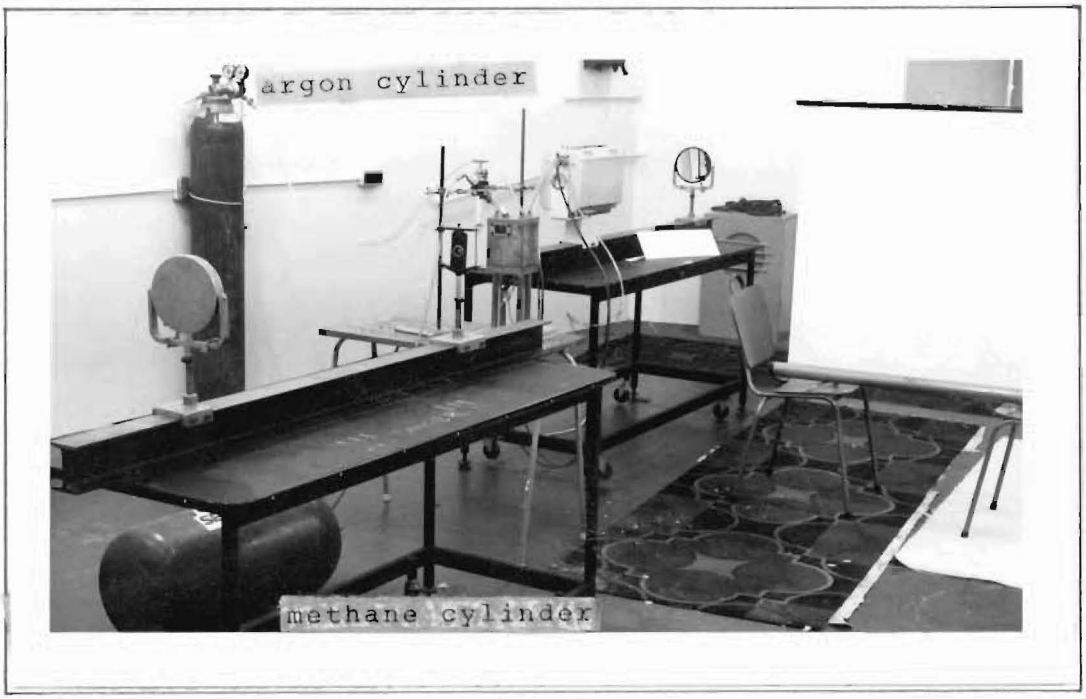

PLATE 3.8 Schlieren photography arrangement

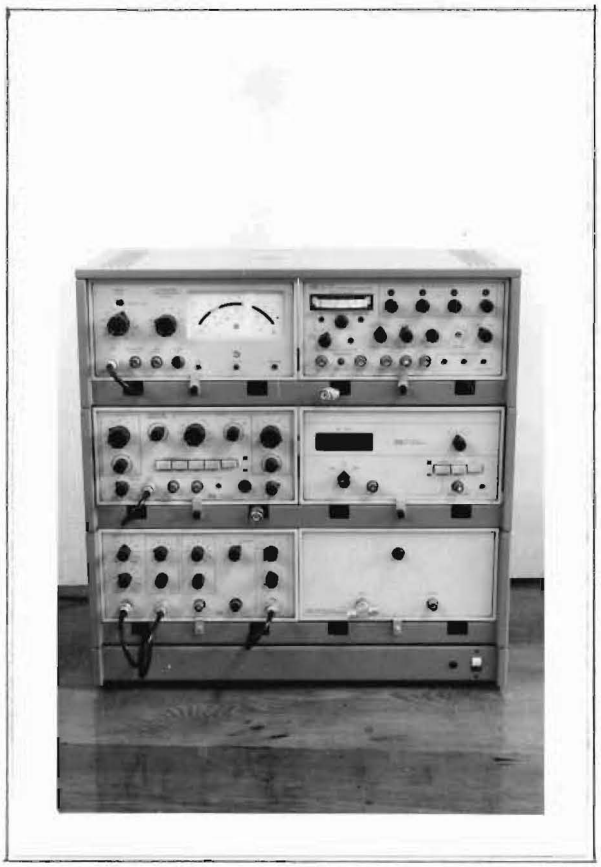

PLATE 3.9 **DISA** 55D01 anemometer unit

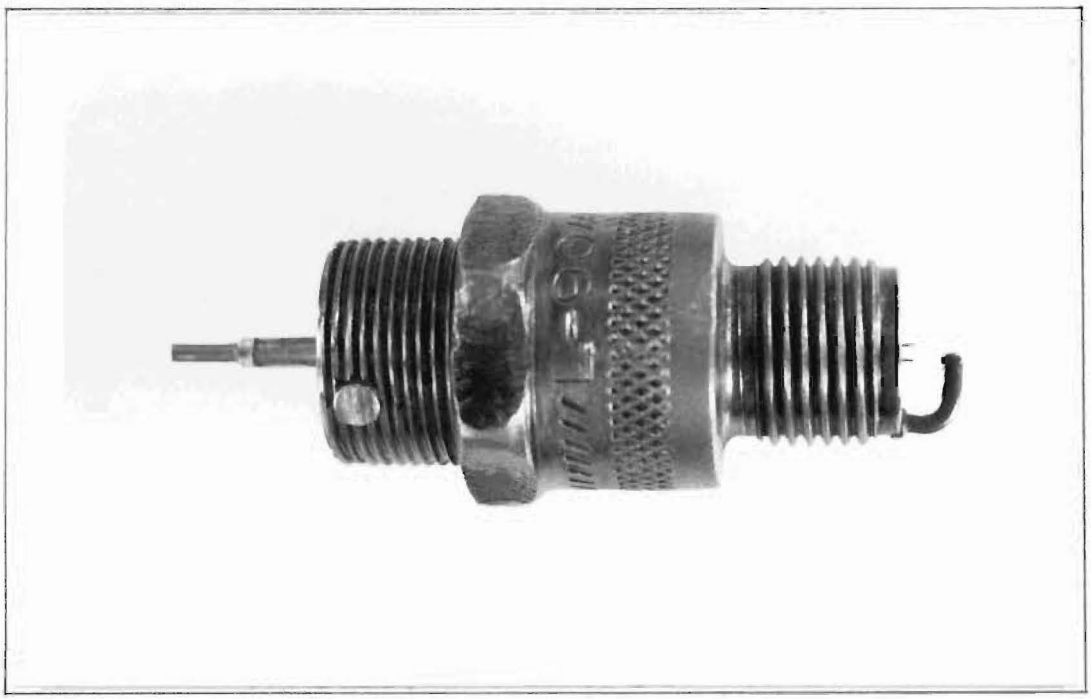

PLATE 3.10 Hot wire probe with the adapter

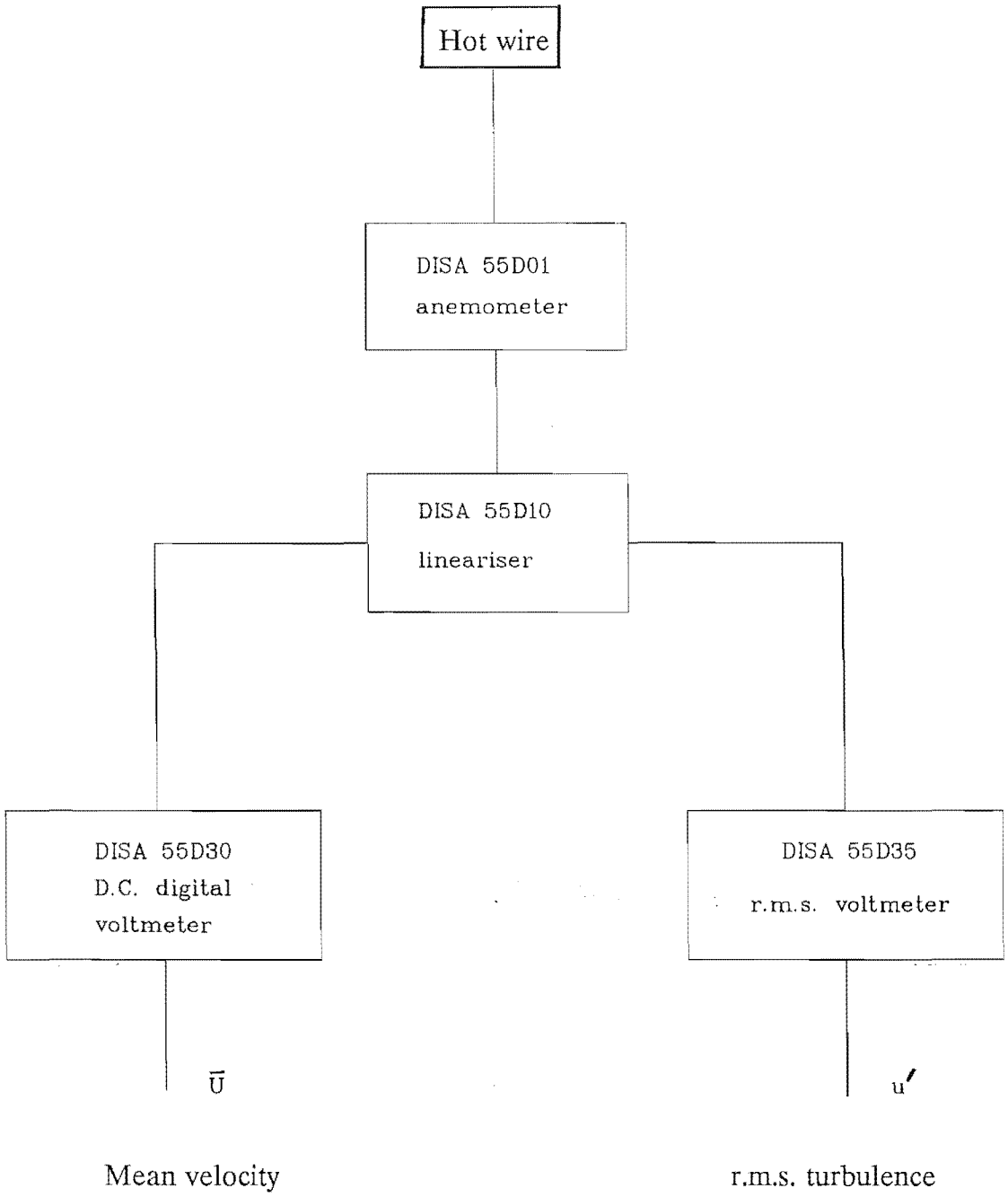

Fig. 3.2 Block diagram of the hot wire anemometer measuring system

CHAPTER 4

EXPERIMENTAL PROCEDURE

The experimental procedure of the present work could be divided into the following sections :-

(1). procedure for the engine combustion experiments

(2). procedure for the combustion chamber simulation

It was envisaged to first conduct the combustion chamber simulation using Schlieren photography and to use these results as a guideline for the engine combustion experiments. However because of unexpected malfunctioning of part of the equipment this order had to be changed. As a result Schlieren photographs were used to verify some of the engine combustion results, instead of using them as a guideline.

4.1 COMBUSTION EXPERIMENTS

4.1.1 Rotameter calibration

A simple method was employed to calibrate the rotameters used in the measurement of the flow rates of methane gas through the spark plug and the gas carburettor. The calibration rig (Fig.4.1) comprised a standard methane gas cylinder, a high pressure regulator, a control valve, a graduated beaker, a container of water and the rotameter to be calibrated. For different methane flow rates at 12 bar, the float position on the rotameter tube scale

and the time taken to displace the known volume of water inside the beaker were recorded. The room temperature and the barometric pressure were also recorded. After correcting these methane flow rates for 12 bar pressure calibration curves at this pressure for each rotameter were plotted as shown in Fig.4.2 and Fig.4.3.

4.1.2 Exhaust gas analyser calibration

The exhaust gas analyser calibration procedure consists of three phases, namely

(1). zero calibration,

(2). span calibration

(3). checker trimmer adjustment

The analyser was warmed up for ten minutes in the **PURGE** mode while the probe was exposed to clean air, before the calibration. For the zero calibration, with the analyser still in the **PURGE** mode, meter readings for HC, CO and CO_2 were set to zero using the **AUTO ZERO** key. Subsequently the span calibration was performed. To accomplish this, the analyser was put in the **STANDBY** mode and a span gas container nozzle was pressed into the span gas inlet on the analyser for 7 - 8 seconds. Next the **SPAN POT** for HC, CO and CO_2 were adjusted to give meter readings as dictated by the span gas composition and the analyser was put in the **PURGE** mode to take the clean air. Finally, with the analyser in the **PURGE** mode and the meter readings of HC, CO and CO_2 set to zero, the checker trimmer was adjusted to give readings of 5000 $\pm$ 150 ppm, 5 $\pm$ 0.14 % vol. and 10 $\pm$ 0.45 % vol.

respectively while the **SPAN CHECK** key was pressed. Further details can be found in the instruction manual (86).

4.1.3 Experimental techniques with the Ricardo engine

The Ricardo engine was warmed up each time before starting the combustion experiments. To quicken the warming up process, an additional water heater was incorporated in the engine set - up. As the cooling water temperature reached around 50°C the engine was turned on. The engine was left running at a required speed until the exhaust temperature reached a steady value and the cooling water temperature approached 70°C. The engine was then considered to be at a steady state and was ready to have the following readings taken for the later performance analysis:-

(1). air inlet temperature

(2). air manometer

(3). spring balance

(4). fuel consumption time

(5). spark timing

(6). exhaust gas species concentrations

All the combustion tests were carried out at the engine speeds of 1000, 1500, 2000 r.p.m unless otherwise stated and the barometric reading was recorded before each set of tests. The accuracy of the exhaust gas analyser was ensured either by performing a quick span check or by re - calibrating with the span gas if necessary.

Since the combustion experiments were carried out in four different configurations, it is appropriate to describe the procedures for each case separately. The stoichiometric composition of the fuels were established with the help of the **Lambda** sensor output voltage signal (Fig. 4.4) and the engine misfire condition was confirmed by monitoring the exhaust hydrocarbon level which had a sharp rise at the onset of misfire.

Unleaded gasoline and 99.6 per cent pure methane gas were used in all the runs whenever the engine had to be fuelled with gasoline and gas respectively. In addition, the temperatures of gasoline fuel, lubricating oil and cooling water were maintained at 20°C, 60°C and 70°C respectively using thermostatic controls, throughout the combustion experiments.

(a). Base line operation with gasoline fuel

At a particular speed the engine was run at wide open throttle (WOT) condition. The gasoline mixture strength was gradually weakened from the stoichiometric proportion by reducing the injected amount of gasoline, until the engine misfired. For each mixture strength the spark timing was adjusted to give the maximum power output (i.e. minimum advance for best torque (MBT) spark setting) and the aforementioned basic readings were recorded. To find the gasoline flow rate, the time taken for 50 ml of gasoline to be consumed by the engine was recorded. Subsequently two more throttle settings (hereafter $WOT_{0.75}$ and $WOT_{0.5}$) were chosen to give approximately 75 per cent and 50 per cent of the brake power values obtained with the WOT setting, at the stoichiometric mixture strength and the

same speed. The engine was run again with the MBT spark setting until it misfired, at $WOT_{0.75}$ and $WOT_{0.5}$ and all the relevant readings were again recorded.

(b). **Charge stratification of a gasoline engine with methane gas**

It can be seen from 3.1.1 (b) that this part of the experiment involved the methane injection through the spark plug in addition to the manifold injection of gasoline fuel. A pressure of 12 bar was chosen to inject the methane gas through the modified spark plug late in the compression stroke for all runs. Apart from the operation with the MBT spark setting, an additional performance optimisation study was undertaken, to examine the effects of the charge stratification process on the gasoline lean limit. However in each set of runs, for a constant methane flow rate, the amount of manifold injected gasoline was gradually decreased until the engine misfired. In addition to the aforementioned basic readings, the methane flow rate through the spark plug was read off from the calibrated rotameter - 1.

(1). **Performance optimisation**

step 1 : the engine was operated over a range of spark timings between 20°BTDC and 50°BTDC whilst the injection timing and the flow rate of the methane gas were held constant. The optimum spark timing was selected on the basis of specific fuel consumption, exhaust emission

(particularly HC emission), lean limit and the range of stable operation.

step 2 : the engine was again operated over a range of injection timings between 40°BTDC and 90°BTDC at the optimum spark timing (from step 1) and for a constant methane flow rate. The optimum injection timing was selected on the basis of aforementioned factors.

step 3 : with the optimum spark timing (from step 1) and the optimum injection timing (from step 2), the engine was operated over a range of methane flow rates. From these results, an optimum point in the operating range was found on the same basis as in the previous steps.

This performance optimisation study was conducted at 1000 r.p.m/WOT and 2000 r.p.m/$WOT_{0.5}$ conditions. For an example, 1000 r.p.m/WOT reads as "at 1000 r.p.m and WOT condition".

(2). Operation with the MBT spark setting

At a fixed methane injection timing the engine was run on three different methane flow rates, while the spark timing was adjusted to MBT for each run. All the relevant readings were recorded. This procedure was repeated for 2000 r.p.m/WOT, 2000 r.p.m/$WOT_{0.5}$, 1500 r.p.m/WOT, and 1500 r.p.m/$WOT_{0.75}$ settings. Injection timing was varied according to the speed.

(c). **Base line operation with methane gas**

To be comparable with the earlier part throttle settings of $WOT_{0.75}$ and $WOT_{0.5}$, two new part throttle settings (hereafter $WOT_{0.75eq}$ and $WOT_{0.5eq}$) with the gas carburettor were selected. These were chosen so that for the same engine speed, the stoichiometric mixture of methane produced the same brake power values as with the stoichiometric mixture of gasoline at $WOT_{0.75}$ and $WOT_{0.5}$ respectively.

The engine was run with the MBT spark setting at WOT, $WOT_{0.75eq}$ and $WOT_{0.5eq}$ settings as the methane gas was carburetted into the engine. The gas mixture was gradually weakened from the stoichiometric proportion until the engine misfired. All the relevant readings (including the methane flow rate through the carburettor read off from the rotameter - 2) were recorded.

(d). **Charge stratification of a methane fuelled engine**

For a fixed methane injection timing the engine was run on three different rates of methane injection through the spark plug, with the MBT spark setting in each case. The carburetted mixture strength was gradually weakened until the engine misfired. This procedure was repeated for 2000 rpm/ WOT, 2000 rpm/ $WOT_{0.5eq}$, 1500 rpm/ WOT, 1500 rpm/ $WOT_{0.75eq}$, 1000 rpm/ WOT settings. All the relevant readings were recorded.

During the course of the charge stratification experiments, the non - return valve and the methane injector were cleaned frequently with **Electrosol M3** evaporating solvent, as there was a continuous deposit of exhaust products

at the valve seat thus allowing exhaust gas to come into contact with the injector needle area.

4.2 COMBUSTION CHAMBER SIMULATION

As mentioned in 3.2, this part of the experiment involved visualisation of the effects of the velocity field on the injected methane puff inside the simulated combustion chamber. Therefore this work was divided into :-

(1). obtaining typical velocity values around the spark gap location corresponding to the various Ricardo engine speeds, from previous works.

(2). establishing the typical velocity field around the spark gap, using the hot wire anemometer system and

(3). visualising the effects of the velocity field on the injected methane puff through Schlieren photography

4.2.1 Hot wire anemometer technique

(a). Hot wire calibration

The hot wire was calibrated by using the TSI calibrator (Plate 4.1) available in the Mechanical Engineering Department. This has three probe locations cascaded in area each with a controlled velocity profile to cover a very wide velocity range from 3 cm/s to Mach 1 (48). The hot wire probe was positioned at the middle calibration range location, during this calibration. By adjusting the pressure regulator and the needle valve on the

calibrator, a few pressure readings in the range of 0.1 - 1 mm water were obtained on the micromanometer. These pressure readings correspond to velocity values in the range of 0 - 3 m/s at the nozzle outlet where the hot wire was positioned perpendicular to the air flow. As a part of the calibration procedure lineariser controls were adjusted so that a linear relationship could be obtained between the range of velocities and the output D.C.voltages of the anemometer (34). This lineariser output was also adjusted in such a way that the output D.C.voltage showed a simple relationship to the velocity. i.e. 1 volt = 1 m/s. These data were recorded and processed by an IBM PC through an analogue - to - digital (A/D) converter, at a sampling frequency of 25 Hz. This procedure was repeated until the intercept of the calibration curve was within±0.3 V which is considered to be the accurate. The typical calibration results are shown in appendix 3.

(b). Velocity field simulation

The variable speed D.C. motor was operated with a D.C. power source. The electric current to the motor was varied so that the fan produced the typical velocity components around the spark gap location. These pre - established velocity values were deduced from the work by Cole et al.(23) for some of the Ricardo E6 engine speeds and resolved into two perpendicular components in the required spark plug plane (Table 4.1). Further, correction to these values were included using the results of Semenov (104) so that reasonable velocity values around the present injection timings could be derived (appendix 4).

The calibrated hot wire probe with the adapter was screwed and sealed with **Loctite** at the spark plug hole on the constant volume bomb, which was filled with air. The position of the hot wire inside the bomb was adjusted so that it was at the same position as the spark gap. The alignment of the hot wire with respect to the mean velocity vector was done by trial and error. This is based on the method (63) where the hot wire probe was rotated to maximise the anemometer output voltage and that direction was assumed to be perpendicular to the mean velocity vector. The speed of the motor was varied so that sets of known velocity components were detected by the hot wire anemometer system. For each case, these analogue signals were recorded and processed by the IBM PC for 500 samples at a sampling frequency of 1000 Hz. This data acquisition system was run with a computer programme called **HWACQ.BAS** with the **QBASIC** compiler and produced the values of mean velocity and turbulent intensity. The corresponding current settings on the D.C.power source were also noted. Consequently a set of data representing typical engine speeds and the corresponding D.C fan current values was obtained (Table 4.2).

4.2.2 Schlieren photography

Schlieren photography was used to capture the positions of the injected methane puff with respect to the spark gap, in the simulated velocity field. The methane injector - modified spark plug assembly was mounted at the spark plug location on the bomb which contained air at atmospheric pressure. The filament lamp (continuous source) incorporated in the argon

light source was switched on to permit the adjustment of the optical system prior to the use of a pulsed light source. The bomb set - up was positioned in such a way that a clear image of the spark gap was formed on a white screen, afterwards the light was reflected onto two concave mirrors and was partly cut off by the knife edge. Subsequently the methane injector was actuated by a D.C.source thus generating a methane puff around the spark gap. To get a clear image of this puff on the screen, the positions of the concave mirrors and the knife edge were adjusted. With this arrangement, a **NIKON** camera without lens was placed in front of the screen and focussed the image on to the film plane. This whole set - up was located inside a completely dark room. Since the appearance of the image ultimately depended on the duration of the pulsed light, it was decided to keep the shutter open until the flash went off. A **400 ASA** film was used for this work and was subsequently push - processed to **1600 ASA** (with a longer processing time of 12 min. at 22° C) using **Microphen** film developer, to allow for very low light intensity at the time of photography.

The D.C.motor was supplied with the pre - established current, in order to produce the required velocity field. Further, the time delay was set to a particular value and the argon pressure at the light source entry was adjusted to 5 cm water. Then the light source was put into the pulse mode and the injector was actuated. The methane puff was then photographed. This procedure was repeated for different velocity fields and different time delays while the gas inside the bomb was purged between each setting, with the compressed air.

During the course of this simulation, the air inside the bomb was at 1 bar. Although this condition did not typify the actual engine combustion chamber values, it is justified, as this present work is very much concerned with the effects of velocity field rather than with absolute values of pressure and temperature which may have some secondary effects on the results. However a reasonable average pressure difference of 4 bar was chosen to inject the methane gas during the Schlieren photography, to be comparable with the injection during engine operation. Therefore the author believes that the possible effects of pressure and temperature on the current work are not substantial enough to affect the final conclusion, eventhough it is not verified in the present work.

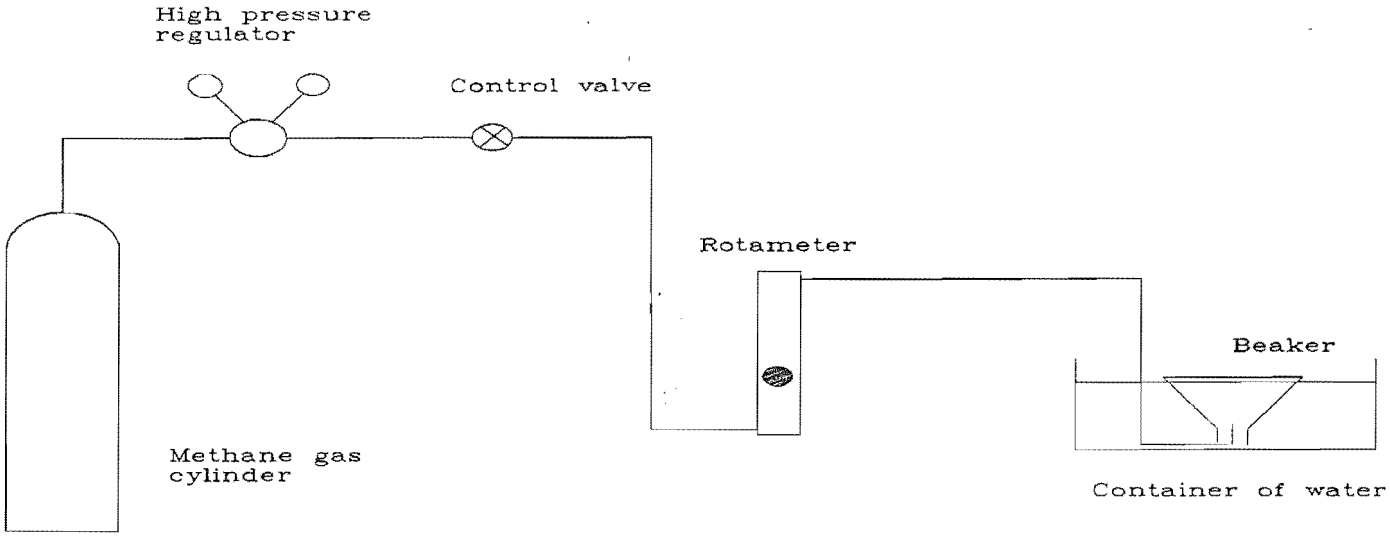

Fig. 4.1 Schematic diagram of the rotameter calibration rig

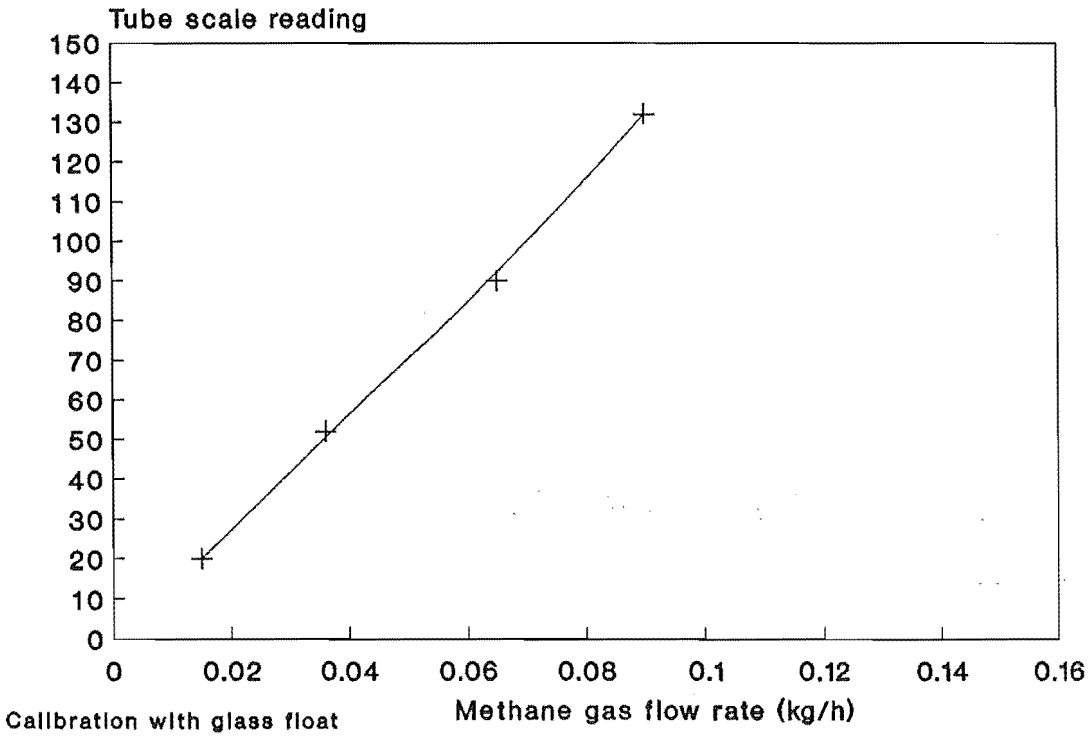

Fig. 4.2 Calibration curve for rotameter - 1 (tube no. 602) at 12 bar and 20°C

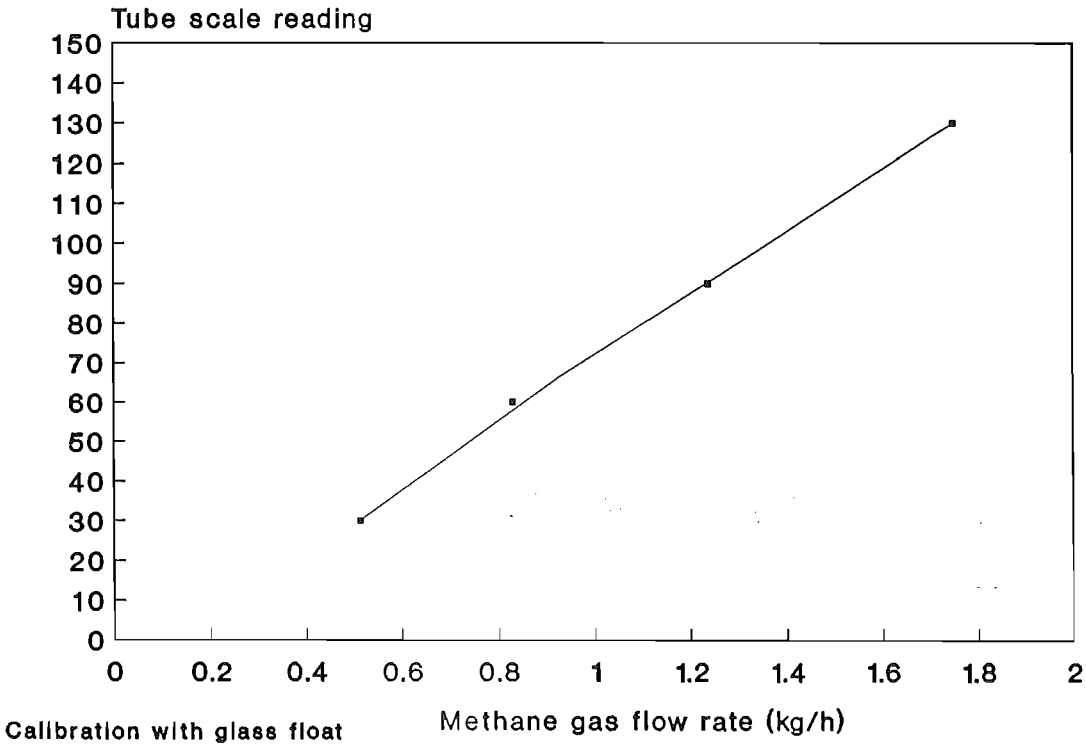

Fig. 4.3 Calibration curve of rotameter - 2 (tube no. 604) at 12 bar and 20°C

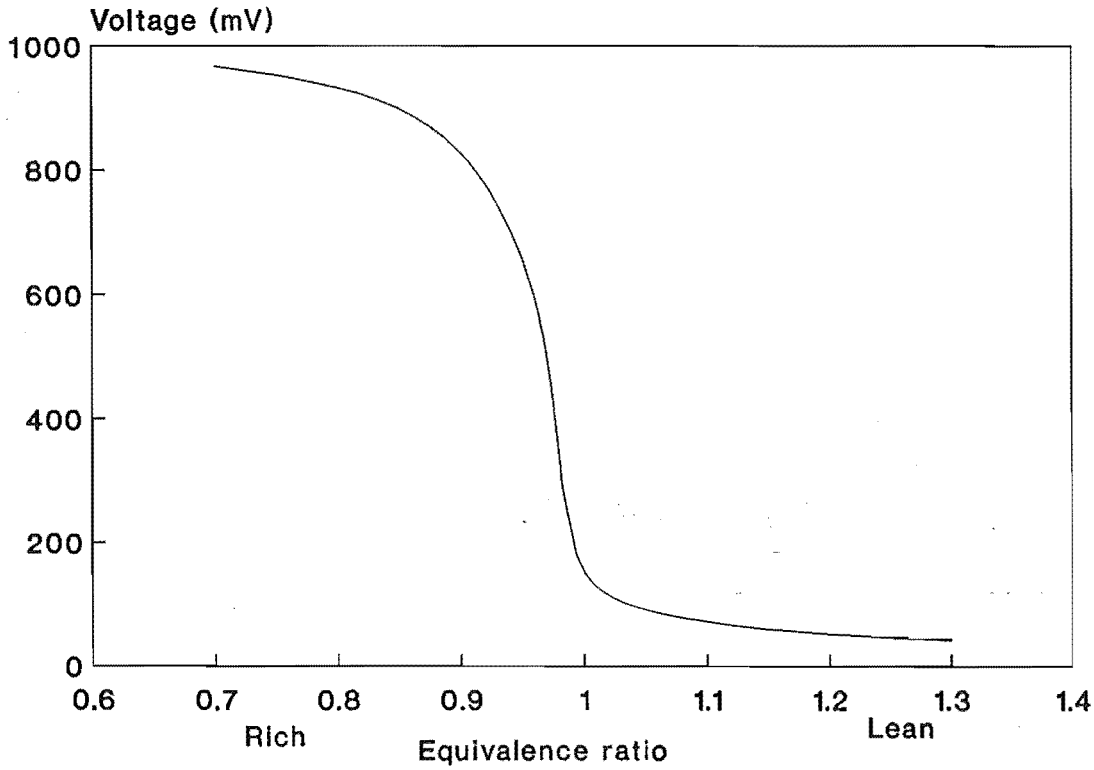

Fig. 4.4 Typical voltage curve of the Lambda sensor

(See Fig. 1.2 for the definition of equivalence ratio and the equivalence ratio of 1 refers to the stoichiometric mixture proportion)

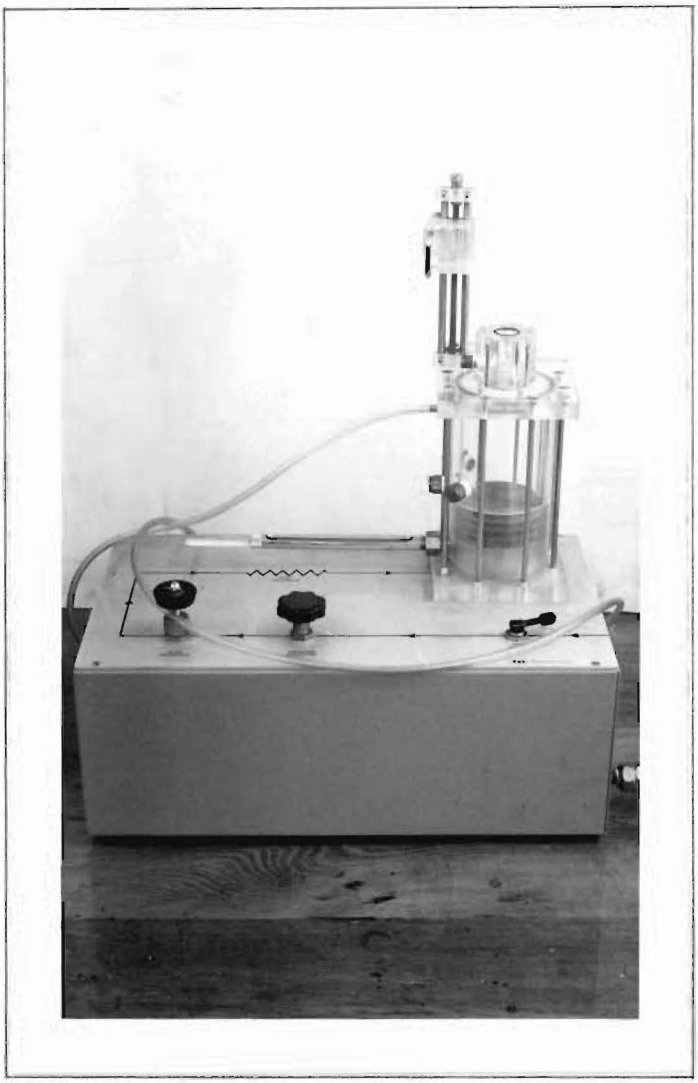

PLATE 4.1 TSI model 1125 calibrator

Engine speed (r.p.m)	Mean velocity (m/s)		r.m.s. turbulence (m/s)	
	X - dir.	Y - dir.	X - dir.	Y - dir.
400	0.398	0.289	-0.299	1.20
600	0.487	0.643	-0.548	1.91
800	0.545	0.863	-0.687	2.729
1000	0.845	1.352	-0.819	3.221
1200	1.067	1.428	-1.302	3.824

TABLE 4.1 Resolved mean and r.m.s. turbulent velocity components in the spark plug plane, in the vicinity of the spark gap. (Spark plug plane is approximately 60° inclined to the plane considered in the work of Cole et al. (23)).

Engine speed (r.p.m)	D.C. fan current settings (mA)
1000	214
1500	258
2000	305

TABLE 4.2 D.C. fan current values representing equivalent Ricardo E6 engine speeds.

CHAPTER 5

DATA ANALYSIS

5.1 NOMENCLATURE

$(A/F)_{ga}$	actual gasoline air - fuel ratio
$(A/F)_{ma}$	actual methane air - fuel ratio
BP	engine brake power (kW)
BP_c	corrected brake power (kW)
C_t	temperature correction factor
L	engine torque (N.m)
$(LCV)_g$	lower calorific value of gasoline (kJ/kg)
$(LCV)_m$	lower calorific value of methane (kJ/kg)
N_e	engine speed (rev/s)
P_a	atmospheric pressure (m Hg)
P_s	standard pressure (m Hg)
R_a	specific gas constant of air (J/kg.K)
S	spring balance reading (N)
T_a	air temperature (K)
T_s	standard temperature (K)
$\bar{U}$	mean velocity (m/s)
V_{ae}	volumetric air flow rate (m^3/h)

V_{as}	volumetric air flow rate at P_s and T_s (m^3/h)
bsfc	brake specific fuel consumption (kg/kW h)
g	gravitational acceleration (m/s^2)
l	manometer reading (mm)
m_{as}	mass flow rate of air at P_s and T_s (kg/h)
m_g	mass flow rate of gasoline (kg/h)
m_{geq}	equivalent gasoline mass flow rate to m_{mp} (kg/h)
m_{mc}	mass flow rate of methane through the gas carburettor (kg/h)
m_{mp}	mass flow rate of methane through the spark plug (kg/h)
n_b	number of dynamometer load weights each of 20 N.
n_s	number of samples
t_g	time taken for 50 ml. of gasoline to be consumed by the engine (s)
u_i	instantaneous velocity of i^{th} sample (m/s)
u'	turbulence intensity (m/s)
λ_g	equivalence ratio of gasoline
λ_m	equivalence ratio of carburetted methane
η_b	brake thermal efficiency (%)
ρ_{as}	density of air at P_s and T_s ($kg/m^{3)}$
ρ_{Hg}	density of mercury (kg/m^3)

5.2 COMBUSTION EXPERIMENTS

5.2.1 Equations for basic engine combustion data analysis

(1). Calculation of air flow rate

For the Alcock viscous flow meter,

According to (85),

$$V_{ae} = 0.000077 \times l \times C_t \times 3600 \tag{5.1}$$

$$V_{as} = \frac{V_{ae} \times T_s \times P_a}{T_a \times P_s} \tag{5.2}$$

$$\rho_{as} = \frac{P_s \times \rho_{Hg} \times g}{R_a \times T_s} \tag{5.3}$$

$$m_{as} = V_{as} \times \rho_{as} \tag{5.4}$$

(2). Calculation of gasoline flow rate

$$m_g = \frac{50 \times 0.75 \times 3600}{t_g \times 1000} \tag{5.5}$$

(3). Calculation of engine torque

From the Ricardo engine instruction manual (98),

$$L = \{ (20 \times n_b) - S \} \times 0.457 \tag{5.6}$$

Where the radius of the torque arm is 0.457 m.

(4). **Calculation of engine brake power**

According to (98),

$$BP = \frac{L \times N_e}{0.457 \times 348.1} \tag{5.7}$$

(5). **Corrected engine brake power**

When the test conditions differ from those standard conditions (760 mm Hg, 20°C) engine power has to be corrected to provide a common basis for comparison of engine performance.

From **Bosch** automotive handbook (14),

$$BP_c = BP \times \frac{760}{P_a} \times \sqrt{\frac{T_a}{293.15}} \tag{5.8}$$

(6). **Brake specific fuel consumption**

(a). **Base line operation with gasoline fuel**

From the basic definition,

$$bsfc = \frac{m_g}{BP} \tag{5.9}$$

(b). **Charge stratification of a gasoline engine with methane gas**

Since this process involved dual - fuel operation, an equivalent gasoline flow rate to the methane flow rate through the spark plug was determined.

$$m_{geq} = m_{mp} \times \frac{(LCV)_m}{(LCV)_g} \tag{5.10}$$

therefore,

$$bsfc = \frac{(m_g + m_{geq})}{BP} \tag{5.11}$$

(c). **Base line operation with methane gas**

Again by definition,

$$bsfc = \frac{m_{mc}}{BP} \tag{5.12}$$

(d). **Charge stratification of a methane fuelled engine**

By considering methane fuel flow through both spark plug and carburettor,

$$bsfc = \frac{(m_{mc} + m_{mp})}{BP} \tag{5.13}$$

(7). **Brake thermal efficiency**

(a). **Base line operation with gasoline fuel**

$$\eta_b = \frac{BP \times 3600}{m_g \times (LCV)_g} \times 100 \tag{5.14}$$

(b). Charge stratification of a gasoline engine with methane gas

$$\eta_b = \frac{BP \times 3600}{(m_g + m_{geq}) \times (LCV)_g} \times 100 \qquad (5.15)$$

(c). Base line operation with methane gas

$$\eta_b = \frac{BP \times 3600}{m_{mc} \times (LCV)_m} \times 100 \qquad (5.16)$$

(d). Charge stratification of a methane fuelled engine

$$\eta_b = \frac{BP \times 3600}{(m_{mc} + m_{mp}) \times (LCV)_m} \times 100 \qquad (5.17)$$

(8). Air - fuel ratio

(a). Base line operation with gasoline fuel

$$(A/F)_{ga} = \frac{m_{as}}{m_g} \qquad (5.18)$$

(b). Charge stratification of a gasoline engine with methane gas

Since methane gas was injected through the spark plug just prior to ignition, it was assumed that it did not have sufficient time to become thoroughly mixed with the available air and consequently it ignited close to the rich limit of flammability.

Air required for methane combustion at limit of flammability =

$$m_{mp} \times 10.27 \tag{5.19}$$

Where the air - fuel ratio (mass basis) at the rich flammability limit of methane is 10.27.

Air available for gasoline combustion =

$$\{ m_{as} - (m_{mp} \times 10.27) \} \tag{5.20}$$

therefore,

$$(A/F)_{ga} = \frac{(m_{as} - m_{mp} \times 10.27)}{m_g} \tag{5.21}$$

(c). **Base line operation with methane gas**

$$(A/F)_{ma} = \frac{m_{as}}{m_{mc}} \tag{5.22}$$

(d). **Charge stratification of a methane fuelled engine**

The assumption that was made in 8(b) is also applicable in this case and provide a similar condition for performance analysis.

therefore,

$$(A/F)_{ma} = \frac{(m_{as} - m_{mp} \times 10.27)}{m_{mc}} \tag{5.23}$$

(9). Equivalence ratio

(a). Gasoline

$$\lambda_g = \frac{(A/F)_{ga}}{14.8} \tag{5.24}$$

(b). Carburetted methane

$$\lambda_m = \frac{(A/F)_{ma}}{17.2} \tag{5.25}$$

Where the stoichiometric ratios (mass basis) of regular unleaded gasoline and methane gas are 14.8 and 17.2 respectively. Moreover $\lambda > 1$ refers to lean mixture conditions.

5.3 COMBUSTION CHAMBER SIMULATION

5.3.1 Hot wire data acquisition system

(1). Mean velocity

$$\overline{U} = \frac{\Sigma u_i}{n_s} \tag{5.26}$$

Where i = 1...n_s

(2). Turbulence intensity

$$u' = \sqrt{\frac{\Sigma (u_i - \overline{U})^2}{(n_s - 1)}} \tag{5.27}$$

Where i = 1...n_s

CHAPTER 6

RESULTS AND DISCUSSION

6.1 GENERAL

If the air - fuel ratio of the supplied mixture to an engine cylinder is increased, a limit is reached at which the mixture fails to burn every cycle due to failure of flame initiation (97) or failure to sustain flame propagation (41). This air -fuel ratio limit is known as lean limit or misfire limit. As discussed in Chapter 1, amongst the factors that influence the lean limit, mixture motion is one of the most important in practical situations like engine combustion chambers. Although Chapter 1 deals primarily with pre - mixed homogeneous charge engines, the effect of mixture motion on stratified charge combustion is also well understood.

It was shown in Chapter 2 that amongst the forms of air motion usually encountered in engine combustion chambers, swirl has the dominant influence on the performance of stratified charge engines (94,110), although turbulence plays the role of local mixing, an important factor in the flame initiation phase. In addition, it was shown that after fuel injection, because of the air motion there is a possibility of forming very lean mixture regions which are too lean to support combustion of the fuel mixture. This results in excessive HC emissions due to volume quenching (50,60). Similarly formation of over - rich fuel mixture in some regions of the combustion field is thought

to be the cause of excessive CO emissions (82,111).

Although flame propagation rates with stratified charge mixtures were generally higher than those with quasi - homogeneous condition, as observed by Karim et al.(56), flame propagation in stratified mixtures are not supported so much by the convective mass transfer of active species into unburnt mixture because of the higher flame temperature in stratified charge mixture. This will result in flame velocities which will not differ too greatly from the quasi - homogeneous values. Further it was shown through mathematical modelling (109) that although initial heat release rates with stratified charge combustion is higher compared to the homogeneous case, flame speed dropped abruptly as the flame moved into exceedingly lean mixtures.

Overall it has been shown that with stratified charge combustion it is possible to burn very lean fuel mixtures compared to its homogeneous counterpart because of its unique flame initiation phase which is of prime importance for the subsequent combustion process.

6.2 EXPERIMENTAL RESULTS

All the results presented in this chapter, using the Ricardo E6 research engine, were obtained at MBT spark timing and a compression ratio of 7:1 unless otherwise stated. The equivalence ratio of a fuel mixture is defined as the ratio of actual air - fuel ratio to the stoichiometric air - fuel ratio and consequently an equivalence ratio greater than one is considered as a lean mixture. HC emission is discussed on a concentration basis and measured in terms of n - hexane equivalent.

6.3 PERFORMANCE OPTIMISATION STUDY

Tests were initially conducted to ensure that the use of the modified spark plug to enable stratification of the charge would work in the Ricardo E6 engine.

Upon injection of methane gas around the spark plug electrodes, a methane puff forms in that locality. Subsequently this methane puff mixes with the available air and forms an ignitable mixture at the interface between the methane puff and the lean mixture in the combustion chamber, thus producing a stratified charge condition. To ensure successful flame initiation, this abovementioned interface should be close to the spark plug electrodes, at the time of ignition. The mixture motion inside the engine cylinder is responsible for positioning the ignitable interface at the spark plug electrodes. Hence a certain time interval exists between methane injection and ignition of the ignitable interface. As the time interval between methane injection and ignition increases the aforementioned interface would move away from the spark plug electrodes due to prevailing velocity field and could not be resulted in a good flame initiation. Because pure methane is injected into the engine cylinder it is expected that once ignition takes place the remainder of the methane puff will burn with conditions close to the rich flammability limit. Initial results were most encouraging but optimisation of the system was required before detailed experimentation could be carried out.

To examine the effects of charge stratification on the combustion process, it was decided to undertake performance optimisation studies at two

different engine speed - throttle setting combinations. As mentioned in Chapter 4, the optimum condition for each set of engine tests determined by the following factors, namely

(1). brake specific fuel consumption

(2). exhaust HC emission

(3). lean limit of combustion

(4). range of stable operation

The optimisation process was divided into optimising three engine operating parameters, namely

(1). spark timing optimisation

(2). methane injection timing optimisation

(3). methane injection rate/duration optimisation

Performance optimisation was carried out in the same order as shown above. As a common practice, during the optimisation of one parameter the other two parameters were kept constant.

6.3.1 Optimisation at 1000 r.p.m and WOT

(a). Spark timing optimisation

This part of the optimisation involved operating the engine with different spark timings, over a range of gasoline equivalence ratios (refer Chapter 5 for the definition of the gasoline equivalence ratio) while keeping the methane injection timing (50°BTDC) and the methane injection rate constant as shown in Figs.6.1 and 6.2. It should be noted that for a given engine speed the methane injection rate was solely controlled by the methane

injection duration (10 ms in this case).

As the spark timing was advanced from 20° to 40° BTDC, the lean limit and bsfc moved in a favourable direction. This is generally in agreement with homogeneous charge operation. The reason for this particular effect in this case could be that at an advanced spark timing since the position of the interface between a compact methane puff and the lean gasoline mixture (hereafter referred as "interface") is close to the spark plug electrodes, at the time of ignition, flame initiation should have occurred under suitable ignition conditions.

But at retarded spark timing, because of the longer time interval between methane injection and ignition, a greater quantity of methane fuel is injected. In addition to the displacement of interface away from the spark gap, the flame must also burn through a larger volume of rich mixture. This initial phase of richer combustion may not be effective, as with the advanced spark timing for subsequent burning of lean gasoline mixture. Mizutani et al. (77) have observed that because of the longer period between injection of light oil and combustion, there was a loss of fuel droplets and consequently this could have an effect on burning of lean mixtures.

In addition, Dent et al.(32) have shown that for a disc type combustion chamber turbulence level at the spark plug location decreased steadily during the compression stroke. But it is well known that turbulence plays an important role in the local mixing of fuel and air and is one of the factors influencing the initial flame development phase. Therefore it could be said that turbulence at retarded spark timing did not promote the initial flame

development process to the degree, that it did with advanced spark timings. This seems to be in agreement with Pitt et al.(95) who have concluded that turbulent diffusion dominates the early stages of the puff - jet ignition process.

The initial stage of combustion has an influence on the subsequent flame propagation (21,57,91). Therefore it is possible that factors discussed above could have affected burning of lean gasoline mixtures at retarded spark timing for the given operating conditions.

On the other hand as the spark timing was retarded towards TDC an increase in the range of knock free operation was observed. In the case of HC emission 25°BTDC spark timing gave the lowest emission for most of the operating range as shown in Fig.6.2. This could be due to the higher exhaust temperatures with the retarded spark timings. However as the mixture becomes much leaner because of stratified charge combustion, advanced spark timing gave lower HC emission but reduced the operating range. In contrast, despite the higher exhaust temperatures, increase in HC emission was observed with 20° BTDC spark timing compared to 25°BTDC spark timing. This may be due to a relatively richer flame initiation condition at this much retarded spark timing.

Furthermore, for the given injection timing (50°BTDC) and injection duration (10 ms), unburnt and/or partially burnt charge will be forced into the hypodermic injection tube as a result of increasing combustion pressure. Consequently this portion of the charge will become quenched inside the hypodermic injection tube (hereafter referred as "quenching") and released during the expansion and subsequent exhaust stroke. This will result in an

increase in HC emission. Calculation of quench distance is shown in appendix 5. As spark timing is advanced, the resulting high combustion pressure will result in even higher level of HC emission. From these observations 25°BTDC was chosen as the optimised spark timing for the next stage of injection timing optimisation.

(b). Methane injection timing optimisation

This part of the optimisation involved operating the engine with different methane injection timings over a range of gasoline equivalence ratios at 25°BTDC spark timing and methane injection duration of 10 ms. The relevant results are shown in Figs.6.3 and 6.4. Although there is not much difference in bsfc values, with 40°BTDC injection timing a little favourable displacement in the lean limit was achieved. Since this was the injection timing closest to the ignition timing compared to the other two settings, flame initiation for this case could have occurred in a favourable environment as noted earlier.

In practice there was not much difference in the operating range in terms of gasoline equivalence ratios for all three injection timings eventhough a limited range is shown for 40°and 70°BTDC in Figs.6.3 and 6.4. However the HC emission with the 50°BTDC injection timing was lower than with the other two injection timings. For the given spark timing (25°BTDC) and injection duration (10 ms), at 40°BTDC injection timing the possibility exists that near pure methane or rich methane - air mixture could be forced back into the hypodermic injection tube under combustion pressure. Consequently

this portion of charge will become quenched and released during expansion and subsequent exhaust stroke. This will result in an increase in HC emission. But in the case of 70° BTDC injection timing, due to longer time interval between methane injection and ignition the flame could have initiated and initially burn in a very rich mixture environment and this could have resulted in relatively higher HC emission than it did with 50° BTDC injection timing.

From these observations 50° BTDC injection timing was chosen with 25° BTDC spark timing for the next part of the optimisation process.

(c). Methane injection rate/duration optimisation

As mentioned earlier for a given engine speed the methane injection rate was governed solely by the injection duration. This was accomplished by an electronic timing device which was designed to give a maximum injection duration of 10 ms (refer Section 3.1).

This optimisation involved operating the engine with three different methane injection rates (which corresponded to 8 ms, 9 ms and 10 ms of injection duration respectively) at 25° BTDC spark timing and 50° BTDC injection timing over a range of gasoline equivalence ratios as shown in Figs.6.5 and 6.6. For these given conditions the lowest of the injection durations tested (i.e. 8 ms) gave an advantage in extending the lean limit.

Again the same injection duration of 8 ms resulted in lower HC emission compared to other injection durations. At reduced injection rate (i.e. low injection duration) the level of HC emission is lower than that of the

higher injection rates due to following reasons. They include :-

(1). the mixture at the lower injection rate is leaner overall

(2). the amount of methane gas quenched inside the hypodermic injection tube will be less

6.3.2 Optimisation at 2000 r.p.m and part throttle ($WOT_{0.5}$)

(a). Spark timing optimisation

The engine was operated for different spark timings over a range of gasoline equivalence ratios, while keeping the methane injection timing (70°BTDC) and a reduced methane injection rate or duration (6 ms) constant as shown in Figs. 6.7 and 6.8. This shorter injection duration was necessary at the engine speed of 2000 r.p.m to maintain an acceptable crank angle duration period.

Again it can be seen that as the spark timing was advanced, the lean limit and bsfc values generally moved in a favourable direction. This could also be explained on the basis of flame initiation condition as discussed in Section 6.3.1. However the lean limit did not improve much with advanced spark timings as it did with 1000 r.p.m/ WOT condition, perhaps because of an increased amount of residual gas prevailing at the time of ignition, due to increased throttling.

Retarded spark timings resulted in low HC emissions, possibly due to higher exhaust temperatures. However as the mixture became much leaner, because of stratified charge combustion low HC emission resulted even with advanced spark timing. The increased level of HC emission with advanced

spark timing, at relatively rich mixtures could be due to gas become quenched inside the hypodermic injection tube as explained in Section 6.3.1. From these observations 40°BTDC spark timing was chosen as the value for injection timing optimisation.

(b). Methane injection timing optimisation

This process involved operating the engine with different methane injection timings over a range of gasoline equivalence ratios, at 40°BTDC spark timing and a methane injection duration of 6 ms, as shown in Figs.6.9 and 6.10. The lean limit at 70°BTDC injection timing was slightly richer than those at the other two time settings. This may be because the time interval between injection and ignition at this high speed was so small for the given operating condition that not enough methane gas would have been present within the spark gap by the time of ignition, consequently affecting the flame initiation phase.

In the case of 70°BTDC injection timing which was the closest to the spark timing (40°BTDC) compared to the other two settings again have resulted in higher HC emission due to the "quenching" effect as noted in Section 6.3.1 and possibly because of the poor flame initiation as noted above. But in the case of 90°BTDC injection timing, in addition to the displacement of the interface away from the spark gap because of a relatively longer time between injection and ignition combined with the expected higher flow velocities (at 2000 r.p.m) around the spark gap, the initial burning will have occurred in a richer mixture environment that results in higher HC emission.

The effect of this condition on the flame initiation is shown in Fig.6.10, as the mixture becomes leaner HC emission for 90°BTDC injection timing increases compared to the 80°BTDC injection timing.

From these results, 80°BTDC injection timing was chosen with 40°BTDC spark timing for the methane injection duration optimisation.

(c). Methane injection rate/duration optimisation

This part of the optimisation involved operating the engine with three different methane injection rates (which corresponded to 5 ms, 6 ms and 7 ms of injection durations respectively) over a range of gasoline equivalence ratios, at 40°BTDC spark timing and 80°BTDC injection timing, as shown in Figs.6.11 and 6.12.

The injection rate corresponding to 6 ms gave an advantage in the bsfc values and in extending the lean limit. Further higher injection rate will result in an increase in HC emission, due to following reasons :-

(1). the mixture at higher injection rates is richer overall

(2). the amount of methane gas quenched inside the hypodermic injection tube will be high

Although this implies that the lowest injection rate (corresponding to 5 ms of injection duration) should have resulted in lower HC emissions, it is suspected that the increased level of residual gas at the greater throttle setting is the cause of higher HC at this injection rate, at leaner equivalence ratios.

6.3.3 Summary of optimisation study

The following table shows a few optimised values of operating parameters that have been obtained during the performance optimisation. Further, the injection timing/duration shown in this table refers to the methane injection through the modified spark plug for charge stratification purpose.

Operating condition	Spark timing (BTDC)	Injection timing (BTDC)	Injection duration (rate) [ms (kg/h)]
1000 r.p.m/WOT	25°	50°	8 (0.05)
2000 r.p.m/$WOT_{0.5}$	40°	80°	6 (0.08)

6.4 ENGINE COMBUSTION EXPERIMENTS AT MBT SPARK SETTING

This part of the experiment was primarily involved with comparing normal homogeneous charge operation (i.e. base line operation) with stratified charge operation. Although a number of combinations of operating condition could be found, for simplicity, charge stratification experiments were confined to a limited range of operating conditions which will be discussed below. Furthermore base line operation is indicated as "**no methane injection**" in the corresponding figures. In addition the brake power (BP) of the engine was corrected to standard atmospheric conditions for the purpose

of comparing engine performances obtained at different ambient operating conditions.

6.4.1 Charge stratification of a gasoline fuelled engine

(a). 2000 r.p.m and WOT condition

To obtain a reasonable charge stratification, the time interval between methane injection and ignition, as governed by the engine speed, plays an important role. Therefore, from the earlier optimisation study for 2000 r.p.m case, an injection timing of 80° BTDC was chosen for this operating condition. The engine was operated with three different methane injection rates and 80° BTDC injection timing, for stratified charge operation. The corresponding results are shown in Figs. 6.13 to 6.16.

There is a general improvement in the gasoline lean limit equivalence ratio with stratified charge operations compared to base line operation (i.e. a shift from 1.35 to 1.47). Although bsfc values are not very favourable with stratified charge combustion in the early part of the operating range, as the mixture becomes leaner (i.e. at higher gasoline equivalence ratios) the effect of charge stratification is well pronounced, especially with the lowest injection rate of 0.064 kg/h (Fig.6.13). This could be due to the fact that the burning of lean mixtures depends very much on the flame initiation phase which is unique with the charge stratification process. A similar trend was observed by Mizutani et al.(77), who have shown that charge stratification through light oil injection was more effective for lean mixture ratios. In addition Pitt et al. (95) have also shown that at stoichiometric mixture ratio there was no

difference in the nature of the combustion between normal spark gap firing and stratified charge combustion through a puff - jet device, in terms of ignition delay. However at lean mixture equivalence ratios there was a marked difference in the combustion process in favour of the stratified charge combustion. But the higher methane injection rates which corresponded to higher injection durations have resulted in higher bsfc values, because of the richer overall mixture as noted earlier.

The brake power (BP) of the engine with stratified charge operation is still comparable with the base line operation, and in some cases even higher as the mixture becomes leaner (Fig.6.14).

In the case of HC emission, stratified charge operation has resulted in higher values when compared to the base line operation (Fig.6.15). The reason for this observation could be the condition at which combustion was initiated, which is assumed to be the rich flammability limit of methane gas. In addition, quenching of unburnt and/or partially burnt charge inside the hypodermic injection tube could also cause an increase in HC emission with stratified charge operation. Further higher methane injection rates have resulted in high HC emission values, perhaps due to the richer overall mixture.

CO emission is almost the same as or a little lower with stratified charge operation than with base line operation as the mixture becomes leaner, indicating better combustion with charge stratification at lean mixture ratios (Fig.6.16).

(b). **2000 r.p.m and part throttle condition** ($WOT_{0.5}$)

Since the engine was operated at the same speed as in 6.4.1.(a), the same injection timing of 80° BTDC was also chosen in this case, for the same reason. The engine was operated with the same three methane injection rates and injection timing as in the case of 2000 r.p.m/ WOT. The corresponding results are shown in Figs. 6.17 to 6.20.

Again an improvement in the gasoline lean limit equivalence ratio is found with stratified charge operation compared to base line operation (i.e. a shift from 1.22 to 1.28) as in the previous case. However the shift in the lean limit is less compared to 2000 r.p.m / WOT condition, possibly because of the existing residual gas inside the combustion chamber at an increased throttling. Further the effectiveness of stratified charge combustion can be seen at lean gasoline equivalence ratios in terms of bsfc values (Fig.6.17) as in the previous case.

BP values with stratified charge combustion are still comparable with base line operation and even greater as the mixture becomes leaner (Fig.6.18).

Again the HC emission is higher with stratified charge operation than with base line operation (Fig.6.19). This could be because of the prevailing amount of residual gas and the reasons stated in the previous case.

As the mixture becomes leaner, CO emission is almost the same or little lower with stratified charge operation than with base line operation (Fig.6.20).

(c). 1500 r.p.m and WOT condition

As no optimisation study was undertaken at 1500 r.p.m, a mean value of 65°BTDC injection timing was taken from the optimised injection timings at 1000 r.p.m (50°BTDC) and 2000 r.p.m (80°BTDC). The engine was operated with three different injection rates and 65°BTDC injection timing, for stratified charge operation. The corresponding results are shown in Figs.6.21 to 6.24.

Gasoline lean limit equivalence ratio has increased from 1.34 to 1.43 with stratified charge operation compared to the base line operation. bsfc values with stratified charge operation are lower than with base line operation at lean equivalence ratios, again indicating the effectiveness of charge stratification at lean mixture ratios (Fig.6.21).

Brake power (Fig.6.22) and CO emission (Fig.6.24) show a rather similar trend, especially at the lean equivalence ratios, as in the previous cases.

In the case of HC emission (Fig.6.23), stratified charge operation has again resulted in higher values than with base line operation, for the same reasons stated in 2000 r.p.m / WOT condition. However the difference in emission values between these two modes of operation seem to be less than in the 2000 r.p.m / WOT condition. This could be because of increased base line HC emission values at 1500 r.p.m compared to 2000 r.p.m, a common observation with pre - mixed charge operation.

CO emission is again almost the same when operating both with and without charge stratification (Fig.6.24).

(d). 1500 r.p.m and part throttle condition ($WOT_{0.75}$)

The engine was operated with the same three injection rates and injection timing, as in the case of 1500 r.p.m / WOT. The results are shown in Figs.6.25 to 6.28.

A favourable shift in the gasoline lean limit equivalence ratio (i.e. from 1.25 to 1.29) is found with stratified charge operation, compared to base line operation. But again, the improvement is less than that with 1500 r.p.m / WOT condition, possibly because of the effect of residual gas, as in the 2000 r.p.m case.

Further, the trends of bsfc (Fig.6.25), BP (Fig.6.26), HC emission (Fig.6.27) and CO emission (Fig.6.28) are rather resemble previous cases, when comparisons are made between stratified charge operation and base line operation.

All the stratified charge combustion results, so far discussed, were obtained when operating the engine in dual - fuel mode, namely injecting gasoline at the inlet manifold early in the induction stroke, then stratifying the mixture by injecting methane through the spark plug just prior to ignition. The following results will deal with fuelling the engine only with methane gas, either in base line operation or in stratified charge operation. Further, as part of the present work, it was found useful to compare the base line

operations with gasoline and methane as the fuel, to investigate briefly the use of alternative fuels.

6.4.2 Comparison of base line operations

The base line operation of the engine with gasoline and methane is compared in Figs.6.29 to 6.36. The part throttle setting used in this comparison work corresponds to $WOT_{0.5}$, hence 2000/PART in the figures means "at 2000 r.p.m and $WOT_{0.5}$ condition". From these figures, the following observations can be made :-

(1). lean mixture limit equivalence ratio is increased significantly with methane gas operation, for all the speed - throttle setting combinations tested because gaseous fuels such as methane mix readily and intimately with air.

(2). BP is decreased with methane gas operation by about 10 - 12 per cent (calculated around stoichiometric mixture ratio) at WOT and all speeds (Fig.6.29). The main reason for this is, reduction in air capacity as methane gas occupies approximately 10 per cent of the available volume in the intake manifold and the engine cylinder. But the reduction in BP values is very much less, around stoichiometric mixture ratio, for part throttle conditions (Fig.6.30). However as the mixture becomes leaner, BP is greater with methane

gas than with gasoline by virtue of its leaner burning capability.

(3). HC emission is low with methane gas, for all the speed - throttle combinations tested (Fig.6.31 and Fig.6.32).

(4). CO emissions are lower with methane gas particularly at lean equivalence ratios (Fig.6.33 and Fig.6.34).

(5). brake thermal efficiency is increased with methane gas for most of the operating conditions tested (Fig.6.35 and Fig.6.36) which implies significant improvement in bsfc at lean equivalence ratios.

The reductions in HC, CO emissions and the improvement in bsfc could be the result of intimate mixing of methane gas with air whereby more complete combustion is achieved.

These observations and the accompanying reasons should answer most of the trends which will be observed in the next section.

6.4.3 Charge stratification of a methane fuelled engine

The engine was operated in similar conditions to those used for dual - fuel stratified charge operation, discussed in section 6.4.1. These conditions included control of speed - throttle setting combinations, methane injection timing and injection rates. The corresponding results are shown in Figs.6.37 to 6.56 and the following results can be inferred from these figures.

They are :-

(1). shift in the lean limit equivalence ratio with this stratified charge operation is relatively large when compared to dual - fuel stratified charge operation under similar operating conditions.

(2). bsfc improvement with this stratified charge operation is also relatively large when compared to dual - fuel stratified charge operation particularly at lean equivalence ratios.

(3). although BP values with this stratified charge operation are comparable to those of the base line operation, they are relatively lower than with dual - fuel stratified charge operation for similar operating condition, especially at WOT setting.

(4). although HC emission is high with this stratified charge operation compared to base line operation, they are still lower than those with dual - fuel stratified charge operation.

(5). at lean equivalence ratios, CO emission with this stratified charge operation is almost the same as with base line operation and they are lower than those with dual - fuel stratified charge operation.

Furthermore the effectiveness of charge stratification at lean equivalence ratios is again highlighted in terms of bsfc. Apart from this, there

is an increased level of HC emission with this stratified charge operation (compared to base line operation with methane gas), perhaps for the same reasons as in the case of dual - fuel operation, namely,

(1). flame initiation at rich flammability limit of methane gas

(2). initial burning in a rich mixture environment

(3). quenching of unburnt or partially burnt charge inside the hypodermic injection tube.

6.5 FLOW VISUALISATION BY MEANS OF SCHLIEREN PHOTOGRAPHS

To find the effect of the velocity field around the spark gap on the injected methane puff, photographs were taken using the Schlieren method. These photographs were taken at two different velocity fields which corresponded to Ricardo engine speeds of 1000 r.p.m (Plate 6.1) and 2000 r.p.m (Plate 6.2). Further, these photographs could be used to verify the explanations that have been put forward in the preceding discussion.

It can be seen from the photographs that as the time from the instant of methane injection increases, the injected methane puff is distorted from its initial compactness and is transformed into a widely scattered shape due to the prevailing complex velocity field and possibly because of outflow of methane gas. This situation arises at a very early stage (on a time scale) with increasing engine speed, as can be seen from the photographs of particular time intervals at given speeds. This observation, combined with the engine

combustion results suggest that the initially small but compact shape of the methane puff around the locality of the spark gap, which governs the position of the interface, is also one of the factors governing the flame initiation phase, as is the turbulence. But no further detail study was undertaken regarding this conclusion as it is out of the scope of the present work.

In addition it can also be seen from the photographs that with increasing time the amount of methane that dispersed away from the ignition source (i.e. displacement of the interface) is high, especially at high speeds, which could have resulted in high HC emission values with retarded spark timings and at lean equivalence ratios.

Further it should be noted that the series of photographs of the methane puff typify only the engine motoring condition. However this is true even with the firing condition but up to the point of ignition, since after ignition the flame induced velocity fields would change the conditions around the spark gap. Since this present work is more concerned with the flame initiation phase which is considered to be influencing the subsequent combustion process, these photographs still can provide useful information.

Apart from this, to typify the actual engine operation with the methane injection timings used, a pressure difference of 4 bar between the regulated gas supply and the constant volume bomb was maintained during the Schlieren photography. However in an actual engine operation with constant methane supply pressure, continuously varying pressure differences could have an effect on the instantaneous shape of the injected methane puff.

Furthermore the velocity field corresponding to 2000 r.p.m had to be extrapolated from the available data points from the work by Cole et al.(23), in connection with the Schlieren photography work. But this is valid as other data points show a linear relationship. However the correction factor involved in obtaining velocity values around the injection timings used in the present work was derived from the work by Semenov (104) for a disc type combustion chamber and for a single engine speed. Because of limited availability of literature on this subject, this correction factor was applied for velocities involved in the combustion chamber simulation work.

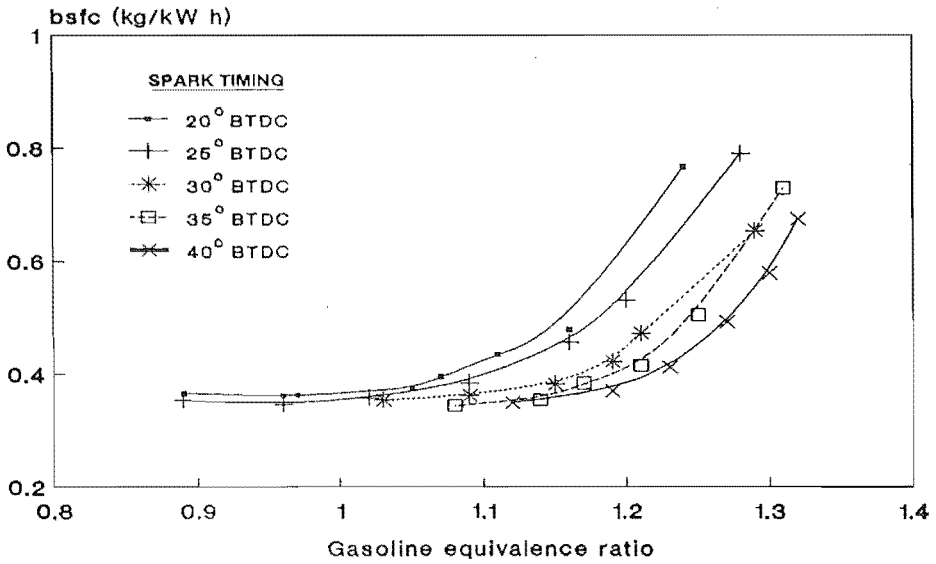

Fig. 6.1 bsfc vs gasoline equivalence ratio for stratified charge operation during spark timing optimisation at 1000 r.p.m/WOT

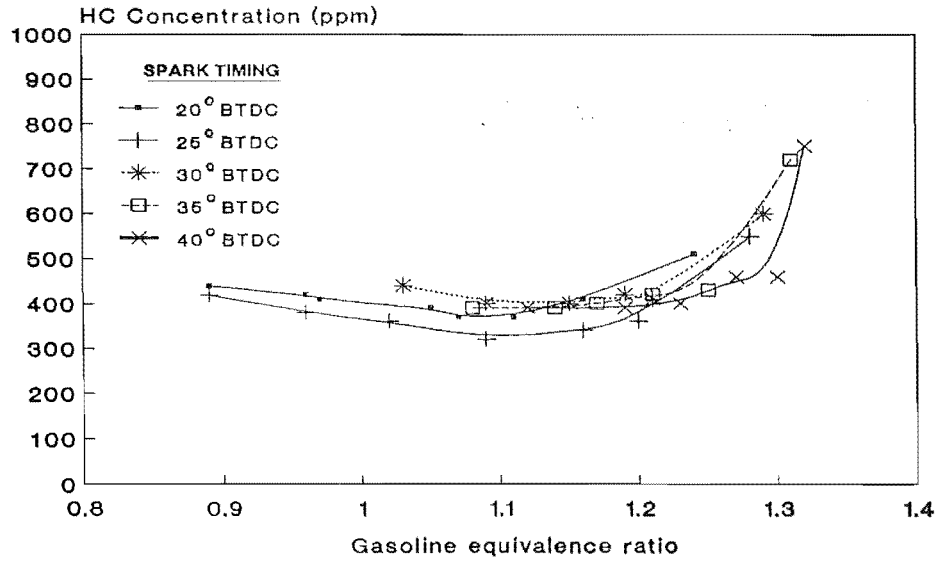

Fig. 6.2 HC emission vs gasoline equivalence ratio for stratified charge operation during spark timing optimisation at 1000 r.p.m/WOT

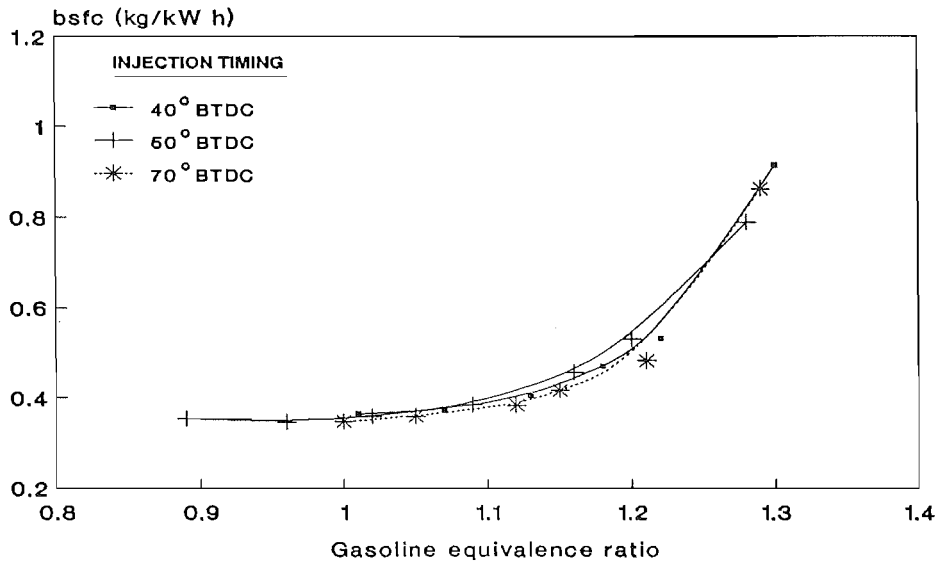

Fig. 6.3 bsfc vs gasoline equivalence ratio for stratified charge operation during injection timing optimisation at 1000 r.p.m/WOT

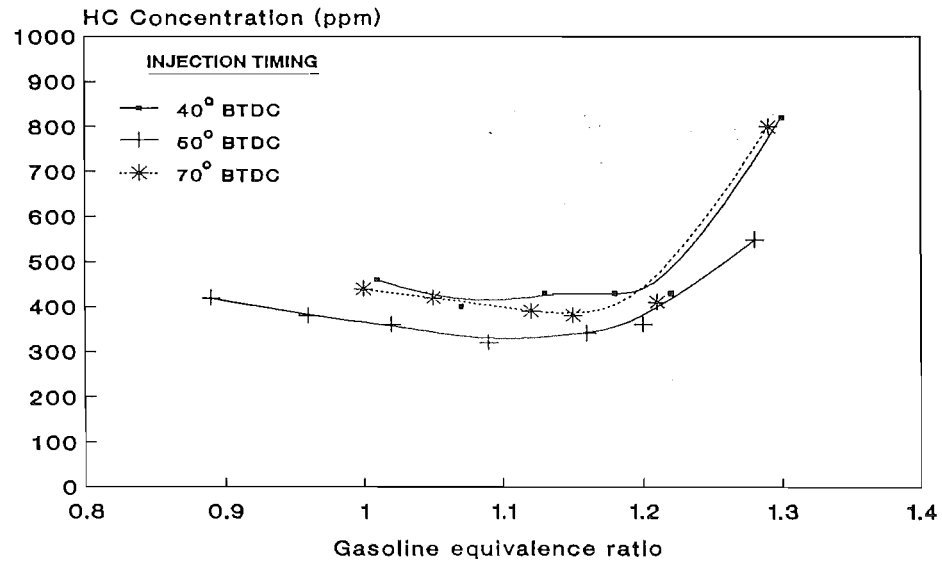

Fig.6.4 HC emission vs gasoline equivalence ratio for stratified charge operation during injection timing optimisation at 1000 r.p.m/WOT

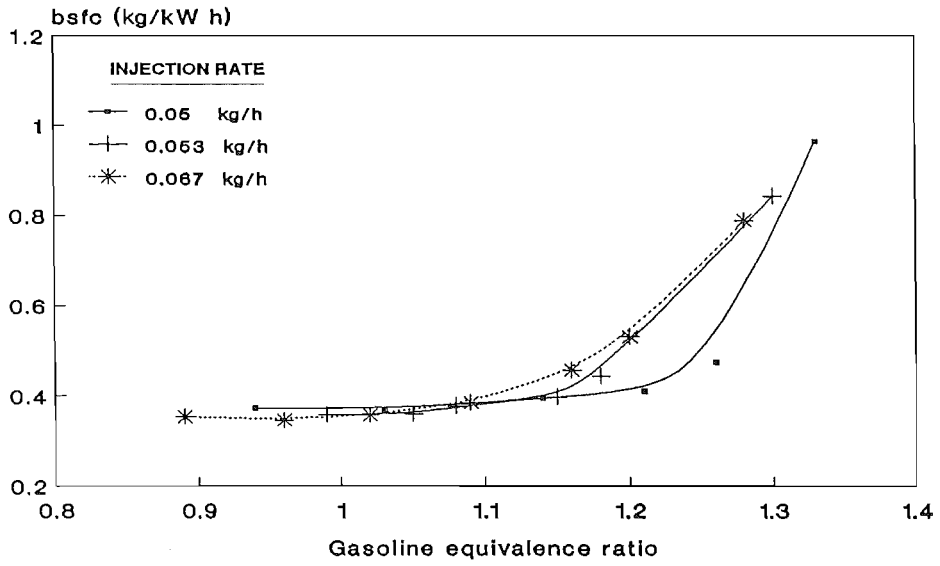

Fig. 6.5 bsfc vs gasoline equivalence ratio for stratified charge operation with different methane injection rates at 1000 r.p.m/WOT

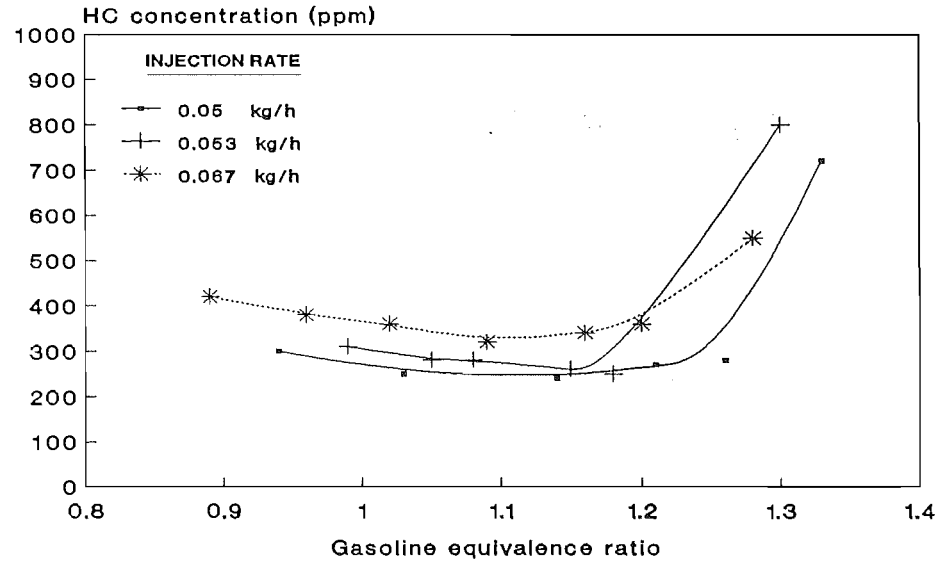

Fig. 6.6 HC emission vs gasoline equivalence ratio for stratified charge operation with different methane injection rates at 1000 r.p.m/WOT

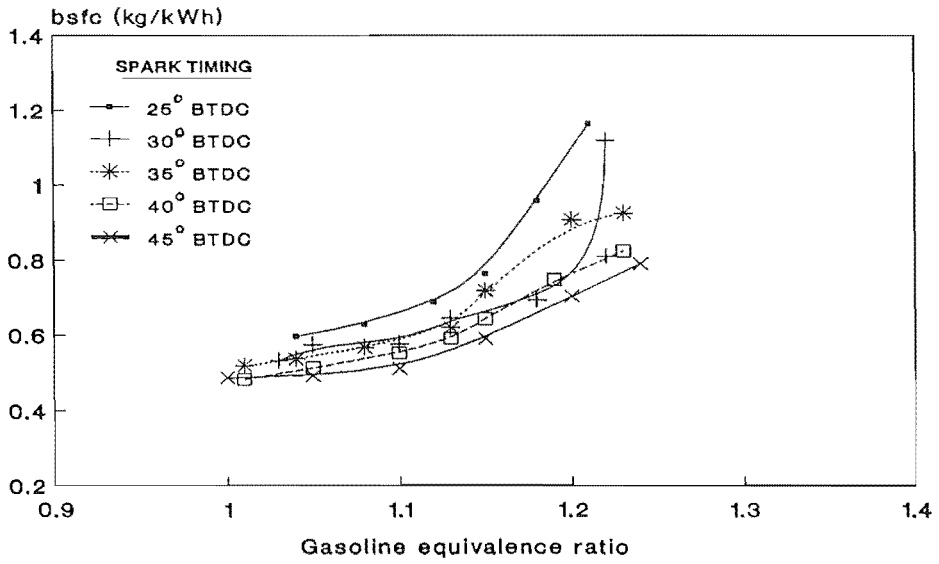

Fig. 6.7 bsfc vs gasoline equivalence ratio for stratified charge operation during spark timing optimisation at 2000 r.p.m/$WOT_{0.5}$

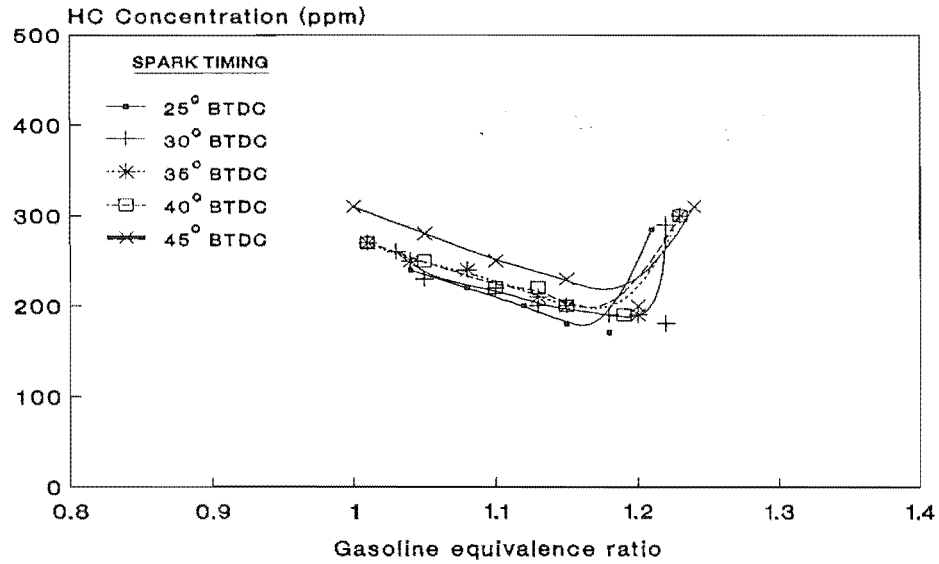

Fig. 6.8 HC emission vs gasoline equivalence ratio for stratified charge operation during spark timing optimisation at 2000 r.p.m/$WOT_{0.5}$

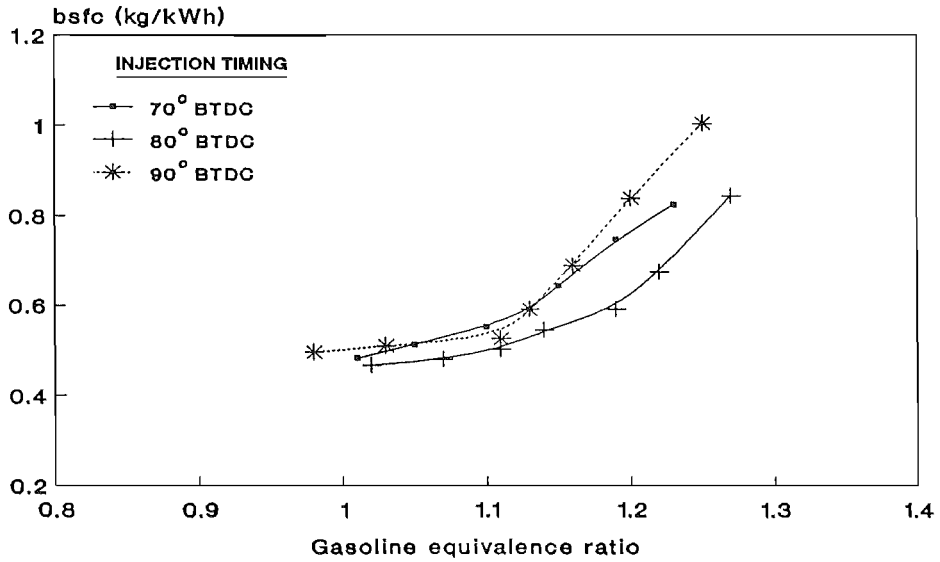

Fig. 6.9 bsfc vs gasoline equivalence ratio for stratified charge operation during injection timing optimisation at 2000 r.p.m/$WOT_{0.5}$

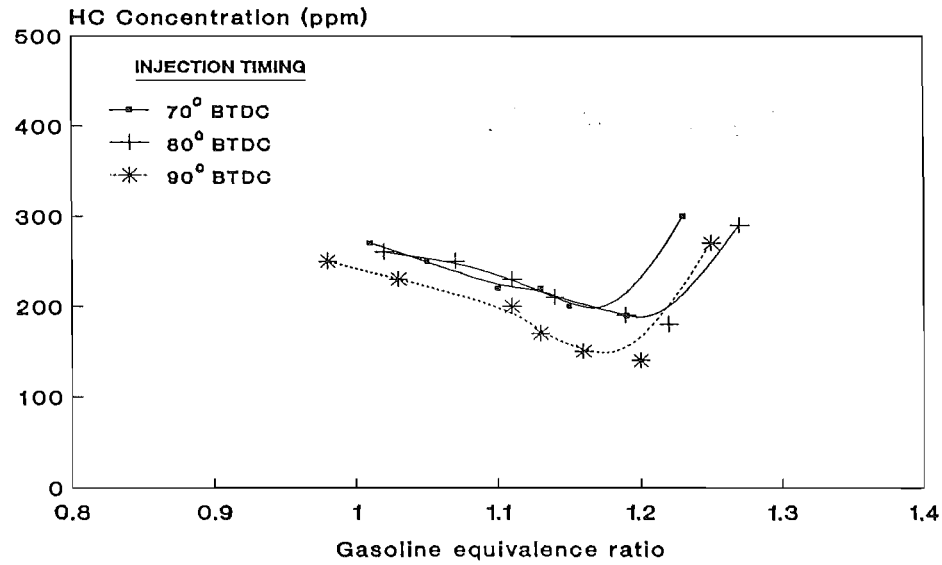

Fig. 6.10 HC emission vs gasoline equivalence ratio for stratified charge operation during injection timing optimisation at 2000r.p.m/$WOT_{0.5}$

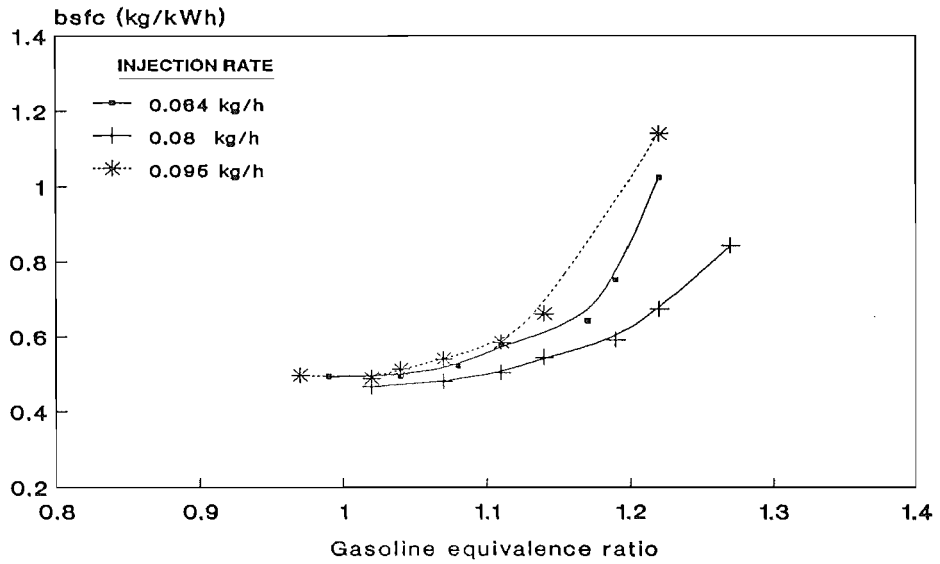

Fig. 6.11 bsfc vs gasoline equivalence ratio for stratified charge operation with different methane injection rates at 2000 r.p.m/$WOT_{0.5}$

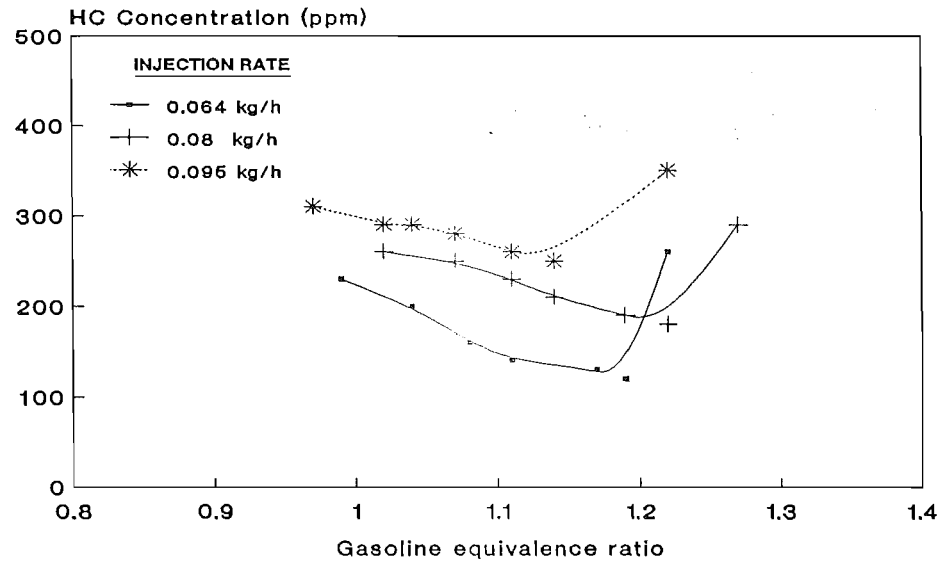

Fig. 6.12 HC emission vs gasoline equivalence ratio for stratified charge operation with different methane injection rates at 2000 r.p.m/$WOT_{0.5}$

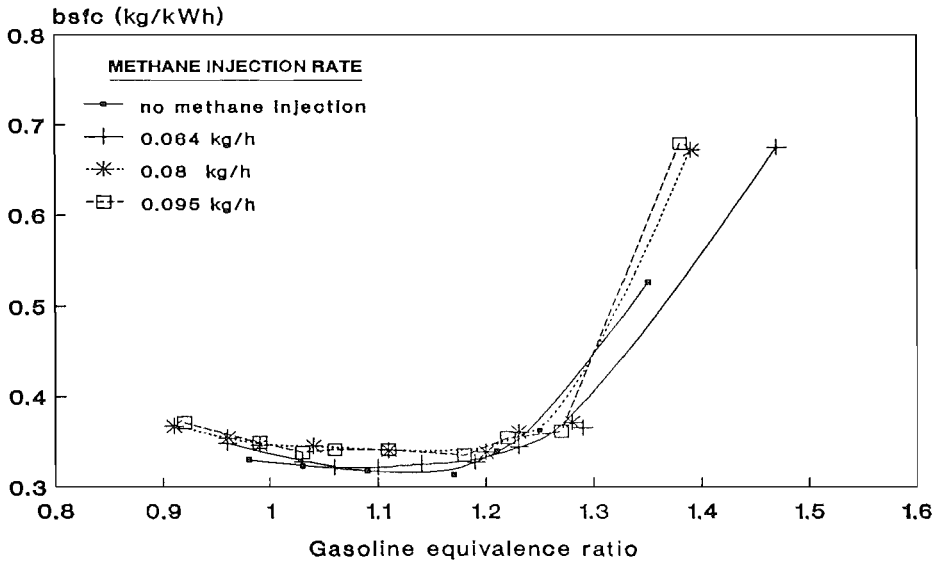

Fig. 6.13 bsfc vs gasoline equivalence ratio with and without charge stratification at 2000 r.p.m/WOT

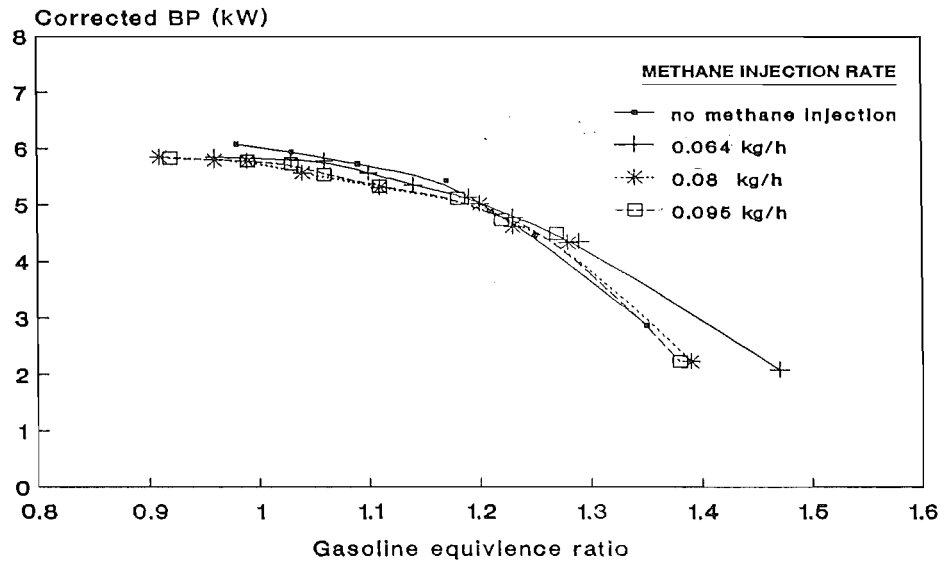

Fig. 6.14 Corrected brake power vs gasoline equivalence ratio with and without charge stratification at 2000 r.p.m/WOT

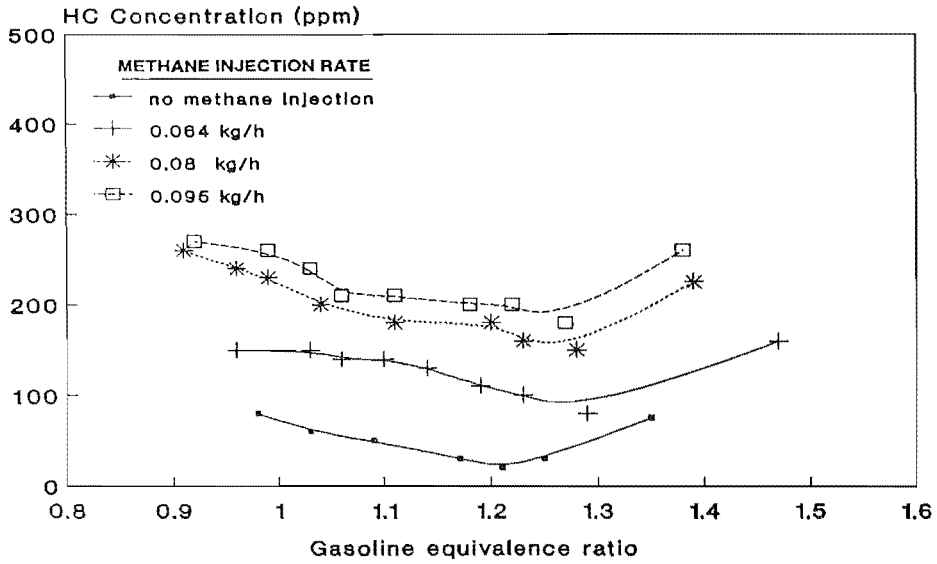

Fig. 6.15 HC emission vs gasoline equivalence ratio with and without charge stratification at 2000 r.p.m/WOT

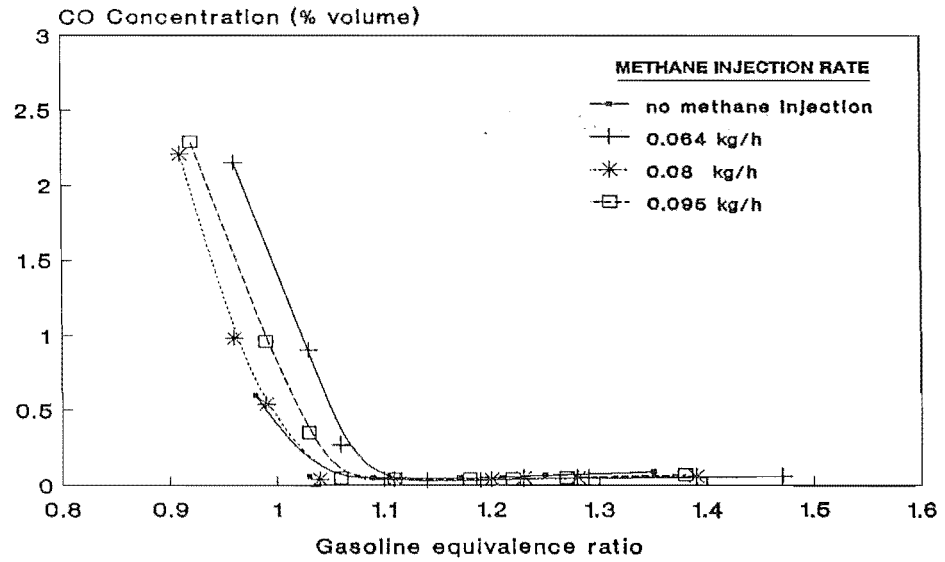

Fig. 6.16 CO emission vs gasoline equivalence ratio with and without charge stratification at 2000 r.p.m/WOT

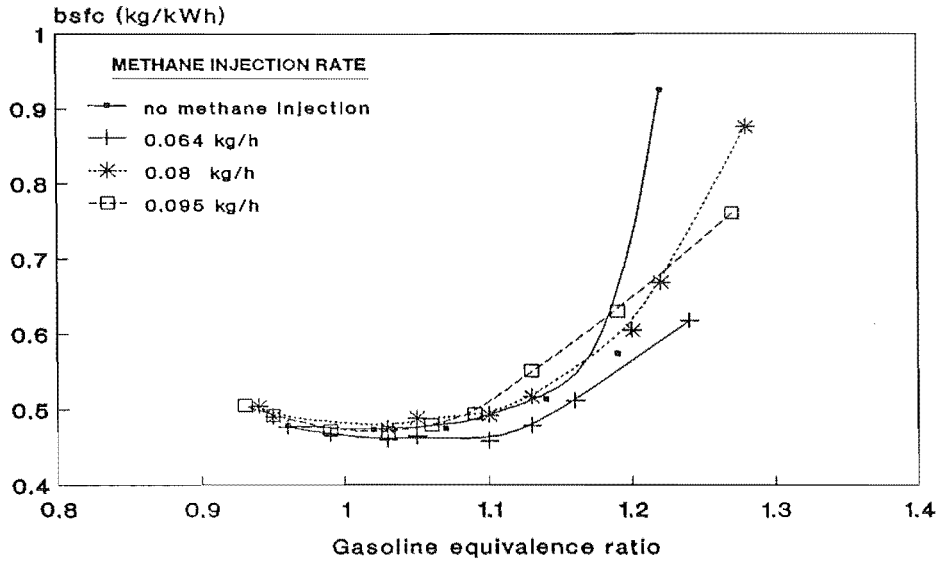

Fig. 6.17 bsfc vs gasoline equivalence ratio with and without charge stratification at 2000 r.p.m/$WOT_{0.5}$

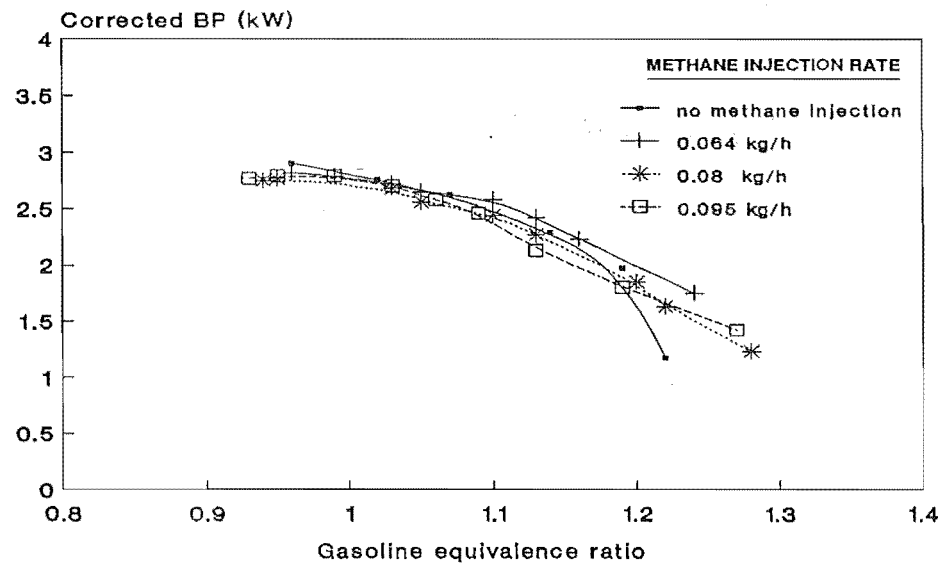

Fig. 6.18 Corrected brake power vs gasoline equivalence ratio with and without charge stratification at 2000 r.p.m/$WOT_{0.5}$

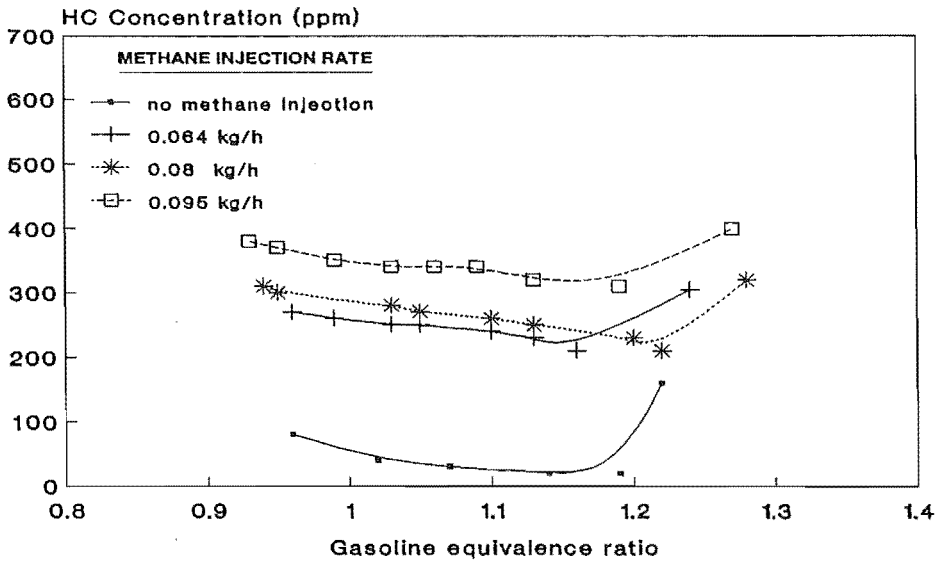

Fig. 6.19 HC emission vs gasoline equivalence ratio with and without charge stratification at 2000 r.p.m/$WOT_{0.5}$

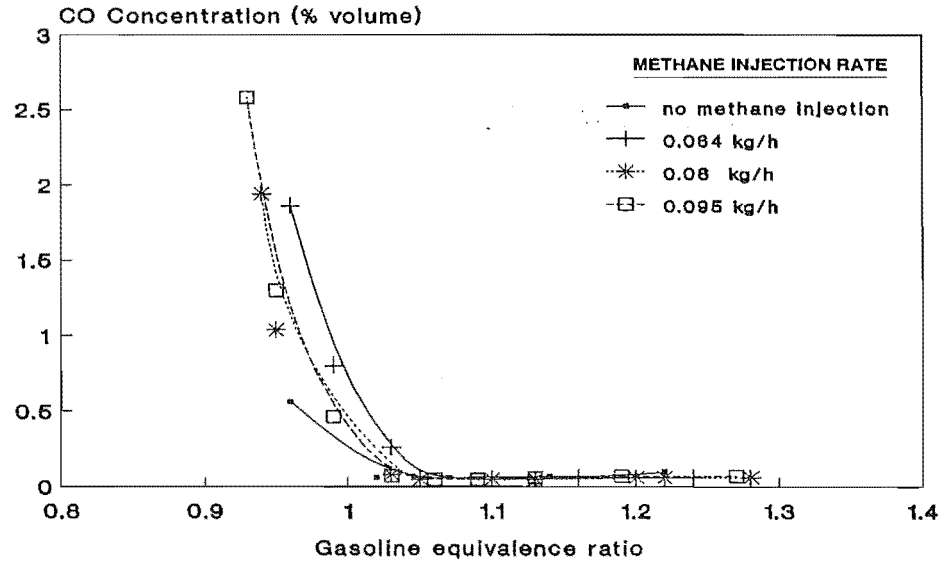

Fig. 6.20 CO emission vs gasoline equivalence ratio with and without charge stratification at 2000 r.p.m/$WOT_{0.5}$

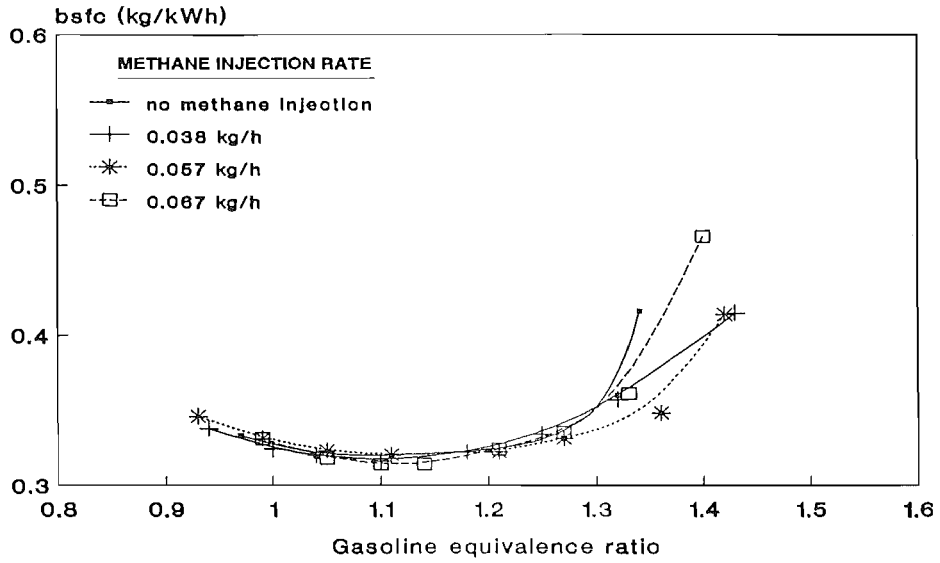

Fig. 6.21 bsfc vs gasoline equivalence ratio with and without charge stratification at 1500 r.p.m/WOT

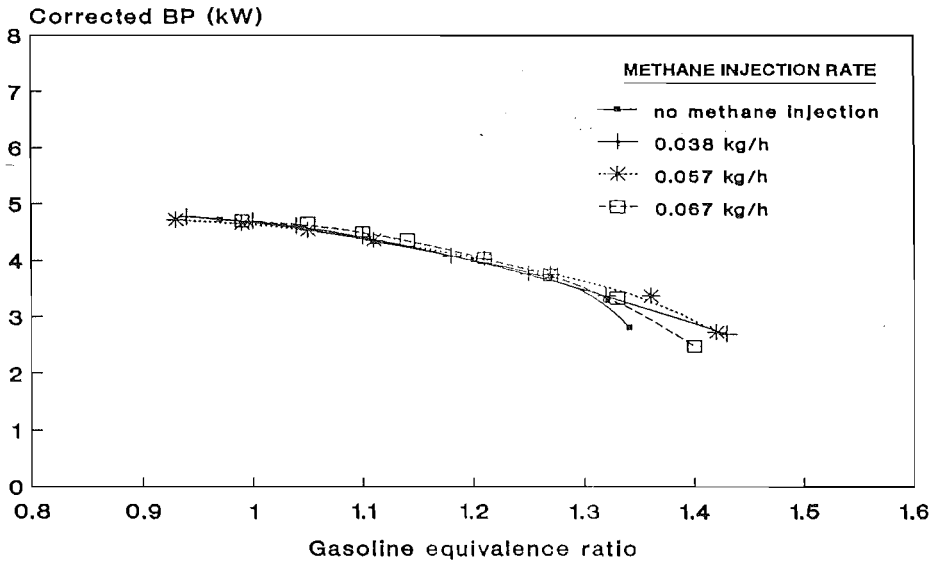

Fig. 6.22 Corrected brake power vs gasoline equivalence ratio with and without charge stratification at 1500 r.p.m/WOT

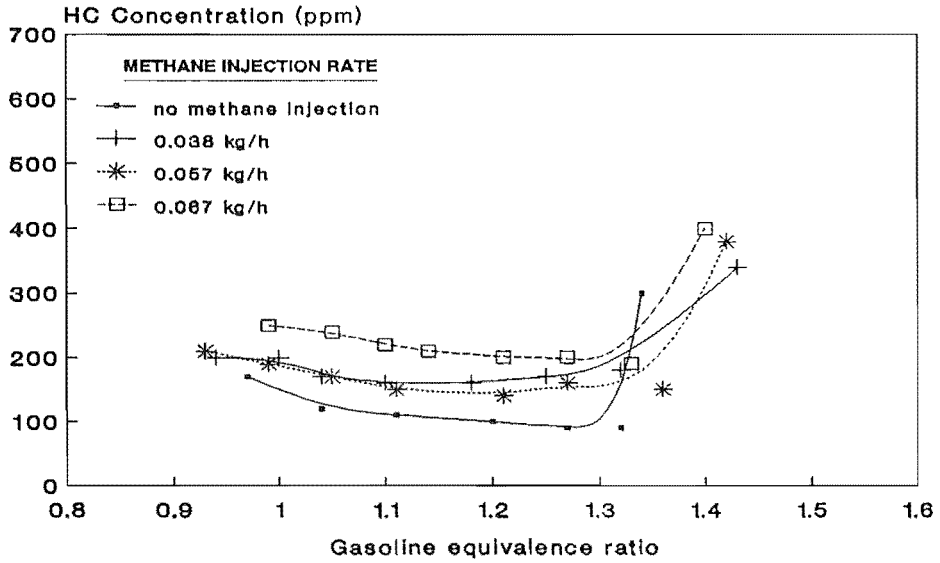

Fig. 6.23 HC emission vs gasoline equivalence ratio with and without charge stratification at 1500 r.p.m/WOT

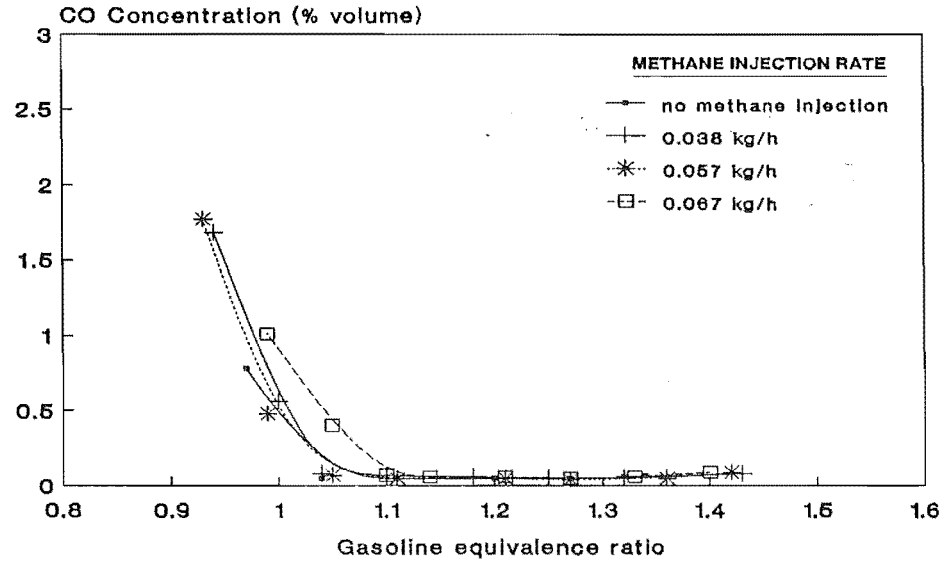

Fig. 6.24 CO emission vs gasoline equivalence ratio with and without charge stratification at 1500 r.p.m/WOT

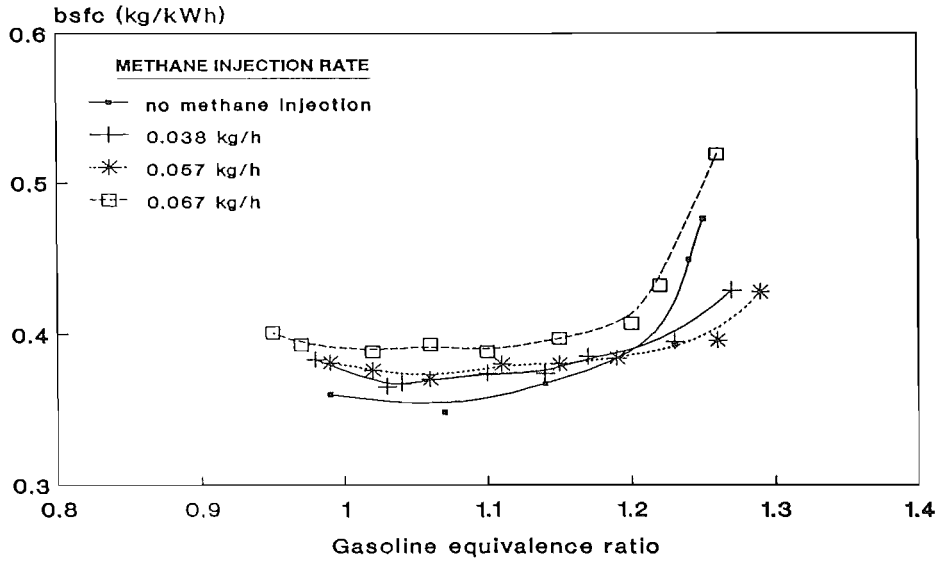

Fig. 6.25 bsfc vs gasoline equivalence ratio with and without charge stratification at 1500 r.p.m/$WOT_{0.75}$

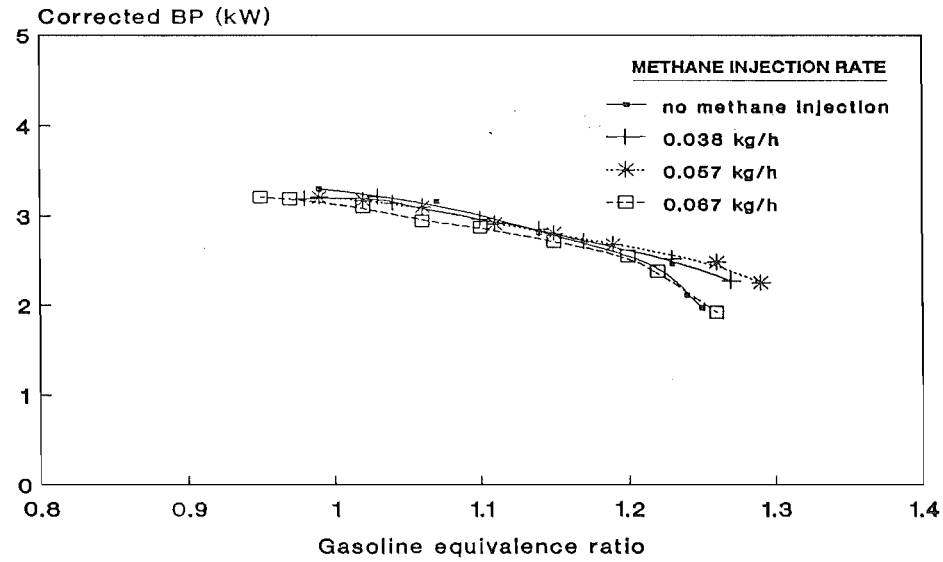

Fig. 6.26 Corrected brake power vs gasoline equivalence ratio with and without charge stratification at 1500 r.p.m/$WOT_{0.75}$

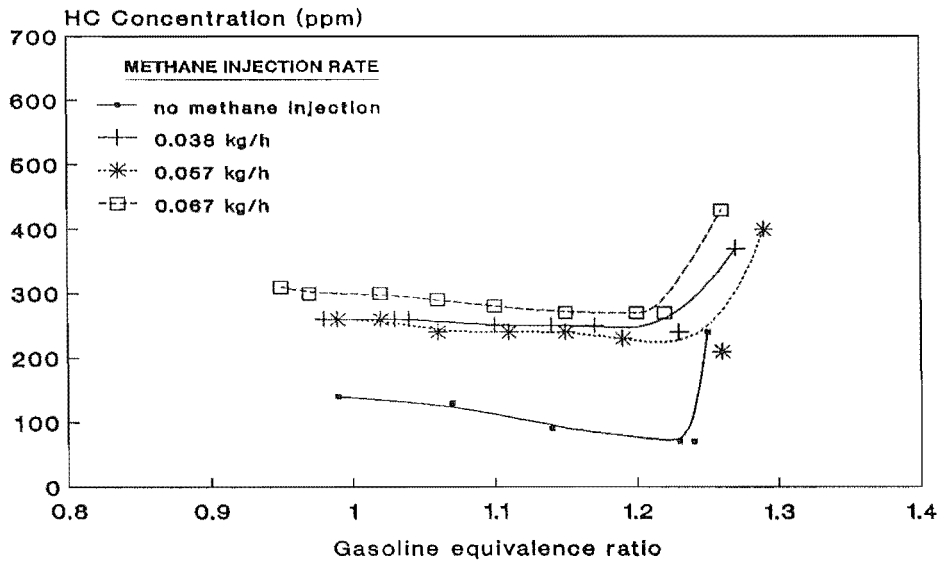

Fig. 6.27 HC emission vs gasoline equivalence ratio with and without charge stratification at 1500 r.p.m/$WOT_{0.75}$

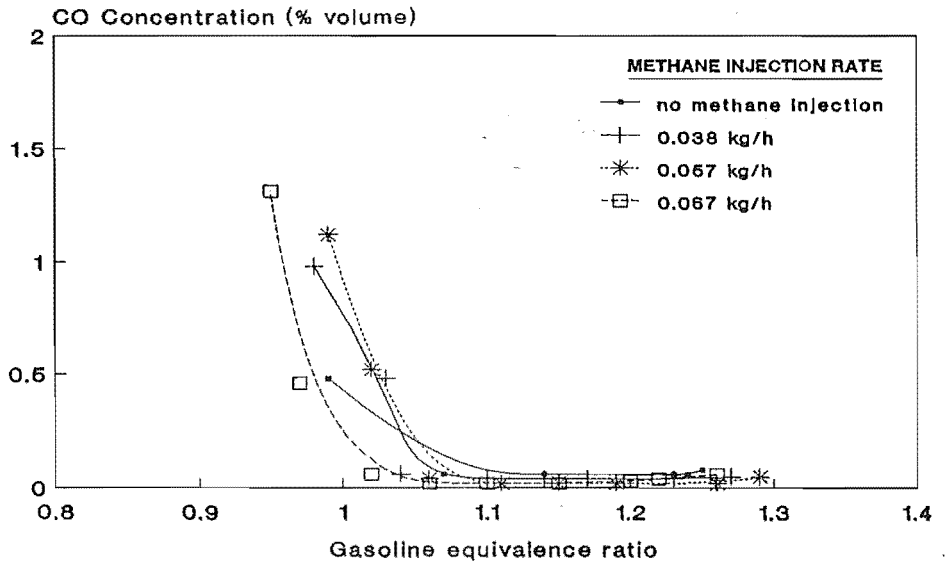

Fig. 6.28 CO emission vs gasoline equivalence ratio with and without charge stratification at 1500 r.p.m/$WOT_{0.75}$

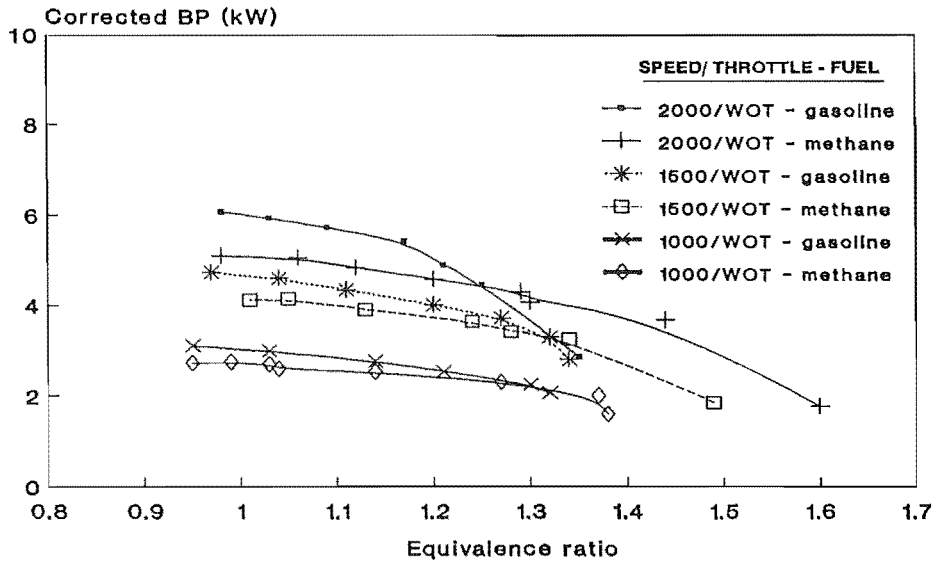

Fig. 6.29 Corrected brake power vs equivalence ratio for base line operation with gasoline and methane at different speeds and WOT

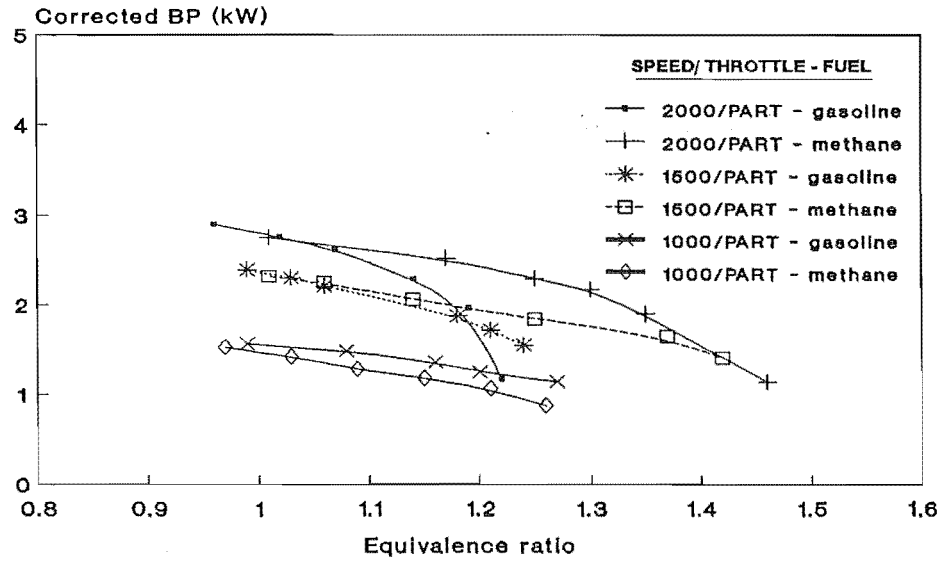

Fig. 6.30 Corrected brake power vs equivalence ratio for base line operation with gasoline and methane at different speeds and part throttle

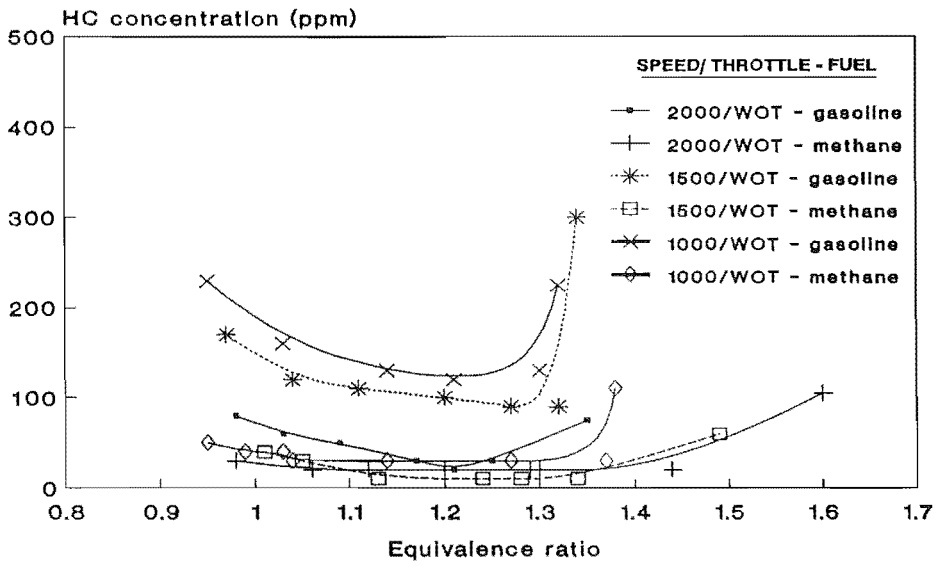

Fig. 6.31 HC emission vs equivalence ratio for base line operation with gasoline and methane at different speeds and WOT

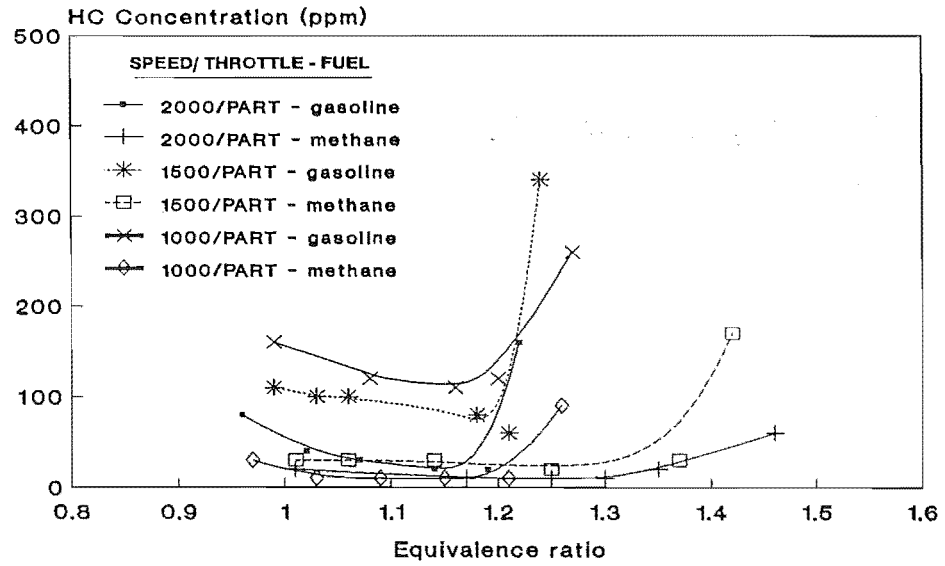

Fig. 6.32 HC emission vs equivalence ratio for base line operation with gasoline and methane at different speeds and part throttle

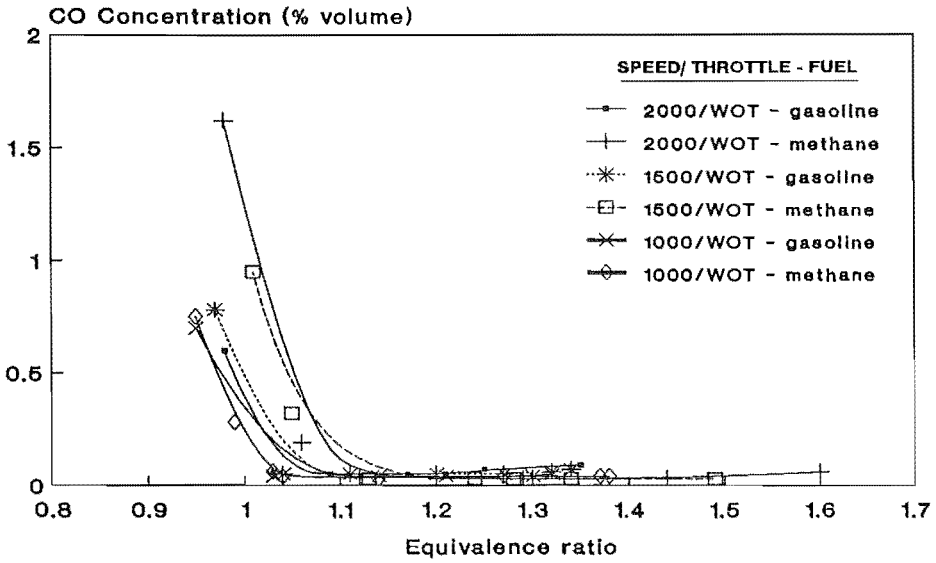

Fig. 6.33 CO emission vs equivalence ratio for base line operation with gasoline and methane at different speeds and WOT

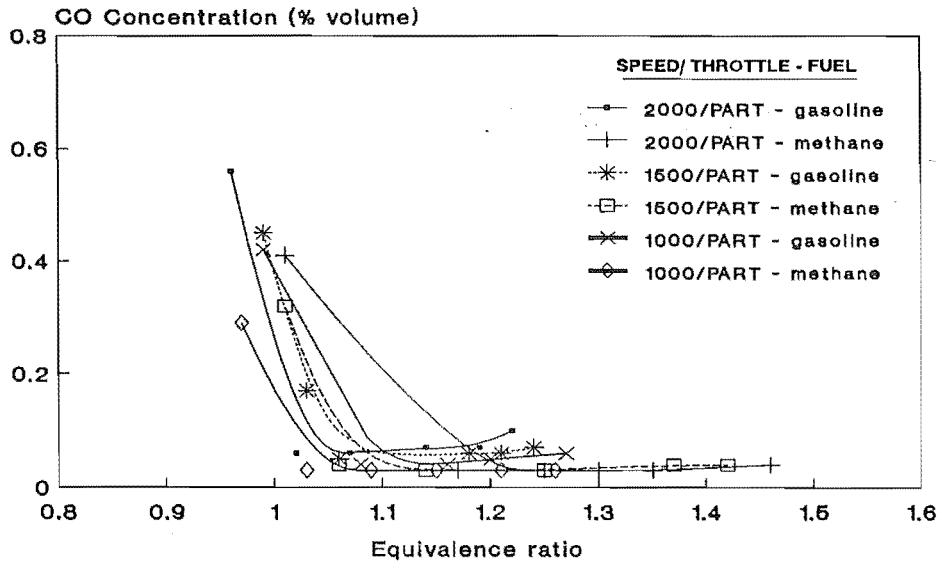

Fig. 6.34 CO emission vs equivalence ratio for base line operation with gasoline and methane at different speeds and part throttle

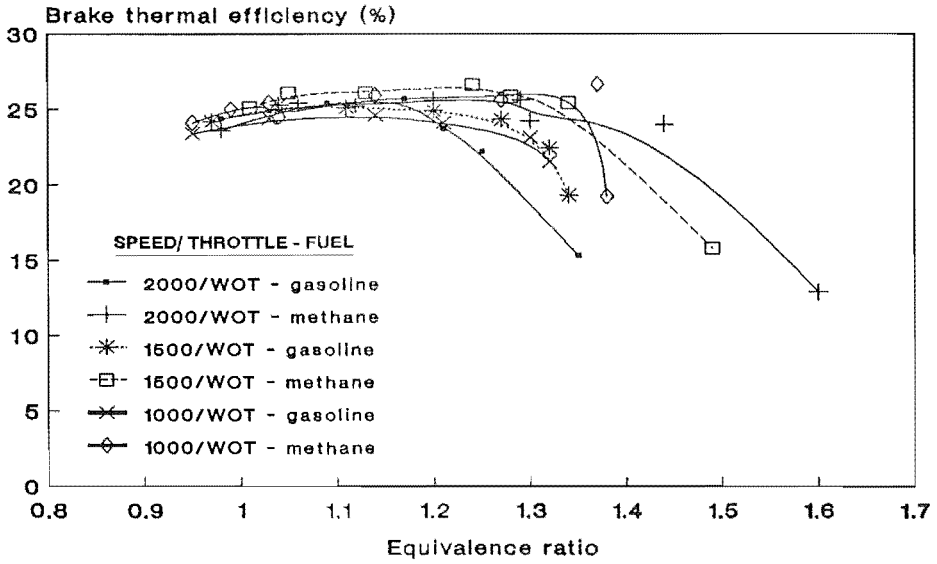

Fig. 6.35 Brake thermal efficiency vs equivalence ratio for base line operation with gasoline and methane at different speeds and WOT

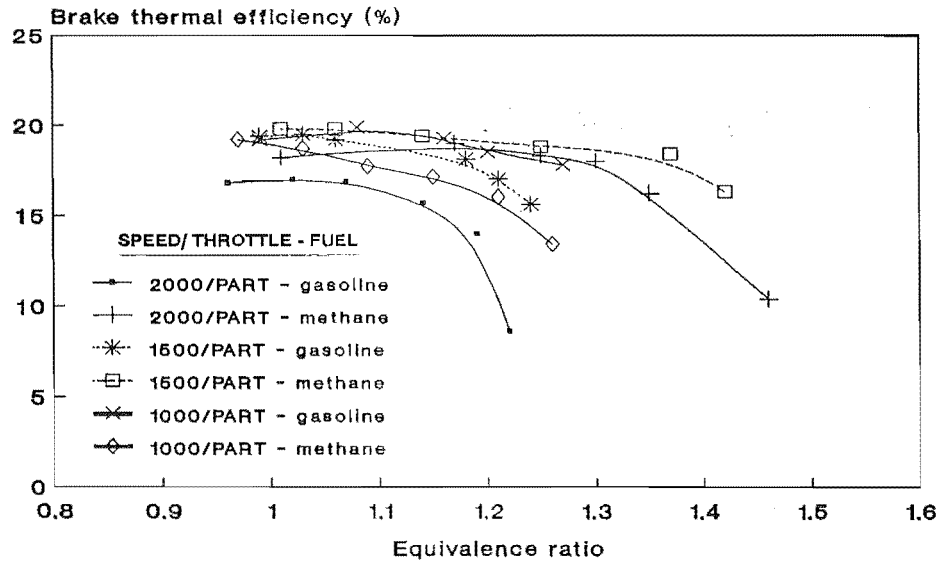

Fig. 6.36 Brake thermal efficiency vs equivalence ratio for base line operation with gasoline and methane at different speeds and part throttle

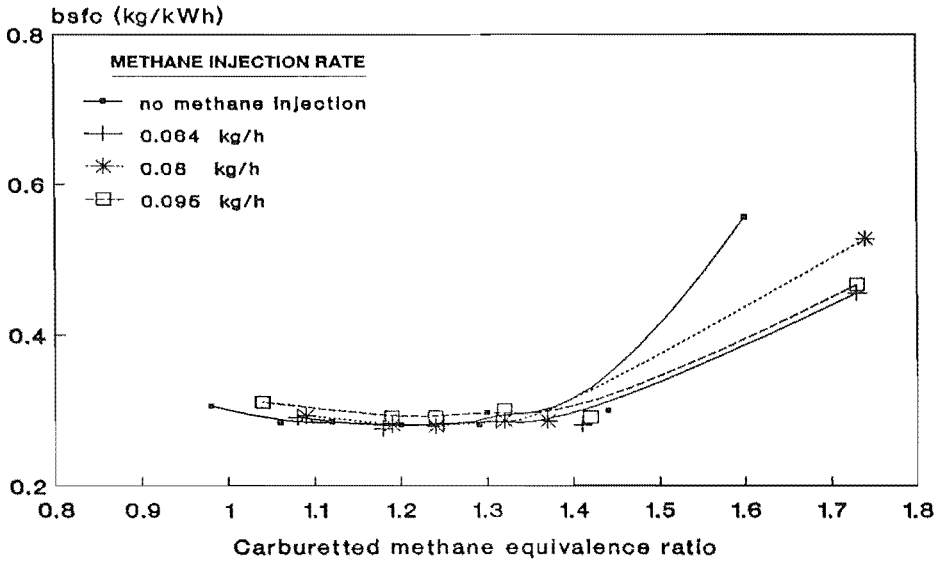

Fig. 6.37 bsfc vs carburetted methane equivalence ratio with and without charge stratification at 2000 r.p.m/WOT

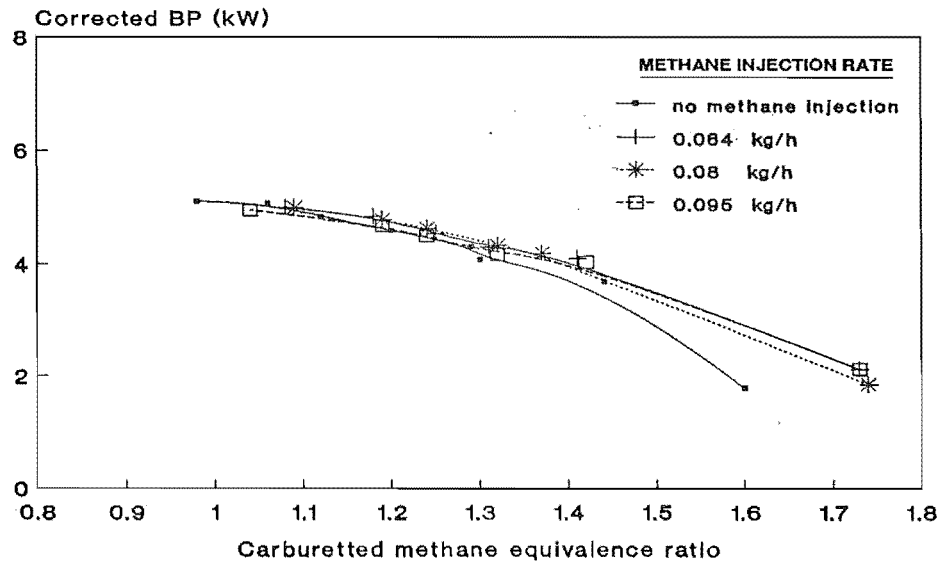

Fig. 6.38 Corrected brake power vs carburetted methane equivalence ratio with and without charge stratification at 2000 r.p.m/WOT

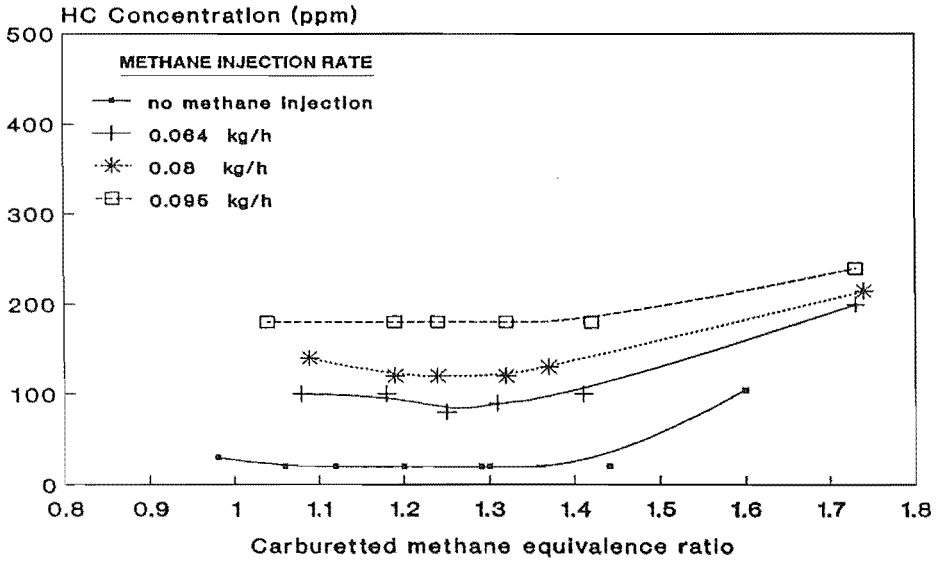

Fig. 6.39 HC emission vs carburetted methane equivalence ratio with and without charge stratification at 2000 r.p.m/WOT

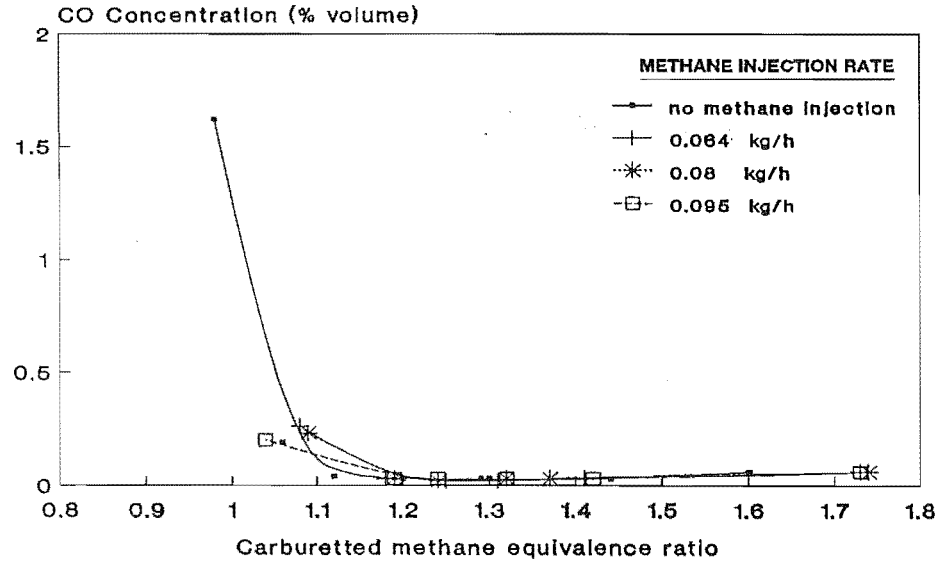

Fig. 6.40 CO emission vs carburetted methane equivalence ratio with and without charge stratification at 2000 r.p.m/WOT

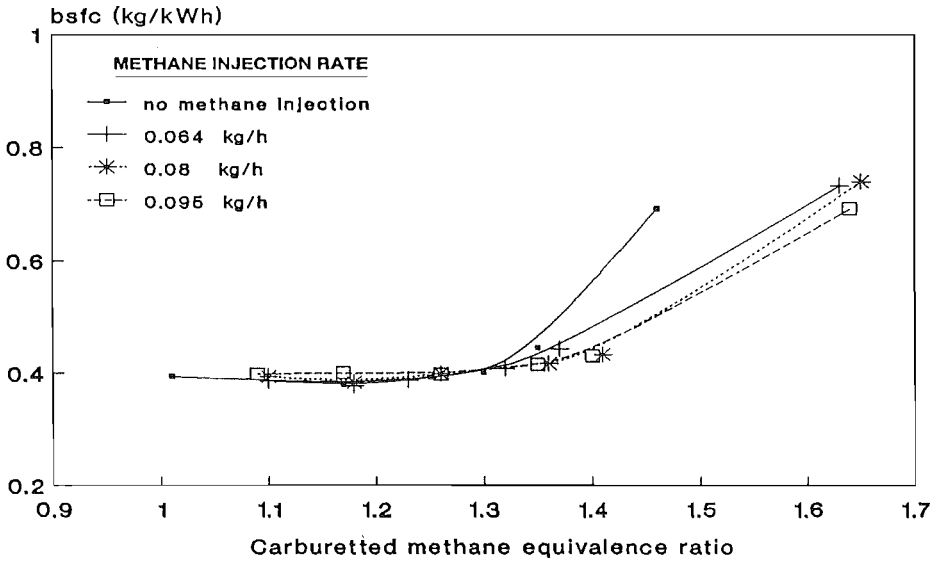

Fig. 6.41 bsfc vs carburetted methane equivalence ratio with and without charge stratification at 2000 r.p.m/$WOT_{0.5eq}$

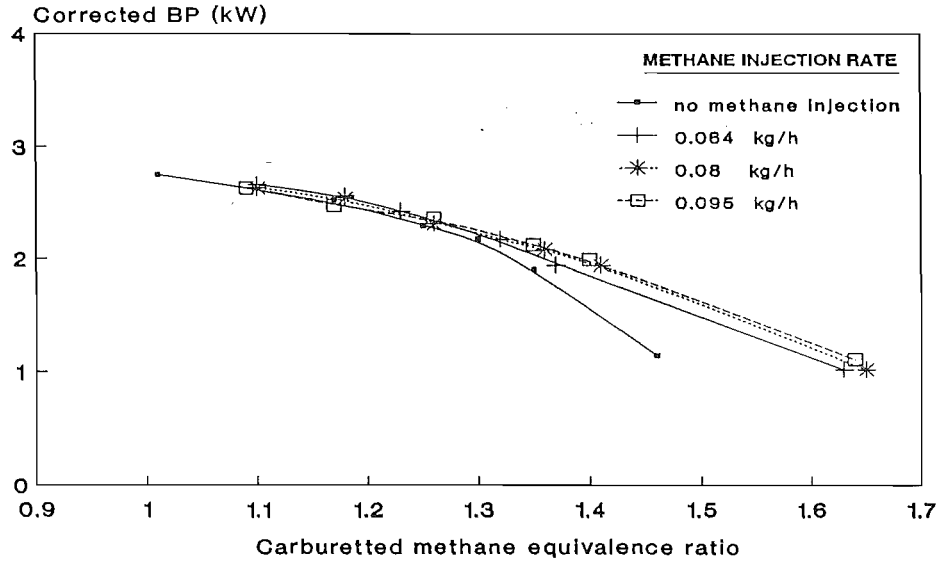

Fig. 6.42 Corrected brake power vs carburetted methane equivalence ratio with and without charge stratification at 2000 r.p.m/$WOT_{0.5eq}$

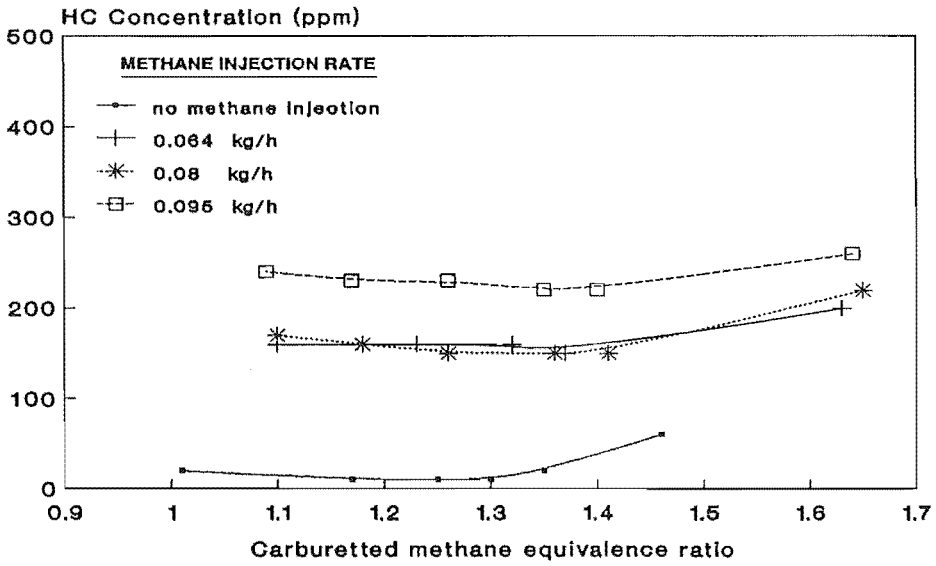

Fig. 6.43 HC emission vs carburetted methane equivalence ratio with and without charge stratification at 2000 r.p.m/$WOT_{0.5eq}$

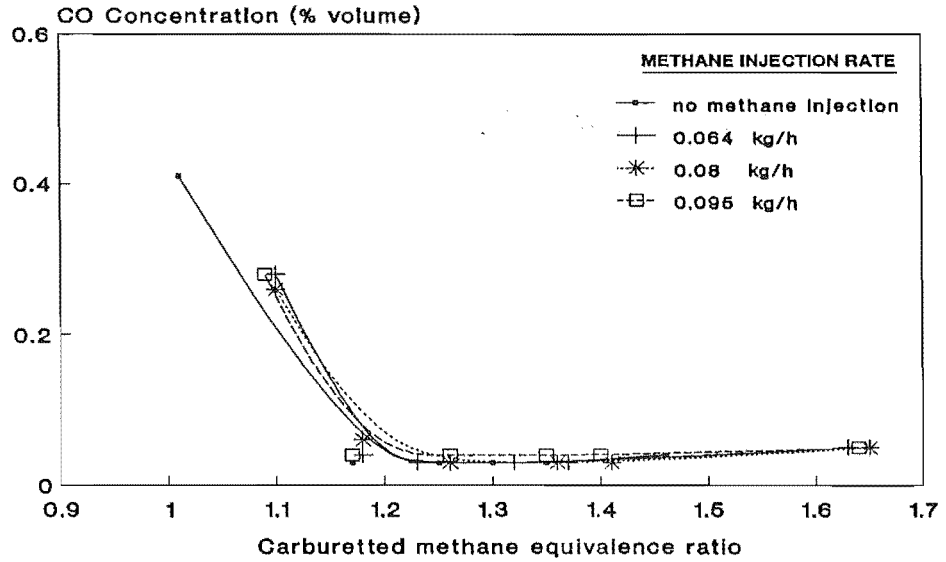

Fig. 6.44 CO emission vs carburetted methane equivalence ratio with and without charge stratification at 2000 r.p.m/$WOT_{0.5eq}$

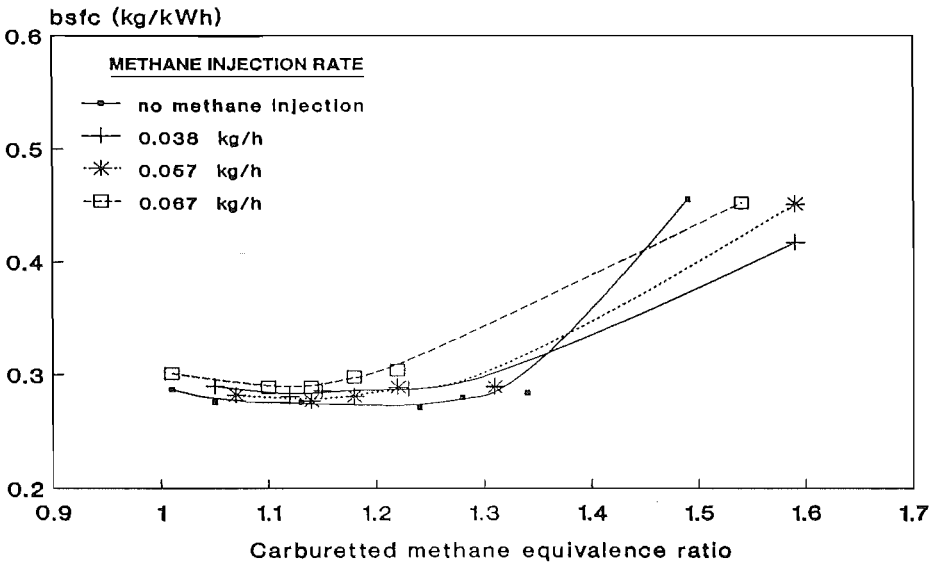

Fig. 6.45 bsfc vs carburetted methane equivalence ratio with and without charge stratification at 1500 r.p.m/WOT

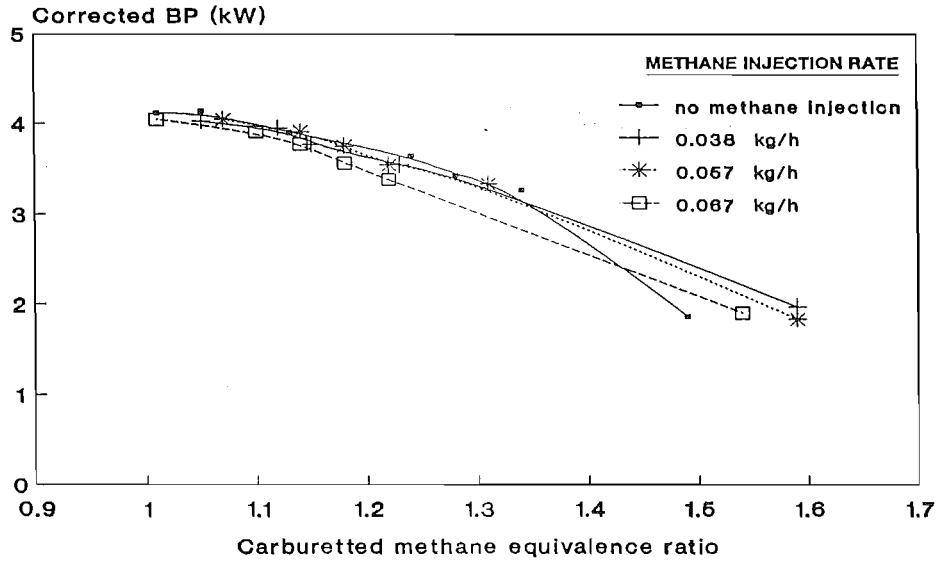

Fig. 6.46 Corrected brake power vs carburetted methane equivalence ratio with and without charge stratification at 1500 r.p.m/WOT

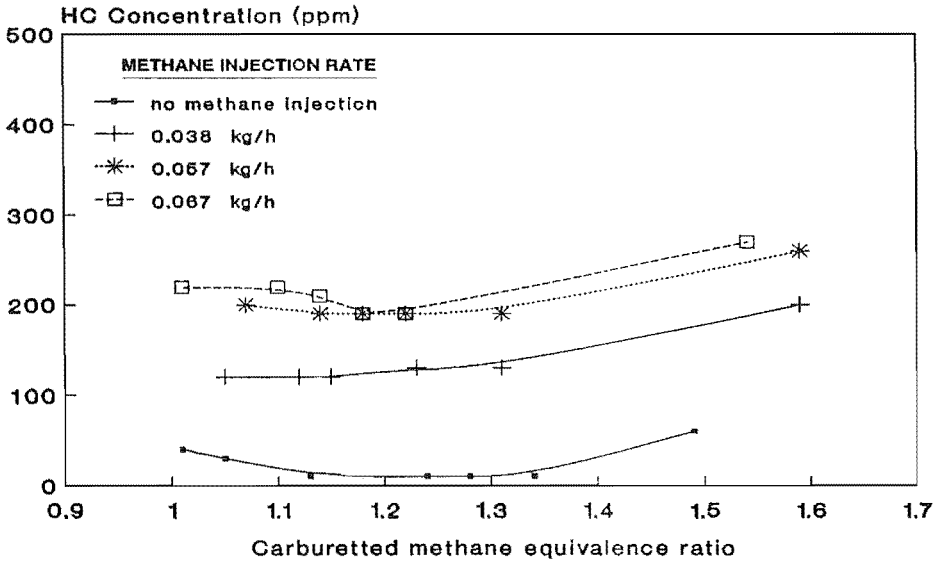

Fig. 6.47 HC emission vs carburetted methane equivalence ratio with and without charge stratification at 1500 r.p.m/WOT

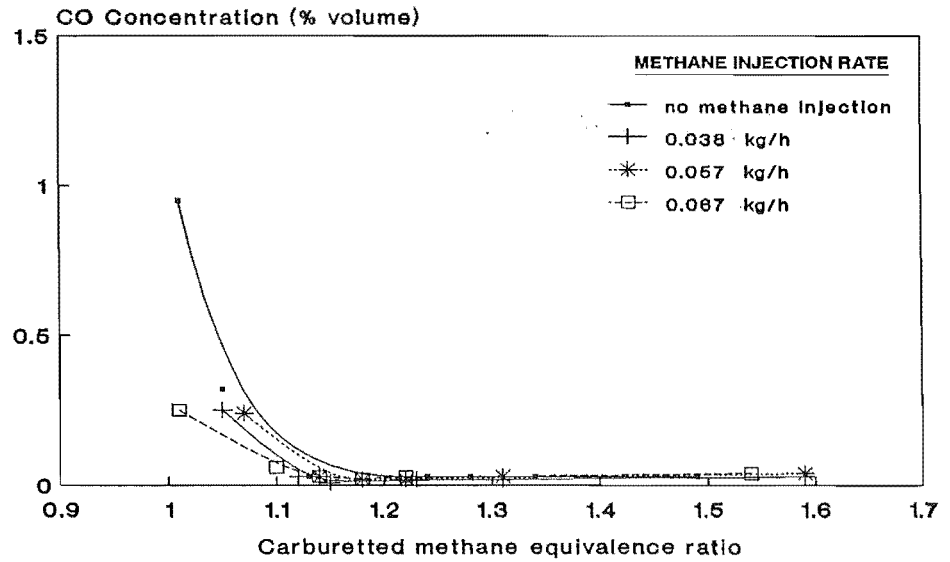

Fig. 6.48 CO emission vs carburetted methane equivalence ratio with and without charge stratification at 1500 r.p.m/WOT

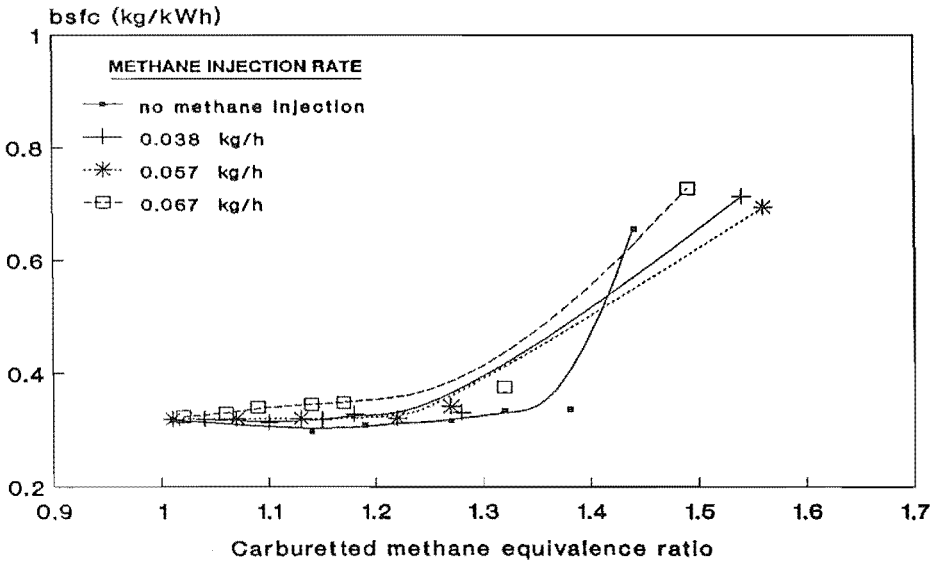

Fig. 6.49 bsfc vs carburetted methane equivalence ratio with and without charge stratification at 1500 r.p.m/$WOT_{0.75eq}$

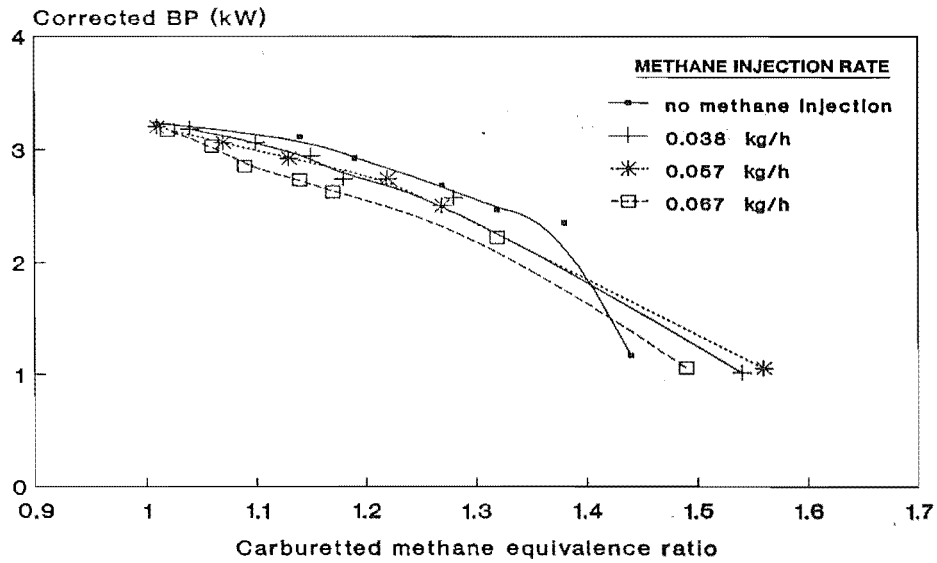

Fig. 6.50 Corrected brake power vs carburetted methane equivalence ratio with and without charge stratification at 1500 r.p.m/$WOT_{0.75eq}$

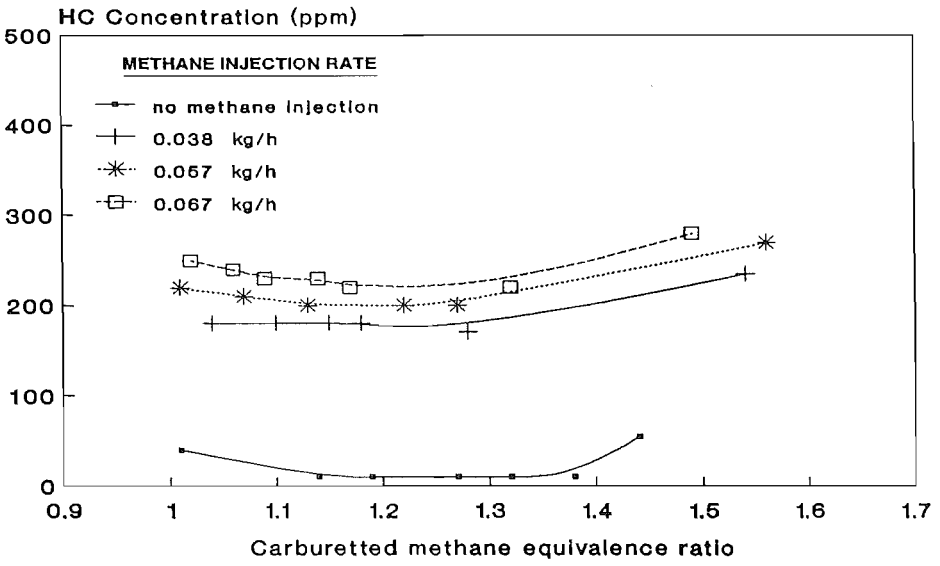

Fig. 6.51 HC emission vs carburetted methane equivalence ratio with and without charge stratification at 1500 r.p.m/$WOT_{0.75\ eq}$

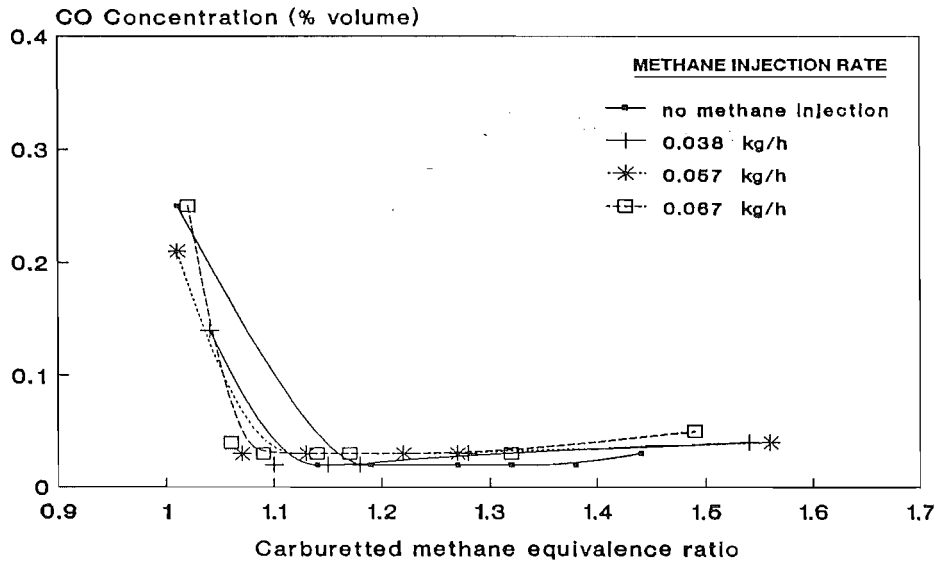

Fig. 6.52 CO emission vs carburetted methane equivalence ratio with and without charge stratification at 1500 r.p.m/$WOT_{0.75\ eq}$

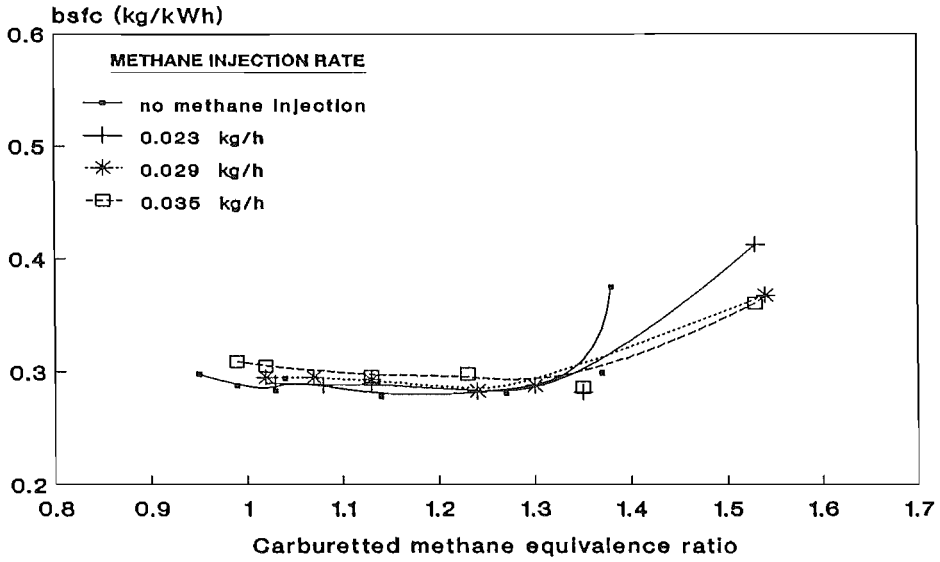

Fig. 6.53 bsfc vs carburetted methane equivalence ratio with and without charge stratification at 1000 r.p.m/WOT

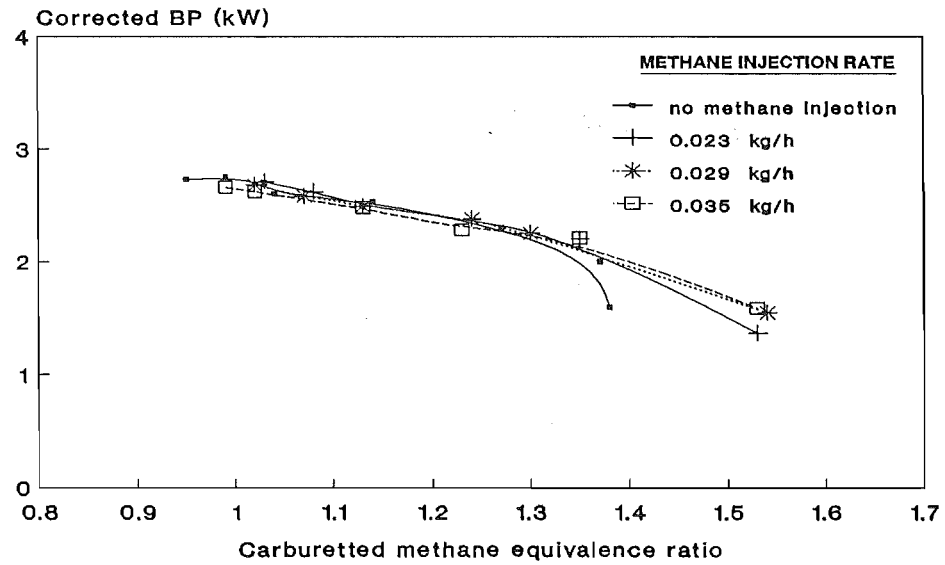

Fig. 6.54 Corrected brake power vs carburetted methane equivalence ratio with and without charge stratification at 1000 r.p.m/WOT

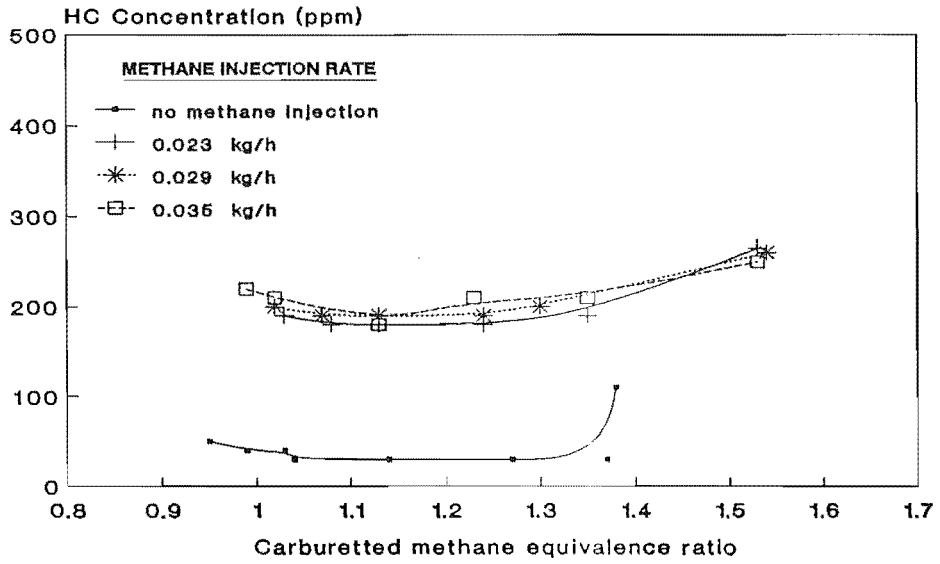

Fig. 6.55 HC emission vs carburetted methane equivalence ratio with and without charge stratification at 1000 r.p.m/WOT

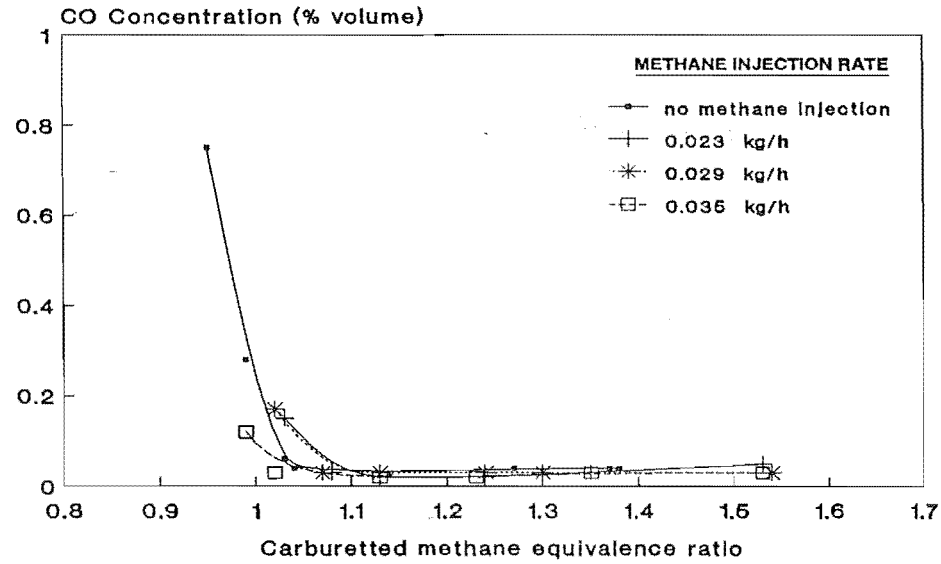

Fig. 6.56 CO emission vs carburetted methane equivalence ratio with and without charge stratification at 1000 r.p.m/WOT

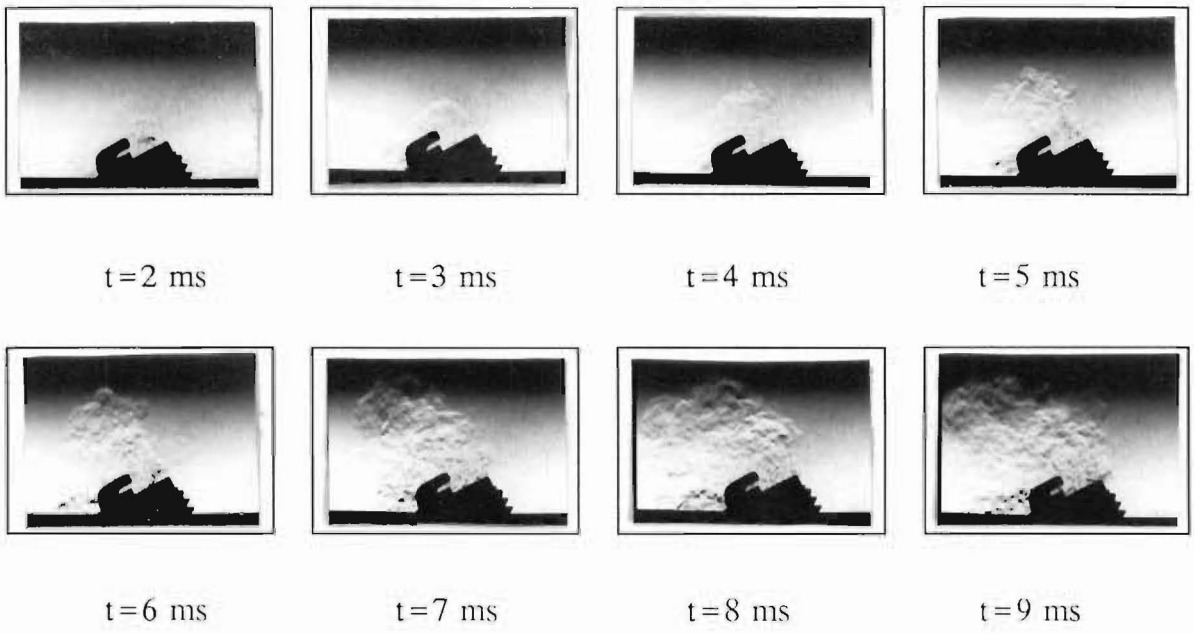

PLATE 6.1 Schlieren photographs of methane puff at 1000 r.p.m

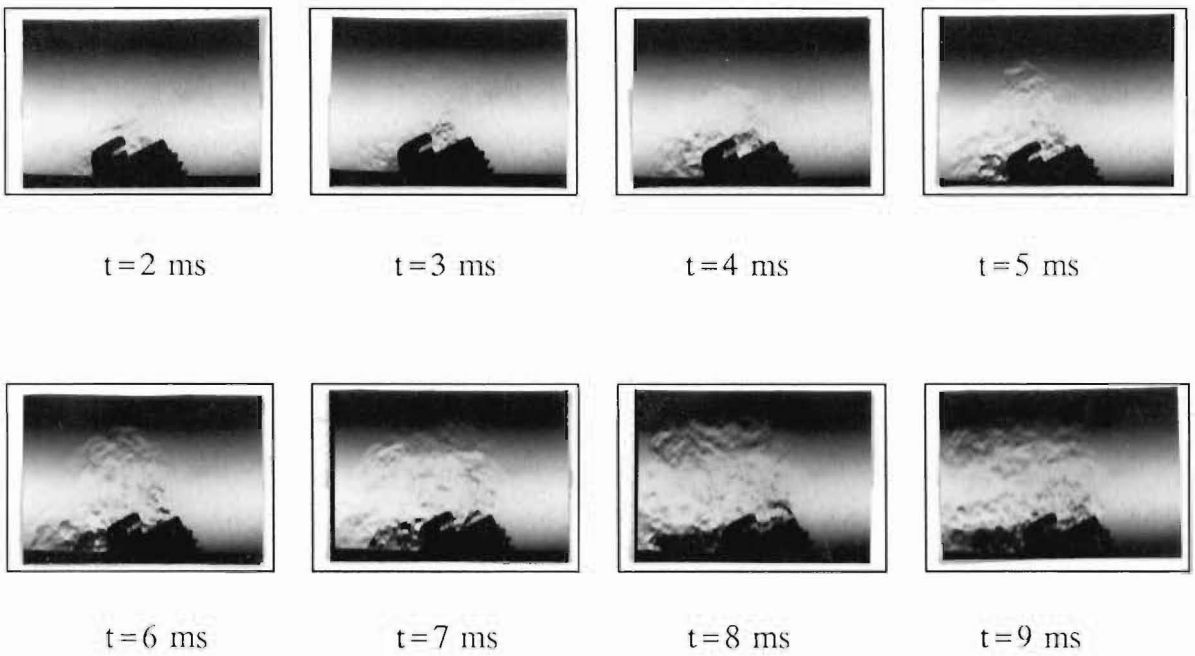

PLATE 6.2 Schlieren photographs of methane puff at 2000 r.p.m

CHAPTER 7

CONCLUSIONS

The results of the engine combustion and combustion chamber simulation experiments led to the following conclusions :-

(1). Comparison of base line operations shows

(a). methane gas can undergo combustion at relatively leaner conditions than gasoline because it mixes intimately and readily with air.

(b). a reduction of about 10 - 12 per cent in brake power with methane gas was found around stoichiometric mixture ratio when compared to gasoline. This can be attributed to reduced air capacity as methane gas occupies about 10 per cent of the available volume in the inlet manifold and in the engine cylinder

(c). low HC and CO emissions with methane gas operation can again be attributed to its intimate mixing with air, resulting in more complete combustion.

(2). lean limit of the fuel mixture is extended through the charge stratification process. Consequently this means that lean mixtures depend very much on the flame initiation

phase for their subsequent combustion.

(3). lean limit of the fuel mixtures at part throttle conditions is not greatly improved relative to WOT conditions, possibly due to the increased amount of residual gas.

(4). with the charge stratification process, lean limit extension with a methane fuelled engine is relatively greater than with a gasoline fuelled engine (i.e. dual - fuel mode). This could be due to the fact that methane gas mix readily and intimately with air.

(5). much more favourable bsfc values at leaner equivalence ratios with charge stratification process indicate the effectiveness of charge stratification at these equivalence ratios. This is in agreement with work of other researchers (77,95).

(6). HC emission with stratified charge operation is generally higher than with base line operation. The main reason could be that injected methane gas has been burnt around its rich flammability limit providing a certain level of incomplete combustion.

(7). high HC emissions with increased methane injection durations could be due to the quenching of unburnt and/or partially burnt charge inside the hypodermic injection tube and because of a overall richer mixture, as explained in the discussion.

(8). CO emission with stratified charge operation is almost the same as or little lower than with base line operation, at leaner equivalence ratios.

(9). BP values with stratified charge combustion are still comparable with those of base line operation and even a little higher as the mixture becomes leaner.

(10). the initially small and compact shape of the methane gas puff, as seen in the Schlieren photographs, could have a positive influence on the flame initiation phase, by having the ignitable interface close to the spark plug electrodes. However further study is needed to draw any firm conclusion.

(11). that because of improved bsfc at lean mixture conditions the idea of injecting a rich mixture near to spark plug electrode tip, just prior to ignition, has been demonstrated to be a most effective way of extending the lean limit combustion of a spark ignited internal combustion engine. Advantage of this system is that it is relatively simple to incorporate into an existing engine. It is more cost effective than any of the current systems described in Chapter 2.

CHAPTER 8

SUGGESTIONS FOR FURTHER RESEARCH

It was stated that the burning of injected methane gas around its rich flammability limit could be responsible for the increased level of HC emission with stratified charge combustion compared to that of base line operation. This is an unavoidable situation when injection timing and ignition timing are close and necessary to attain a reasonable degree of charge stratification. Therefore it would be interesting to see the changes in the HC emission level, if a richer pre - mixed methane charge compared to leaner main body of fuel, is introduced through the spark plug, instead of virtually pure methane gas. It could also be worth considering to have a properly designed gas injector which is suitable for high pressure applications, to avoid any leakage problem. Measurement of NO_x concentration could be added to the presently measured pollutant types.

Although a reasonable procedure was adopted in the present work to define equivalent part throttle settings for carburetted methane gas operation relative to gasoline operation, an attempt could be made to define equivalent part throttle settings in terms of inlet manifold vacuum pressure. In addition a method should be found to monitor the instantaneous values of mixture air - fuel ratio; perhaps the possibility of incorporating a data acquisition system to the present engine set - up could be investigated.

Further it was noted with constant volume bomb work that having a constant pressure difference between the regulated gas supply and bomb may not accurately model the actual appearance of the methane puff in the engine combustion chamber, due to continuously changing pressure differences. Although the extent to which it could affect the test results is not very clear, an attempt could be made to have Schlieren photographs taken at different times from the point of methane injection while maintaining appropriate pre - calculated pressure differences.

Finally an attempt could be made to measure the velocities in the Ricardo E6 engine cylinder, rather than completely relying on the previous works, perhaps using the laser Doppler velocimeter system.

REFERENCES

(1). **ADAMCZYK, A.A. and KACH, R.A.** The effect of oil layers on hydrocarbon emissions : low solubility oils. Combustion Science and Technology, 36: 227 - 234. 1984.

(2). **ADAMS, W.E., MARSEE, F.J., OLREE, R.M. and HAMILITON, J.C.** Emissions, fuel economy and durability of lean burn engines. SAE paper 760227, 1976.

(3). **AL-MAMAR, F.N.A.A., SHEPPARD, C.G.W. and DESOKY, A.R.A.** Combustion in the divided chamber spark ignition engine. C46/83, Combustion in Engineering, I Mech E Conference Publications, 1: 73 - 80. 1983.

(4). **ALPERSTEIN, M., SCHAFER, G.H. and VILLFORTH, F.J.** Texaco's stratified charge engine - multifuel, efficient, clean and practical. SAE paper 740563, 1974.

(5). **BALLAL, D.R. and LEFEBVRE, A.H.** Effect of electrode spacing on spark ignition of flowing mixtures. Combustion Institute European Symposium, 236 - 241. 1973.

(6). **BALLES, E.N., EKCHIAN, J.A. and HEYWOOD, J.B.** Fuel injection characteristics and combustion behaviour of direct - injection stratified charge engine. SAE paper 841379, 1984.

(7). **BARTON, R.K., KENEMUTH, D.K., LESTZ, S.S. and MEYER, W.E.** Cycle by cycle variation of a spark ignition engine - a statistical analysis. SAE paper 700488, 1970.

(8). **BISHOP, I.N. and SIMKO, A.** A new concept of stratified charge combustion - the Ford combustion process. SAE paper 680041, 1968.

(9). **BLACKMORE, D.R. and THOMAS, A.** Fuel economy of the gasoline engine. 1st. ed. London, The Macmillan Press Ltd., 1977. 268p.

(10). **BLUMBERG, P.N. and KUMMER, J.T.** Prediction of NO formation in spark ignition engines - an analysis of methods of control. Combustion Science and Technology, 4: 73 - 95. 1971.

(11). **BLUMBERG, P.N.** Nitric oxide emissions from stratified charge engines : prediction and control. Combustion Science and Technology, 8: 5 - 24. 1973.

(12). **BOLT, J.A. and HOLKEBOER, D.H.** Lean fuel/ mixtures for high - compression spark ignited engines. SAE Trans., 70: 195 - 202. 1962.

(13). **BOLT, J.A. and HARRINGTON, D.L.** The effects of mixture motion upon the lean limit and combustion of spark ignited mixtures. SAE paper 670467, 1967.

(14). **Bosch** automotive handbook. 2nd. ed. 1986. 707p.

(15). **BRANDSTETTER, W.R., DECKER, G., SCHAFER, H.J. and STEINKE,D.** The Volkswagenwerk PCI stratified charge concept - results from the 1.6 liter air cooled engine. SAE paper 741173, 1974.

(16). **BREISACHER, P., NICHOLS, R.J. and HICKS, W.A.** Exhaust emission reduction through two - stage combustion. Combustion Science and Technology, 6: 191 - 201. 1972.

(17). **BURT, R., ROBERTS, D.D. and WOODWORTH, J.A.** A comparison of fuel - economy, exhaust emissions, and performance of three European cars operating on homogeneous fuel - air mixtures. C148/79, Fuel economy and emissions of lean burn engines, I Mech. E Conference Publications, 205 - 221. 1979.

(18). **CHAPMAN, P.R.** Catalyst systems for the control of emissions from motor vehicles and industrial processes. Proceedings of Seventh International Clean Air Conference, 533-549. 1981.

(19). **CHMELA, F.** High compression stratified charge engines and their suitability for conventional and alternative fuels. C400/80, Stratified Charge Automotive Engines, I Mech. E Conference Publications, 69 - 76. 1980.

(20). **CICCARONE, A., ANTONINI, C. and VIRGILIO, U.** Fuel consumption in European passenger cars powered by gasoline, diesel and direct injection stratified charge engine. SAE 760796, 1976.

(21). **CLARKE, J.S.** Initiation and some controlling parameters of combustion in the automobile engine. SAE Trans., 70: 240 - 261. 1962.

(22). **COLE, D.E. and MIRSKY, W.** Mixture motion - its effect on pressure rise in a combustion bomb ; a new look at cyclic variation. SAE paper 680766, 1968.

(23). **COLE, J.B. and SWORDS, M.D.** Optical studies of the flow field in a motored E6 Engine. C102/79, Fuel economy and emissions of lean burn engines, I Mech E Conference Publications, 165-175. 1979.

(24). **CRAVER, R.J., PODIAK, R.S.and MILLER, R.D.** Spark plug design factors and their effect on engine performance. SAE paper 700081, 1970.

(25). **CURRY, S.** A three - dimensional study of flame propagation in a spark ignition engine. SAE Trans., 71: 628 -650. 1963.

(26). **DAILY, J.W.** Cycle - to - cycle variations : a chaotic process ?. Combustion Science and Technology, 57: 149 - 162. 1988.

(27). **DAIMLER - BENZ AG** Publication. Exhaust gas emission regulations communicated by **R.K.Green.**

(28). **DANIEL, W.A.** Engine variable effects on exhaust hydrocarbon composition (a single - cylinder engine study with propane as the fuel). SAE paper 670124, 1967.

(29). **DANIEL, W.A.** Why engine variables affect exhaust hydrocarbon emission. SAE paper 700108, 1970.

(30). **DATE, T., YAGI, S., ISHIZUYA, A. and FUJII, L.I.** Research and development of the Honda CVCC engine. SAE paper 740605, 1974.

(31). **DE SOETE, G.G.** Compared effects of single chamber and dual chamber charge stratification on NO_x emission and combustion efficiency. C252/76, Stratified Charge Engines, I Mech.E Conference Publications, 95 - 102. 1976.

(32). **DENT, J.C. and SALAMA, N.S.** The measurement of the turbulence characteristics in an internal combustion engine cylinder. SAE paper 750886, 1975.

(33). **DISA** Instruction and service manual for type 55D01 anemometer unit. DISA Elektronik A/S, DK2730 Herlev, Denmark, 1968. 72p.

(34). **DISA** Instruction and service manual for type 55D10 linearizer unit. DISA Elektronik A/S, DK2730 Herlev, Denmark, 1970. 28p.

(35). **FANSLER, T.D. and FRENCH, D.T.** Swirl, squish and turbulence in stratified charge engines : laser velocimetry measurements and implications for combustion. SAE paper 870371, 1987.

(36). **GAY, E.J.** Military multifuel compression ignition engines and their fuel requirements. API mid-year meeting, 1960.

(37). **GIRARD, P., HUNEAM, M., RABASSE, C. and LEYER, J.C.** Flame propagation through unconfined and confined hemispherical stratified gaseous mixtures. Seventeenth Symposium (International) on Combustion, 1247 - 1255. 1978.

(38). **GLOVANETTI, A.J., EKCHIAN, J.A., HAYWOOD, J.B. and FORT, E.F.** Analysis of HC emissions in direct injection spark ignition engine. SAE paper 830587, 1983.

(39). **GRUDEN, D. and HAHN, R.** Performance, exhaust emissions and fuel consumption of an I C engine operating with lean mixtures. C111/79, Fuel economy and emissions of lean burn engines, I Mech. E Conference Publications, 177 - 184. 1979.

(40). **HANSEL, J.G.** A turbulent combustion model of cycle to cycle combustion variation in spark ignition engines. Combustion Science and Technology, 2: 223 - 225. 1970.

(41). **HANSEL, J.G.** Lean automotive engine operation - HC exhaust emissions and combustion characteristics. SAE paper 710164, 1971.

(42). **HARROW, G.A. and CLARKE, P.H.** Mixture strength control of engine power : fuel economy and specific emissions from gasoline engines running in fully vaporized fuel/air mixtures. C90/79, Fuel economy and emissions of lean burn engines, I Mech. E Conference Publications, 39 - 50. 1979.

(43). **HASALETT, R.A., MONAGHAN, M.L. and McFADDEN, J.J.** Stratified charge engines. SAE paper 760755, 1976.

(44). **HATTORI, T., GOTO, K. and OHIGASHI, S.** Study of spark ignition in flowing lean mixtures. C101/79, Fuel economy and emissions of lean burn engines, I Mech. E Conference Publications, 153 - 163. 1979.

(45). **HEYWOOD, J.B.** Pollutant formation and control in spark ignition engines. Prog.Energy and Combustion Science, 1: 135 - 164. 1976.

(46). **HIRES, S.D., EKCHIAN, A., HEYWOOD, J.B., TABACZYNSKI, R.J. and WALL, J.C.** Performance and NO_x emissions modelling of a jet ignition pre - chamber stratified charge engine. SAE paper 760161, 1976.

(47). **HOLDER, D.W. and NORTH, R.J.** Schlieren methods. London, National Physics Laboratory, Her Majesty Stationery Office, 1963. 106p.

(48). Hot wire - Hot film - ion anemometer systems. Thermo - Systems Inc., Minnesota, USA, 1975. 100p.

(49). **HUGHES, D.W. and GOULBURN, J.R.** Fuel vaporisation - economy with reduced exhaust emission. Proc.Inst.of Mech. Engrs., 190: 1 -11. 1976.

(50). **JOHNSTON, S.C.** Precombustion fuel/air distribution in a stratified charge engine using laser Raman spectroscopy. SAE paper 790433, 1979.

(51). **JONES, C. and LAMPING, H.** Curtiss - Wrights development status of the stratified charge rotating combustion engine. SAE paper 710582, 1971.

(52). **KAISER, E.W., ROTHSCHILD, W.G. and LAVOIE, G.A.** The effect of fuel and operating variables on hydrocarbon species distributions in the exhaust from a multi - cylinder engine. Combustion Science and Technology, 32: 245 - 265. 1983.

(53). **KAISER, E.W., ROTHSCHILD, W.G. and LAVOIE, G.A.** Storage and partial oxidation of unburned hydrocarbons in spark - ignited engines - effect of compression ratio and spark timing. Combustion Science and Technology, 36: 171 - 189. 1984.

(54). **KALGHATGI, G.T.** Effect of a spark aider fuel additive on the misfire characteristics of a spark ignition engine. Combustion Science and Technology, 62: 1 -19. 1988.

(55). **KARIM, G.A. and TSANG, P.** Flame propagation through atmospheres involving concentration gradients formed by mass transfer phenomena. Journal of Fluids Engineering, ASME Trans., 97: 615 - 617. 1975.

(56). **KARIM, G.A., TSANG, P., SARPAL, G.S. and BADR, O.** A fundamental study into flame propagation through stratified mixtures. C255/76, Stratified Charge Engines, I Mech.E Conference Publications, 121 - 126. 1976.

(57). **KOMIYAMA, K. and HEYWOOD, J.B.** Predicting NO emissions and effects of EGR in spark ignited engines. SAE paper 730475, 1973.

(58). **KRIEGER, R.B. and DAVIS, G.C.** The influence of the degree of stratification on jet - ignition engine emissions and fuel consumption. C254/76, Stratified Charge Engines, I Mech.E Conference Publications, 109 - 119. 1976.

(59). **KUCK, H.A. and BRANDSTETTER, W.R.** Investigations on a single cylinder stratified charge engine with a scavenged prechamber. C92/75, Combustion in Engines, I Mech.E Conference Publications, 105 - 112. 1975.

(60). **LANCASTER, D.R.** Diagnostic investigation of hydrocarbon emissions from a direct injection stratified charge engine with early injection. C397/80, Stratified Charge Automotive Engines, I Mech. E Conference Publications, 33 - 40. 1980.

(61). **LAVOIE, G.A. and BLUMBERG, P.N.** Measurements of NO emissions from a stratified charge engine : comparison of theory and experiment. Combustion Science and Technology, 8: 25 - 37. 1973.

(62). **LIEBMAN, I., CORRY, J. and PERLEE, H.E.** Dynamics of flame propagation through layered methane - air mixtures. Combustion Science and Technology, 2: 365 - 375. 1971.

(63). **LOMAS, C.G.** Fundamentals of hot wire anemometry. 1st. ed. Cambridge, Cambridge University Press, 1986. 211p.

(64). **LUCAS, G.G., BRUNT, M.F. and ANTON, R.** The effect of squish on charge turbulence and flame propagation. C87/79, Fuel economy and emissions of lean burn engines, I Mech. E Conference Publications, 1 - 18. 1979.

(65). **MA, T.H.** Effect of cylinder charge motion on combustion. C81/75, Combustion in Engines, I Mech.E Conference Publications, 1 - 12. 1975.

(66). **MARSEE, F.J. and OLREE, R.M.** Distribution factors that influence emissions and operation of lean burn engines. C99/79, Fuel economy and emissions of lean burn engines, I Mech. E Conference Publications, 129 - 136. 1979.

(67). **MATSUOKA, S., YAMAGUCHI, T. and UMEMUKI, Y.** Factors influencing the cyclic variation of combustion of spark ignition engine. SAE paper 710586, 1971.

(68). **MATTAVI, J.N., GROFF, E.G. and MATEKUNAS, F.A.** Turbulence flame motion and combustion chamber geometry - their interactions in a lean - combustion engine. C100/79, Fuel economy and emissions of lean burn engines, I Mech. E Conference Publications, 137 - 151. 1979.

(69). **MAY, M.G.** The high compression lean burn spark ignited 4 - stroke engine. C97/79, Fuel economy and emissions of lean burn engines, I Mech. E Conference Publications, 107 - 116. 1979.

(70). **MAYO, J.** The effect of engine design parameters on combustion rate in spark ignited engines. SAE paper 750355, 1975.

(71). **MEURER, J.S. and URLAUB, A.C.** Development and operational results of the M.A.N. FM combustion system. SAE paper 690255, 1969.

(72). **MEURER, J.S.** Present experience with stratified charge engines working with initial separation of mixture components. C250/76, Stratified Charge Engines, I Mech.E Conference Publications, 81 - 87. 1976.

(73). **MITCHELL, E., COBB, J.M. and FROST, R.A.** Design and evaluation of a stratified charge multifuel military engine. SAE paper 680042, 1968.

(74). **MITCHELL, E., ALPERSTEIN, C., COBB, J.M. and FAIST, C.H.** A stratified charge multi - fuel military engine - a progress report. SAE paper 720051, 1972.

(75). **MIYAKE, M., OKADA, S., KAWAHARA, Y. and ASAI, K.** A new stratified charge combustion system (MCP) for reducing exhaust emissions. Combustion Science and Technology, 12: 29 - 46. 1976a.

(76). **MIYAKE, M.** Recent development of Mitsubishi's stratified charge engine MCP. C259/76, Stratified Charge Engines, I Mech.E Conference Publications, 157 - 166. 1976b.

(77). **MIZUTANI, Y. and MATSUSHITA, S.** Fuel vapor - spray - air mixture operation of a spark ignition engine. Combustion Science and Technology, 8: 85 - 94. 1973.

(78). **NAKAJIMA, Y., SUGIHARA, K. and TAKAGI, Y.** Lean mixture or EGR - which is better for fuel economy and NO_x reduction. C94/79, Fuel economy and emissions of lean burn engines, I Mech. E Conference Publications, 81 - 86. 1979.

(79). **NEWHALL, H.K. and STARKMAN, E.S.** Direct spectroscopic determination of nitric oxide in reciprocating engine cylinders. SAE paper 670122, 1967.

(80). **NEWHALL, H.K.** Kinetics of engine generated nitrogen oxides and carbon monoxide. Twelfth Symposium (International) on Combustion, 603 - 613. 1969.

(81). **NEWHALL, H.K. and EL MESSIRI, I.A.** A combustion chamber designed for minimum exhaust emissions. SAE paper 700491, 1970.

(82). **OBLANDER, K., ABTHOFF, J. and FINK, R.** Stratified charge engines with open and subdivided combustion chamber. C251/76, Stratified Charge Engines, I Mech.E Conference Publications, 89 - 94. 1976.

(83). **OBLANDER, K., ABTHOFF, J. and FRICKER, L.** From engine testbench to vechicle - an approach to lean burn by dual ignition. Fuel economy and emissions of lean burn engines, I Mech. E Conference Publications, 19 - 24. 1979.

(84). **OGASAWARA, M., NISHIDA, O., TAKAGI, T. and OHKI, T.** Control of nitric oxide and carbon monoxide emission by two - stage combustion process. C245/76, Stratified Charge Engines, I Mech.E Conference Publications, 37 - 44. 1976.

(85). Operating instructions for Alcock viscous flow air meter no. 1092V. 11p.

(86). Operation manual for HORIBA (MEXA - 534GE) automotive emission analyzer.

(87). **PATTERSON, D.J.** Cylinder pressure variations - a fundamental combustion problem. SAE paper 660129, 1967.

(88). **PATTERSON, D.J. and HENEIN, N.A.** Emissions from combustion engines and their control. Michigan, Ann Arbor Science Publishers, 1972. 355p.

(89). **PERKINS, H.C.** Air pollution. 1st. ed. New York, McGraw Hill Book Company, 1974. 407p.

(90). **PETERS, B.D. and QUADER, A.A.** "Wetting" the appetite of spark ignition engines for lean combustion. SAE paper 780234, 1978.

(91). **PETERS, B.D.** Mass burning rates in a spark ignition engine operating in the partial burn regime. C92/79, Fuel economy and emissions of lean burn engines, I Mech. E Conference Publications, 63 - 70. 1979.

(92). **PISCHINGER, F. and KLEINSCHMIDT, W.** Study of NO, NO_2 and CO formation in spark - ignited engines by using extended reaction - kinetics. Combustion Institute European Symposium, 457 - 462. 1973.

(93). **PISCHINGER, F.F. and KLOCKER, K.J.** Single - cylinder study of stratified charge process with pre chamber - injection. SAE paper 741162, 1974.

(94). **PISCHINGER, F. and ADAMS, W.** Influence on intake swirl on the characteristics of a stratified engine with pre - chamber injection. C391/80, Stratified Charge Automotive Engines, I Mech. E Conference Publications, 1 - 7. 1980.

(95). **PITT, P.L., RIDLEY, J.D. and CLEMENTS, R.M.** Low energy ignition of an ultra lean methane fueled internal combustion engine. Combustion Science and Technology, 38: 217 - 225. 1984.

(96). **PURINS, E.A.** Pre - chamber stratified charge engine combustion studies. SAE paper 741159, 1974.

(97). **QUADER, A.A.** Lean combustion and the misfire limit in spark ignition engines. SAE paper no.741055, 1974.

(98). **Ricardo** Consulting Engineers. The Ricardo E6/MK 6 variable compression engine. Serial no.138/82, 1982. 26p.

(99). **ROBISON, J.A.** Humidity effects in engine nitric oxide emissions at steady state coditions. SAE paper 700467, 1970.

(100). **SAKAI, Y., KUNII, K., TSUTSUMI, S. and NAKAGAWA, Y.** Combustion characteristics of the torch ignited engine. SAE paper 741167, 1974.

(101). **SAKAI, Y., KUNII, K., SASAKI, M., KAKUTA, N. and AIHARA, H.** Combustion characteristics of a torch ignited engine - analytical measurements of gas temperature and mixture formation. C247/76, Stratified Charge Engines, I Mech.E Conference Publications, 55 - 63. 1976.

(102). **SCHWARZ, H.** Ignition systems for lean burn engines. C95/79, Fuel economy and emissions of lean burn engines, I Mech. E Conference Publications, 87 - 96. 1979.

(103). **SCUSSEL, A.J., SIMKO, A.O. and WADE, W.R.** The Ford PROCO engine update. SAE paper 780699, 1978.

(104). **SEMENOV, E.S.** Studies of turbulent gas flow in piston engines. NASA Technical Translation, F97, 122-147. 1963.

(105). **SIMKO, A., CHOMA, M.A. and REPKO, L.L.** Exhaust emission control by the Ford programmed combustion process - PROCO. SAE paper 720052, 1972.

(106). **SYED, S.A. and BRACCO, F.V.** Further comparisons of computed and measured divided chamber engine combustion. SAE paper 790247, 1979.

(107). **TANUMA, T., SASAKI, K., KANEKO, T. and KAWASUKI, H.** Ignition, combustion and exhaust emissions of lean mixture in automotive engines. SAE paper 710159, 1971.

(108). **WATFA, M. and DANESHYAR, H.** Formation of nitric oxide (NO), carbon monoxide (CO) and unburnt hydrocarbons (HC), in spark ignition engines. C99/75, Combustion in Engines, I Mech.E Conference Publications, 165 - 183. 1975.

(109). **WESTBROOK, C.K.** Fuel motion and pollutant formation in stratified charge combustion. SAE paper 790248, 1979.

(110). **WITZE, P.O.** Influence of air motion variation on the performance of a direct injection stratified charge engine. C394/80, Stratified Charge Automotive Engines, I Mech. E Conference Publications, 25 - 31. 1980.

(111). **WOOD, C.D.** Performance of a stratified charge engine. SAE paper 790434, 1979.

(112). **YAGI, S., FUJII, I., AJIKI, Y. and TSUDA, T.** The antiknock quality in the stratified charge engine with an auxiliary combustion chamber. C395/80, Stratified Charge Automotive Engines, I Mech. E Conference Publications, 49 - 54. 1980.

(113). **YOUNG, A.W.** Energy use conservation and outlook in transport. Fourth New Zealand Energy Conference, 143 - 149. 1979.

(114). **ZIEGLER, G.F.W., MALY, R.R. and WAGNER, E.P.** Effect of ignition system design on flammability requirements in ultra-lean turbulent mixtures. C47/83, Combustion in Engineering, I Mech E Conference Publications, 1: 81 - 92. 1983.

BIBLIOGRAPHY

(1). **BENSON, R.B. and WHITEHOUSE, N.D.** Internal combustion engines. Pergamon Press, 1979. 430p.

(2). **BONE, W. and TOWNEND, D.** Flame and combustion in gases. Longmans, Green and Co. Ltd, 1927. 548p.

(3). **BRADSHAW, P.** An introduction to turbulence and its measurement. 1st. ed. Pergamon Press, 1971. 218p.

(4). **FERGUSON, C.R.** Internal combustion engines: applied thermosciences. John Wiley & Sons, 1986. 546p.

(5). **FULLER, D.E.** Mixture motion in an engine cylinder. Cambridge, University of Cambridge, 1975. 183p. (Thesis: Ph.D. : Engineering)

(6). **HINZE, J.O.** Turbulence - an introduction to its mechanism and theory. McGraw Hill Book Company, 1959. 586p.

(7). **LEWIS, B. and von ELBE, G.** Combustion, flame and explosions of gases. 2nd. ed. Academic Press Inc., 1961. 731p.

(8). **ROSE, J.W. and COOPER, J.R.** Technical data on fuel. 7th. ed. The British National Committee, World Energy Conference, 1977. 343p.

(9). **STONE, R.** Introduction to internal combustion engines. 1st. ed. Macmillan Publishers, 1985. 319p.

(10). **WEST, J.P. and BROWN, L.G.** Compressed natural gas. New Zealand Energy Research and Development Committee, publication P14, 1979. 85p.

(11). **ZOELLNER, S.A. and RAINE, R.R.** A feasibility study of gas injection systems for natural gas fuelled automotive engines. New Zealand Energy Research and Development Committee, publication P110, 1986. 77p.

APPENDIX 1

A.1.1 GENERAL SPECIFICATIONS OF COMBUSTION APPARATUS

A.1.1.1 Ricardo E6/MK 6 Engine

serial no.	138/82
no. of cylinders	1
bore	76.2 mm.
stroke	110 mm.
capacity	507 cc.
compression ratio	4.5 - 20:1
Valve timing :	
inlet valve opens	8° BTDC
inlet valve closes	36°ABDC
exhaust valve opens	42°BBDC
exhaust valve closes	8°ATDC
Tappet clearence :	
inlet	0.15 mm
exhaust	0.25 mm

A.1.1.2 Auxiliary items

gasoline pump	**Bosch**; 0580 464 008;
gasoline injector	**Bosch**; 0280 150 151

air meter	**Alcock** viscous type
	serial no. 1092 V
thermo-couple	K type; Ni Cr/Ni Al
	-200°to 1250°C
ignition system	Lumenition MK 16
spark plug	**NGK**; gap setting of 0.64 mm.
dynamometer	**BKB**; swinging field
	400 V DC
	serial no. 55077 - 3
methane cylinder	170 bar.
methane injector	**Bosch**; 0 280 150 201; 3 V
h.p. regulator	Span instruments; 0 - 200 bar.
gas carburettor	E6M 140
l.p. regulator	max. inlet pressure: 20 bar.
	outlet pressure: 1 bar.
	flow rate: 3 kg/h.
fuel controller	no. 2601;
	H.K.L.Gas Power Ltd. UK.
rotameter - 1	**Matheson**;
	max. operating pressure:
	17 bar.
	flow range : up to 1.4 l/min.
	at 760 mm Hg & 21°C.

rotameter - 2	**Matheson;** max. operating pressure : 17 bar. flow range : up to 24 l/min. at 760 mm Hg & 21°C.
gas filter	**Nupro** filter with 2 micron sintered element.
exhaust analyser	**Horiba;** MEXA - 534GE HC : 0 - 10,000 ppm (n - hexane equivalent) CO : 0 - 10 % vol. CO_2 : 0 - 20 % vol. O_2 : 0 - 20 % vol.

APPENDIX 2

A.2.1 GENERAL SPECIFICATIONS OF COMBUSTION CHAMBER SIMULATION APPARATUS

A.2.1.1 Constant volume bomb

bomb size	130 mm x 130 mm x 140 mm
	with two 40 mm x 30 mm
	glass windows and 76.2 mm
	bore
	internal volume = 0.638 l
D.C. motor	operating voltage : 3 V
	no load speed : 9500 r.p.m
fan	35 mm o.d; 8 blades
D.C.power source	**HEATHKIT;**
	settings : 0 - 1.5 A; 5 - 50 V

A.2.1.2 Schlieren apparatus

light source	argon jet type
	power to spark gap : 3 J
	light duration : 0.2 s
	rise time : 0.07 s
	triggering voltage : 30 -70 V
delay circuit	delay time : 0 - 100 ms

argon cylinder	standard; 170 bar
methane cylinder	standard; 170 bar
methane injector	**Bosch**; 0 280 150 201; 3 V
spark plug	**NGK**; gap setting of 0.64 mm

A.2.1.3 Hot wire anemometer system

hot wire	**DISA** ; length = 1.25 mm
	diameter = 5 μ m
	platinum plated tungsten
anemometer	**DISA** type 55D01
linearisер	**DISA** type 55D10
D.C. voltmeter	**DISA** type 55D30
r.m.s. unit	**DISA** type 55D35
calibrator	**TSI** model 1125

APPENDIX 3

A.3.1 LINEAR CURVE FIT DATA OF HOT WIRE CALIBRATION

file name	\A2D\ZC2
probe serial no.	z11-1
resistance at room temperature	3.5 ohms.
operating resistance	6.3 ohms.
slope	1.052536
intercept	- 6.250115E - 02 V
room temperature	295.15 K.
pressure	1.012 bar.

These calibration constants were obtained by using a computer programme called **HWCAL.BAS** with the **QBASIC** compiler.

APPENDIX 4

A.4.1 CORRECTION FACTOR FOR MEAN VELOCITY

The velocity values that derived from the work of Cole et al.(23) corresponded to a crank angle position around TDC. Since a velocity field between 40° to 80° BTDC injection timing was required for the combustion chamber simulation work (Section 4.2), a correction factor for the mean velocity was derived from the results of Semenov (104) as shown below.

According to (104), Fig. 13,

For a cylindrical combustion chamber and at 900 r.p.m,

Average velocity at TDC = 1.143 m/s

Average velocity between

40° to 80° BTDC = 1.429 m/s

Therefore,

Ratio of average velocity = 1.429/1.143

= 1.25

This value of 1.25 was used to correct the mean velocities that obtained from the work of Cole et al.(23) for the necessary velocity field simulation.

APPENDIX 5

A.5.1 CALCULATION OF QUENCH DISTANCE

A.5.1.1 Nomenclature

M	molecular weight (kg/kmol)
P_c	mixture pressure at the end of the polytropic compression (bar)
T_c	mixture temperature at the end of the polytropic compression (K)
T_{ig}	ignition temperature of the mixture (K)
U_F	laminar burning velocity of mixture at 1 bar and 20°C (m/s)
X	mole fraction
c_p	specific heat at constant pressure (kJ/kg K)
k	thermal conductivity (kW/m K)
q_d	quench diameter for a tube (mm)
q_f	quench distance for a single flat plate (mm)
q_p	quench distance for parallel plates (mm)
μ	dynamic viscosity (kg/m s)
ρ	mixture density at 1 bar and 20°C (kg/m^3)

Subscripts

i	species i
j	species j
m	mixture of species i and j
(-)	overbar denotes mean value

A.5.1.2 Equations for quench distance calculation

The mixture under consideration is assumed to be rich and consists of methane and air.

The properties of the mixture can be calculated as follows (1)*

$$C_{pm} = \frac{\sum_{i-1}^{2} M_i \, X_i \, C_{pi}}{\sum_{i-1}^{2} M_i \, X_i} \qquad \text{(A5.1)}$$

$$k_m = \sum_{i-1}^{2} \frac{k_i}{1 + \frac{1}{X_i} \sum_{\substack{j-1 \\ j \neq i}}^{2} X_j \, G_{ij}} \qquad \text{(A5.2)}$$

Where,

$$G_{ij} = \frac{1.065 \left[1 + \left(\frac{\mu_i}{\mu_j}\right)^{1/2} \left(\frac{M_j}{M_i}\right)^{1/4}\right]}{2\sqrt{2} \left(1 + \frac{M_i}{M_j}\right)^{1/2}} \qquad \text{(A5.3)}$$

---

* See the references for the appendix 5 at the end of this appendix

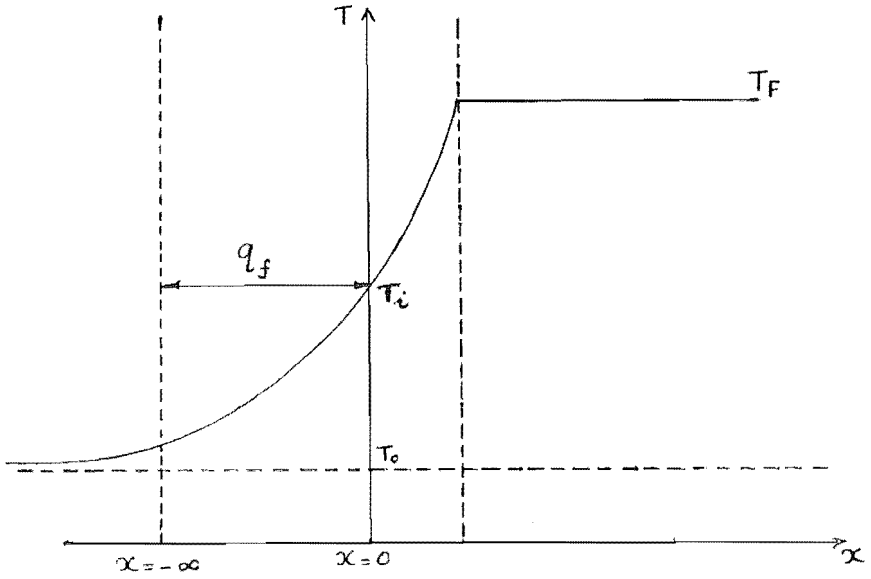

Fig. A5.1 Temperature plot for a flame front

According to the thermal theory of flame propagation the quench distance at a single flat plate may be approximated to (2),

$$q_f = \frac{4.6 \times \overline{k}_m}{\overline{c}_{pm} \times (\rho U_F)} \qquad \text{(A5.4)}$$

Where $\overline{k}$, $\overline{c}_p$ are mean values of thermal conductivity and specific heat respetively, between T_{ig} and T_c.

The quench diameter for a cylindrical tube based on surface area (3) may be represented as,

$$q_d = \frac{q_p}{0.65} \qquad \text{(A5.5)}$$

$$q_d = \frac{2 \times q_f}{0.65} \qquad \text{(A5.6)}$$

For a polytropic compression index of 1.25 and initial conditions (1 bar and 20°C) and at a worst situation of P_c = 50 bar, T_c was calculated as 640 K.

With a reasonable ignition temperature of 650°C for methane - air mixture, the quench diameter (q_d) was found to be approximately 2.8 mm. Since this quench diameter is larger than the hypodermic injection tube (diameter = 1.5 mm) which was used in the stratified charge experiments, the possibility of unburnt and/or partially burnt gases have become quenched inside the hypodermic tube is justified.

A.5.2 References

(1). **GREEN, R.K.** The influence of turbulence on the quenching effects in the combustion process in constant volume explosion flames. Leeds, University of Leeds, 1975. 270p. (Thesis: Ph.D. : Engineering).

(2). **BRADLEY, J.N.** Flame and combustion phenomena. 1st. ed. Methuen and Co. Ltd., 1969. 210p.

(3). **POTTER Jr., A.E.** Flame quencing. Prog. in Combustion Science and Technology no.1, Pergamon Press, 1960. p.145 - 181.